

MAX-PLANCK-GESELLSCHAFT

Dissertation zur
Erlangung des Grades Dr. rer. nat.

Systems Analysis of the spatial Regulation of oncogenic Ras signalling

vorgelegt von

Kaatje Friederike Heinelt

Matrikel-Nr. 173007

Peterstr. 1 | 26316 Varel

angefertigt am

Max-Planck-Institut für

Molekulare Physiologie

Arbeitsgruppe Bastiaens

Dortmund, im März 2017

1. Gutachter: Prof. Dr. Philippe Bastiaens

2. Gutachter: PD Dr. Leif Dehmelt

Eidesstattliche Versicherung

Ich versichere hiermit an Eides statt, dass ich die vorliegende Dissertation mit dem Titel
„Systems Analysis of the spatial Regulation of oncogenic Ras Signalling“ selbstständig und
ohne unzulässige fremde Hilfe angefertigt habe. Ich habe keine anderen als die angegebenen
Quellen und Hilfsmittel benutzt sowie wörtliche und sinngemäße Zitate kenntlich gemacht.

Die Arbeit hat in gegenwärtiger oder in einer anderen Fassung weder der TU Dortmund noch
einer anderen Hochschule im Zusammenhang mit einer staatlichen oder akademischen
Prüfung vorgelegen.

Ort, Datum

Unterschrift

Table of contents

1	Abstract.....	1
2	Zusammenfassung	3
3	Introduction	5
3.1	Ras family.....	5
3.1.1	Ras GTPases – an overview	5
3.1.2	The GTPase cycle of Ras proteins.....	6
3.1.2.1	Ras and its interaction with GEFs.....	8
3.1.2.2	Ras and its interaction with GAPs.....	9
3.1.3	The clinically most notable members of the Ras subfamily.....	11
3.1.4	Downstream effector signalling of Ras.....	16
3.1.5	Kras	21
3.1.6	Kras mutations and their impact in cancer.....	22
3.1.7	Inhibition of oncogenic Ras – The “undruggable” protein	27
3.1.8	The principle of oncogene addiction	28
3.1.9	Another way to target Ras – small molecule PDEδ inhibitors.....	31
3.2	Organoids as a new model system.....	32
4	Objectives	34
5	Material.....	35
5.1	Cell lines used	35
5.2	Antibodies	35
5.2.1	Primary antibodies for Western Blots.....	35

5.2.2	Secondary antibodies for Western Blots	35
5.2.3	Primary antibodies for Immunofluorescence.....	36
5.2.4	Secondary antibodies for Immunofluorescence.....	36
5.3	Materials and Media for cell culture	36
5.4	Transfection	37
5.5	Oligonucleotides	37
5.5.1	Primer for LIC.....	37
5.5.2	Primer for sequencing	38
5.5.3	Primer for genotyping	40
5.6	Animal resources, organoid preparation and organoid culture.....	41
5.6.1	Mice	41
5.6.2	Material and Media for organoid culture.....	42
5.7	Bacteria	43
5.8	Plasmids	43
5.8.1	Eukaryotic Vectors	43
5.8.2	Viral Vectors.....	43
5.9	Media for Bacteria.....	43
5.10	PFA preparation	44
5.10.1	4% PFA in PBS	44
5.10.2	4% PFA in PME.....	44
5.11	Commercial Material and Kits.....	44
5.12	Inhibitors.....	45
5.13	Standards	45
5.14	General chemicals.....	45

5.15	Buffer	47
5.16	Devices and expendables	47
5.17	Microscopes	49
6	Methods	50
6.1	Culture of cell lines	50
6.2	Freezing and thawing cell lines	51
6.3	Transfection of cell lines	52
6.3.1	Transfection with Fugene	52
6.3.2	Transfection with Effectene	52
6.3.3	Transfection with Lipofectamine 2000.....	53
6.4	Preparation of small intestine organoids	54
6.5	Culture of small intestine organoids	55
6.6	Freezing and thawing organoids	57
6.7	Retroviral infection of organoids	58
6.8	Whole cell lysates	61
6.8.1	Mammalian cells	61
6.8.2	Organoids	62
6.9	SDS-PAGE	63
6.10	Western Blot – Tank Blot method	64
6.11	Immunodetection	65
6.12	Antibody stripping of Western Blot membranes	66
6.13	Bradford assay	66
6.14	DNA preparation using Quick-DNA™ Universal Kit	67

6.15	Determination of DNA concentration with NanoDrop Spectral photometer.....	67
6.16	Bacterial culture.....	67
6.17	Transformation of bacteria.....	68
6.18	Polymerase Chain Reaction (PCR) methods.....	69
6.18.1	Ligation independent cloning.....	70
6.18.2	Genotyping PCR (Organoids).....	70
6.19	DNA preparation M&N Midi kit.....	71
6.20	DNA preparation using Roti®-Prep Plasmid Mini Kit.....	72
6.21	Agarose Gelelectrophoresis.....	72
6.22	Purification of DNA from Agarose gels.....	73
6.23	Restriction digest.....	73
6.24	Dephosphorylation of 5'-phosphorylated DNA.....	74
6.25	PCR product purification.....	74
6.26	Ligation.....	75
6.27	Sequencing using BigDye® Terminator kit.....	75
6.28	Preparation of Cryoslices using a Cryostat.....	77
6.29	Immunofluorescence.....	78
6.29.1	Cells.....	78
6.29.2	Organoids on slides.....	78
6.29.3	Organoids in SPIM.....	79
6.30	Life cell imaging experiments.....	81
6.30.1	In cells.....	81
6.30.2	In organoids with SPIM.....	81

7	Results	84
7.1	Comparison of the localization of different over expressed Ras isoforms upon Deltarasin and Deltazinone 1 treatment in MDCK cells	84
7.2	Comparison of the effect of Deltarasin and Deltazinone 1 treatment on localization of endogenous Ras in A431 cells	87
7.3	Deltarasin relocalizes Ras in colorectal cancer cells	88
7.4	Comparison of the effect of Deltarasin and Deltazinone 1 treatment on Localization of mCherry KrasWT in PancTuI cells	90
7.5	Characterization of small intestine organoids	95
7.6	Infection with Cre recombinase leads to DNA recombination and expression of mTFP-KrasG12D protein in small intestine organoids.....	96
7.6.1	Cre-mediated DNA recombination in organoids to switch mTFP-KrasG12D expression on	97
7.6.2	mTFP Kras expression in organoids	101
7.7	Deltarasin causes mTFP-KrasG12D relocalization in small intestine organoids.....	106
8	Discussion	109
8.1	mCherry KrasWT and mCitrine HrasG12V relocalize in parallel in MDCK cells upon PDE δ inhibition by Deltarasin but not by Deltazinone 1	109
8.2	Endogenous Ras relocalizes in Kras-independent cells upon PDE δ inhibition by Deltarasin in a dose dependent manner	112
8.3	mCherry KrasWT relocalizes in Kras-dependent cells upon PDE δ inhibition by Deltarasin and Deltazinone 1	113
8.4	Why use small intestinal organoids?.....	115
8.5	The mTFP-KrasG12D organoid system.....	116
8.6	Ras status in small intestinal organoids after recombination.....	118

8.7	Endogenous levels of mTFP-KrasG12D relocate small intestinal organoids upon PDEδ inhibition by Deltarasin.....	120
9	Outlook	122

1 Abstract

Ras (Rat sarcoma) isoforms are small GTP-binding proteins that play a major role in the signalling networks controlling cell growth and survival. The Kras isoform is of particular interest as in many severe kinds of cancer the presence of oncogenic Kras mutations is associated with a poor prognosis.

Kras is associated with the plasma membrane due to its farnesyl moiety and a polybasic motif and functions as a signalling hub. If Kras gets lost from the plasma membrane due to spontaneous dissociation or endocytosis, it will equilibrate over the extensive endomembrane system inside the cell. With Kras no longer present at the plasma membrane, its activation and the following activation of subsequent pathways can no longer take place. However, to remain on the plasma membrane, Kras has to be constantly enriched there. This enrichment must be actively maintained in the cell by an energy-driven mechanism involving the solubilising factor PDE . Consequently, inhibition or down-modulation of PDE results in mislocalisation of Kras, making PDE an interesting target for anti-cancer drug development. In 2013 a small molecule, Deltarasin, was identified as a potent inhibitor of PDE causing a redistribution of Kras from the plasma membrane towards endomembranes when applied to cells.

This work investigates whether small molecule PDE inhibitors such as Deltarasin affect (K) Ras localization in space and time. It demonstrates that PDE inhibition causes Ras relocation from the plasma membrane towards the endomembranes in different human cancer cell lines and in murine small intestine organoids, which express endogenous levels of oncogenic Kras.

Nonetheless, it has been shown that Deltarasin has certain side effects, e.g. it becomes cytotoxic at higher concentrations. Hence, a new PDE inhibitor, Deltazinone 1, which is supposed to be less cytotoxic in comparison to Deltarasin, was synthesized. In order to determine whether it represents a viable alternative to Deltarasin, its ability to relocate Kras in a panel of cancer cell lines was tested and it was indeed possible to mislocalise Kras with this inhibitor in Kras-dependent PancTu1 cells. Deltazinone 1 and Deltarasin both had a demonstrable effect on cell growth/survival, respectively. In this way it appears that PDE constitutes a valid target for the pharmacological therapy of Kras-dependent tumours.

This work demonstrates that two specific PDE inhibitors with completely different lead structures are capable of mislocalising Kras to endomembranes. In sum, it demonstrates that

the availability of PDE is essential to ensure (K) Ras localization at the plasma membrane in Kras-dependent cancer cells and thus that the survival of those cells are ultimately dependent on PDE .

2 Zusammenfassung

Bei Ras (Rat sarcoma) Isoformen handelt es sich um kleine GTP-bindende Proteine, die eine wichtige Rolle in Signalwegen zur Kontrolle des Wachstums und Überlebens von Zellen spielen. Dabei ist besonders die Kras Isoform von Bedeutung, da in vielen Krebsarten das Vorhandensein onkogener Mutationen von Kras mit einer schlechten Prognose verbunden ist.

Kras kann mittels seines Farnesylschwanzes und einer Abfolge basischer Aminosäuren an die Plasmamembran binden und wirkt dort als Knotenpunkt im Verlauf der Signalübertragung. Wenn Kras durch spontane Dissoziation oder Endocytose die Plasma Membran verlässt, equilibriert es über das im Inneren der Zelle vorhandene ausladende System von Endomembranen. In Folge dessen können die Aktivierung von Kras und auch die der nachfolgenden Signalwege nicht länger stattfinden. Kras muss kontinuierlich an der Plasmamembran angereichert werden, um dort verbleiben zu können. Diese Anreicherung ist ein aktiver Prozess und wird durch einen Energie-abhängigen Mechanismus aufrecht erhalten, an welchem der Lösungsfaktor PDE beteiligt ist. Folglich führen Inhibition oder Herabregulierung von PDE zu einer falschen Lokalisation von Kras in der Zelle, was PDE zu einem überaus interessanten Zielprotein für die Entwicklung neuer Medikamente zur Behandlung von Krebs macht. Im Jahr 2013 wurde ein kleines Molekül mit dem Namen Deltarasin identifiziert, von welchem gezeigt werden konnte, dass es ein potenter Inhibitor für PDE ist. Es führt zu einer Umlagerung von Kras von der Plasmamembran in Richtung der Endomembranen, wenn es zu Zellen gegeben wird.

In dieser Arbeit wird untersucht, inwieweit PDE Inhibitoren auf Basis kleiner Moleküle, wie z.B. Deltarasin, die Lokalisation von (K)Ras in Raum und Zeit beeinflussen. Es kann in verschiedenen humanen Krebszelllinien und in Dünndarmorganoiden aus der Maus, welche endogene Level von oncogenem Kras exprimieren, gezeigt werden, dass die Inhibition von PDE zu einer Relokalisation von Ras von der Plasmamembran in Richtung der Endomembranen führt.

Dennoch wurde gezeigt, dass Deltarasin unerwünschte Nebeneffekte hat, beispielsweise wirkt es in höheren Konzentrationen cytotoxisch. Daher wurde ein neuer Inhibitor für PDE, Deltazinone 1, synthetisiert, welcher weniger cytotoxisch sein sollte. Um herauszufinden, ob er eine gute Alternative zu Deltarasin darstellt, wurde seine Fähigkeit zur Relokalisation von Kras in einem Panel von Krebszelllinien überprüft. Es war tatsächlich möglich Kras mittels dieses Inhibitors in Kras-abhängigen PancTu1 Zellen von der Plasmamembran in Richtung

der Endomembranen zu verlagern. Da Deltazinone 1 und Deltarasin beide nachweislich Effekte auf Wachstum und Überleben von Zellen haben, scheint PDE ein lohnendes Ziel für die pharmakologische Therapie Kras-abhängiger Tumore zu sein.

Diese Arbeit zeigt, dass zwei spezifische PDE Inhibitoren mit vollkommen verschiedenen Leitstrukturen Kras in Richtung der Endomembranen mislokalisieren können. Zusammengefasst zeigt sie, dass das Vorhandensein von PDE essentiell ist, um in Kras-abhängigen Krebszellen die Lokalisation von (K)Ras an der Plasmamembran zu gewährleisten. Somit hängt das Überleben dieser Zellen komplett von PDE ab.

3 Introduction

Ras proteins are the biological background of this work. Accordingly, their role in signal transduction under both normal and pathological conditions and the manner in which they are regulated to be at the right place at the right time are outlined in this chapter.

3.1 Ras family

3.1.1 Ras GTPases – an overview

The Ras (Rat sarcoma) protein superfamily comprises more than 150 members in humans and is divided into five major branches based on sequence and functional similarities: Ras, Rho, Rab, Ran and Arf (Wennerberg et al., 2005). All members of the Ras superfamily are small GTPases that act as molecular switches that cycle between inactive GDP-bound and active GTP-bound states and share a common biochemical mechanism (Vetter and Wittinghofer, 2001). Members of the Ras branch play a major role in the signalling networks controlling cell growth and survival (Nandan and Yang 2011; Courtney et al., 2010) and were found to be some of the first oncogenes (Der et al., 1982; Shimizu et al., 1983).

Ras proteins share a similar topological structure, which is characterized by a G-domain with 6 α -strands flanked by 5 β -helices and 10 connecting loops (Figure 1, Milburn et al., 1990). The proteins have a molecular weight of 21 kDa and are 188/189 amino acids in length.

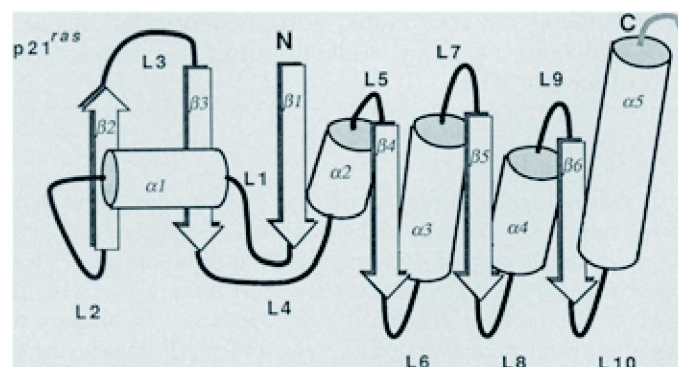


Figure 1: Topological structure of Ras proteins

The topological structure of Ras proteins: β -helices are represented by cylinders and α strands by arrows. The current assignments of the beginning and the ending residue numbers for each secondary structural element are; α 1 (1-9), α 2 (38-46), α 3 (50-58), α 4 (77-84), α 5 (110-117), β 1 (140-144), β 2 (15-26), β 3 (67-75), β 4 (87- 104), β 5 (126-137), β 6 (151-171), L1 (10-14), L2 (27-37), L3 (47-49), L4 (59-66), L5 (76), L6 (85-86), L7 (105-109), L8 (118-125), L9 (138-139), and L10 (145-150). A shaded string represents the COOH-terminal 18 residues that are lacking or disordered in the crystal structures. (Milburn et al., 1990)

The catalytical G domains that form the guanine nucleotide-binding pocket of all Ras proteins are highly conserved. They share 100% identity in the N-terminal lobe 1 (residues 1686) and have an identity of 90% in the C-terminal lobe 2 (residues 876171) (Buhrman, et al., 2011). The only region of significant difference between the Ras-isoforms is the C-terminal hypervariable region (HVR), which contains isoform-specific trafficking and membrane binding determinants. Each Ras-isoform therefore shares overlapping but distinct localizations at the plasma membrane and on intracellular organelles (Eisenberg et al., 2013).

Lobe 1, the effector lobe containing protein/protein interaction sites with effectors, includes the catalytic machinery with the active site for GTP hydrolysis (switch I, switch II, residues 10-17 of the P-loop) and a large part of the nucleotide binding pocket.

Lobe 2, on the other side of the molecule, contains the membrane-interacting portions of Ras and is called the allosteric lobe. It contains several affinity hot spots that interact directly with membrane components, the allosteric site and the allosteric switch components. The active site and allosteric site of Ras are connected together through helix 3 at one edge of the interlobal region and switch II at the other (Buhrman, et al., 2011; Buhrman, et al., 2010). Many residue differences between the Ras-isoforms outside the hypervariable C-terminal region can be found in the hot spots that interact with membranes of that lobe (Nussinov et al., 2013).

The third domain is the HVR, which is terminated by a CAAX box motif (Cox and Der, 2002). Here C is a cysteine, A must be an aliphatic amino acid (leucine, isoleucine, or valine) and X can be any amino acid. This motif, when coupled together with residues immediately upstream (e.g. cysteine residues modified by the fatty acid palmitate) comprises the targeting sequences for interactions with distinct membrane compartments inside the cell. It is also the recognition sequence for farnesyltransferase and geranylgeranyltransferase I, which lead to addition of farnesyl or geranylgeranyl isoprenoid to the cysteine residue of the CAAX motif (Wennerberg et al., 2005).

3.1.2 The GTPase cycle of Ras proteins

In general all Ras proteins function as molecular switches that cycle between inactive guanosine diphosphate (GDP)-bound and active guanosine triphosphate (GTP)-bound states (Figure 2; King et al., 2013). They become activated by binding GTP in response to receptor protein tyrosine kinases or other growth factor-dependent stimuli and both interact with and activate downstream targets in this GTP-bound active state (Figure 2; Scheffzek et al., 1997).

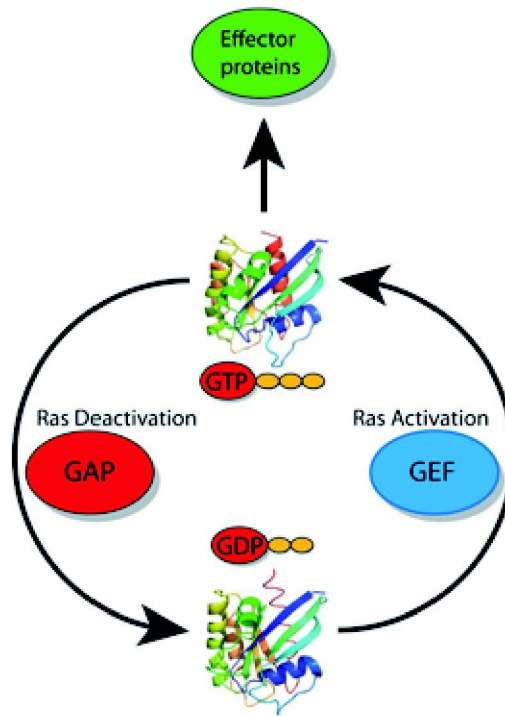


Figure 2: GTPase cycle

Ras cycles between a GTP-bound state (top) in which it interacts with downstream effector proteins, and a GDP-bound state (bottom) in which it is inactive. Different proteins regulate the activity of Ras. The activity of the proteins that activate Ras (called GEFs) and deactivate Ras (called GAPs) is also strictly controlled by the cells. (Hein et al., 2013)

Guanine-nucleotide exchange factors (GEFs) such as Son of sevenless (SOS) stimulate the guanine-nucleotide exchange, allowing GTP, more prevalent in the cell than GDP, to bind and thus activate Ras. This is necessary as Ras has no preference in binding GTP or GDP, therefore stimulating the guanine-nucleotide exchange by GEFs allow GTP to bind and subsequently activate the protein (Boriack-Sjodin et al., 1998; Scheffzek et al., 1997; Bos et al., 2007). Ras has only weak intrinsic GTPase activity and therefore the conversion back to its inactive state is dependent upon Ras GTPase-activating proteins (Ras-GAPs), closing the GTPase cycle (Bos et al., 2007; Donovan et al., 2002). Ras-GAPs increase the intrinsic GTP hydrolysis by several orders of magnitude and thus help to make Ras inactive (Scheffzek et al., 1997). Both GEFs and GAPs are usually multidomain proteins. As many of these domains are protein or lipid interaction domains it is likely that they serve as localization signals and/or as scaffolds for the formation of protein complexes (Bos et al., 2007).

3.1.2.1 Ras and its interaction with GEFs

All GEFs for Ras have a common ~250 amino acid CDC25 homology catalytic domain (the RasGEF domain) and an adjacent ~50 amino acid N-terminal Ras exchange motif (REM; the RasGEFN domain). Three main classes of RasGEFs (Sos, Ras-GRF, and RasGRP) exist and can be distinguished by additional flanking domains and motifs that facilitate their activation or possess additional catalytic functions. CDC25 homology domains possess the ability to concurrently activate other Ras family proteins. Links between Ras activation and the function of Ras and Rho family proteins are provided by the presence of separate Rho-specific GEF catalytic domains in Sos and Ras-GRF proteins. The N-termini of Sos proteins contain the CDC25 domain and additionally Dbl homology (DH; also called RhoGEF) and pleckstrin homology (PH) domains (Mitin et al., 2005). The tandem DHóPH domain cluster is a signature motif of Dbl family proteins, comprising the majority of GEFs for the Rho family of GTPases (Rossman et al., 2006). The GDP/GTP exchange on Rho GTPases is mediated by the catalytic DH domain, while the PH domain is responsible for modulating the activity of the DH domain e.g. by promoting membrane association, facilitating GTPase substrate binding, or by controlling intramolecular interactions. Thus, Sos proteins are capable to perform GEF catalytic activity on Ras and Rac GTPases (Mitin et al., 2005).

After activation of receptor protein tyrosine kinases a GEF such as Sos is transported from the cytoplasm to the activated receptor by adapter proteins such as Grb2 in a phosphotyrosine-dependent manner. The SH3 domains of Grb2 are bound to a proline rich region in the C terminus of Sos and this Grb2óSos complex interacts with phosphotyrosine residues on activated receptors via the SH2 domains of Grb2. Receptor activation results in an increase in the effective concentration of Sos in the vicinity of the plasma membrane localized Ras, facilitating the exchange of bound guanine nucleotide for free cellular guanine nucleotides (Boriack-Sjodin et al., 1998). The affinity of most small G proteins such as Ras for GDP/GTP is in the lower nanomolar to picomolar range. A slow dissociation rate of nucleotides with a half-life on the order of one or more hours is the direct consequence of this high affinity. In biological processes exchange of GDP for GTP and subsequent activation Ras occurs within minutes or even less. Therefore, the activity of GEFs is required for the exchange of GDP for GTP as GEFs accelerate the exchange reaction by several orders of magnitude (Vetter and Wittinghofer, 2001; Bos et al., 2007). GEFs modify the nucleotide-binding site in such a way that the nucleotide affinity is decreased which catalyzes the dissociation of the nucleotide from Ras. Thus, the nucleotide is released and subsequently replaced. The affinity of Ras for

GTP and GDP is similar and the GEF does not favour rebinding of GDP or GTP. Thus, the resulting increase in GTP-bound over GDP-bound is due to the approximately ten times higher cellular concentration of GTP compared to GDP (Bos et al. 2007). Distinct RasGEFs are capable to determine the membrane compartments in which Ras becomes activated as well as the effectors or downstream pathways that are utilized (Mitin et al., 2005).

The nucleotide binding site of Ras opens as a result of the displacement of Ras Switch 1, which is caused by the insertion of a helical hairpin formed by aH and aI of Sos when Sos binds to Ras. The insertion of helix aH into the Ras active site leads to the introduction of a hydrophobic side chain (Leu 938) which blocks magnesium binding, and an acidic side chain (Glu 942) which overlaps the side where the γ -phosphate of the nucleotide would otherwise be bound (Boriack-Sjodin et al., 1998).

Ras Glu 62 and 63 are crucial for its interaction with Sos: Although mutation of both negative charged glutamic acids to positive charged histidines had no effect on the stability of Ras-GDP complexes, the ability of mutants to be activated by the CDC25 domain of the GEF was severely compromised (Boriack-Sjodin et al., 1998).

3.1.2.2 Ras and its interaction with GAPs

In about 30% of human tumours, oncogenic mutations of Ras that lead to impaired intrinsic GTPase activity and insensitivity to GAPs are found. These changes result in an inability to switch off the transmitted signal. In unstimulated cells, WT Ras is found in the inactive (GDP) state due to the presence of the negative regulator GAP, while oncogenic Ras remains in the active (GTP) state (Scheffzek et al., 1997). Ras GAPs have a common ~250 amino acid catalytic domain, but otherwise exhibit no crucial sequence similarity or domain architecture in the sequences that flank this catalytic domain (Mitin et al., 2005).

Many parts of the Ras molecule play a role in its interaction with its GAP. Participants in the interaction include residues 10 to 16 of the phosphate binding (P-) loop, residues 30 to 37 of switch region I, 60 to 76 of switch region II and possibly residues 87 to 98 of helix a3 (Scheffzek et al., 1997).

Polar interactions (involving several water molecules) and van der Waals interactions build the partly hydrophobic interface of the complex between Ras and RasGAP and may explain why the oncogenic mutation Gln61Leu in Ras, which cannot hydrolyze GTP efficiently, has a higher affinity than the wild type for GAP-334 (Scheffzek et al., 1997).

While Ras is localized in the complex with its GAP, loop L4 and helix a2 in the switch II region are well defined. In contrast, in isolated Ras these structures are highly mobile. In the complex, residues 61 to 63 of L4 are arranged in a short 310 helix which precedes a2. Tyrosine-64 plays a major role in forming the polar contact between Ras and its GAP by contributing to the formation of the hydrophobic interface, consistent with the observation that it can be mutated to Phe but not to Glu without affecting the interaction. Switch II may be further stabilized by interactions between Glu62 or Glu63 of Ras and arginines of the GAP. Ras-mediated GTP hydrolysis is blocked if glutamine-61 is mutated to any amino acid other than Glu leading to tumour formation. Gln61 points toward the phosphate chain of the nucleotide in the complex with GAP-334 and is stabilized in its orientation by a hydrogen bond with the main chain carbonyl group of the invariant Arg789 (Scheffzek et al., 1997). In this stabilized transition state the nucleophilic attack of a water molecule on the γ -phosphate of GTP is possible, and thus this state is a requirement for the Mg^{2+} -dependent hydrolysis reaction (Vetter and Wittinghofer, 2001). Another important position in Ras is Gly12, which contacts the loop L1c region of GAP-334 at Arg789 in the complex via van der Waals interactions. This explains the block in GAP-accelerated GTP hydrolysis for Gly12 mutants. Although they bind to GAP with an affinity similar to wild type Ras, it appears from the structure that even replacement with alanine would be highly unfavourable, leading to steric clashes with the main chain of Arg789 and with the side chain NH₂ of Gln61, thus preventing proper hydrolysis of GTP (Scheffzek et al., 1997).

Therefore, the most frequently occurring oncogenic mutations in Ras proteins are missense gain-of-function mutations at one of three mutational hotspots: G12, G13 and Q61. They are considered to be defective in GAP-mediated GTP hydrolysis, resulting in an accumulation of constitutively GTP-bound Ras in cells. Ras can further be activated in cancer by loss of its GAPs (e.g. neurofibromin 1) or persistent receptor mediated activation of GEFs (e.g. Sos) (Hobbs et al., 2016).

The α -molecular switch model is based on the changes in conformation that occur upon hydrolysis of GTP to GDP in switch I (residues 30-40) and switch II (residues 60-76) (Milburn et al., 1990; Buhrman et al., 2011). In addition to this model, other structural features also need to be considered. In GTP-bound Ras there is an equilibrium between two distinct conformational states modulated by an allosteric switch mechanism (Buhrman et al., 2010). The Ras form that is predominately found under solution conditions used for in vitro hydrolysis rate measurements has a disordered active site, with switch II containing the

catalytic residue Q61. Its allosteric site is empty, which could explain the slow GTP hydrolysis rates measured for Ras in vitro (Buhrman et al., 2011). The other conformational state displays an ordered active site, with Q61 positioned near the catalytic centre and a shift in helix 3/loop 7 toward helix 4. It has been proposed that this is the active state in which intrinsic hydrolysis is somehow promoted by an allosteric modulator (Buhrman et al., 2010). In the crystals investigated, bound calcium acetate was found in the allosteric site, which mimicked the modulator during the experiment (Buhrman et al., 2010). In the complex of Ras with GAPs, which promotes hydrolysis of GTP, an ordered switch II region combined with a shift of helix 3 toward helix 4 is also found. The difference is the insertion of the arginine finger from RasGAP into the active site (Scheffzek et al., 1997; Buhrman et al., 2011).

3.1.3 The clinically most notable members of the Ras subfamily

The clinically most notable members of the Ras subfamily are Harvey-Ras (Hras), neuroblastoma-Ras (Nras), and 2 variants of Kirsten-Ras (Kras), Kras4a and Kras4b. The two variants of Kras are produced by alternative splicing from the same gene (McCubrey et al., 2006). The N-terminal catalytic domains (amino acids 16-165) of Hras, Nras and Kras are highly conserved (90-100% identical). Therefore, the Ras isoforms differ primarily with respect to the sequence of the hypervariable region (HVR), which contains the protein sequences necessary for Ras to associate with the inner leaflet of the plasma membrane, and in the types of posttranslational modifications that characterize each Ras isoform. The HVR comprises the minimal Ras anchor which comprises the carboxy-terminal CAAX motif in addition to a second signal, which can be a single palmitoylation site (C181) in Nras, two palmitoylation sites in Hras (C181 and C184) and a polybasic domain of six contiguous lysine residues in Kras (K175-K180) (Figure 3; Hancock, 2003).

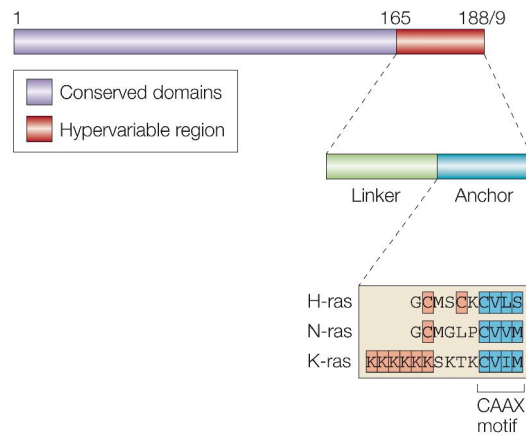


Figure 3: Domain structure of the Ras proteins

The N-terminal catalytic domains of all Ras isoforms are highly conserved. The C-terminal hypervariable regions (HVR) diverge significantly. The HVR comprises anchor sequences that also operate as Ras trafficking signals. The minimal Ras anchor comprises the carboxy-terminal CAAX motif in addition to a second signal. The second signal (in orange) can be a single palmitoylation site (C181) in Nras, two palmitoylation sites in Hras (C181 and C184) and a polybasic domain (six contiguous lysine residues) in Kras (K1756K180). In this figure Kras refers to the ubiquitously expressed Kras4B, and not to the alternatively spliced isoform Kras4A. The sequence between the anchor and the conserved domain constitutes the linker domain. (Hancock, 2003).

In order to be able to associate with cell membranes, Ras proteins undergo posttranslational modifications as they are synthesized as cytosolic precursors. In a first step, the protein farnesyl transferase, a cytosolic enzyme, attaches a farnesyl group to the cysteine residue of the CAAX motif. The farnesylated CAAX sequence is a localization motif for the ER and consequently Ras is targeted to the ER's cytosolic surface. Here, the AAX tripeptide is removed by an endopeptidase, Rce1 (Ras and a-factor converting enzyme). The -carboxyl group on the c-terminal farnesylated cysteine is then methylated by isoprenylcysteine carboxyl methyltransferase (Icmt). After methylation, Ras proteins move to the plasma membrane by one of two routes, depending on a second targeting signal located amino-terminal to the farnesylated cysteine. In the case of Hras and Nras, palmitoylation on cysteines in the HVRs occurs and they enter the exocytic pathway, trafficking to the plasma membrane via the Golgi. As Kras has a polybasic stretch rather than cysteine residues, it bypasses the Golgi and reaches the plasma membrane through direct vesicular transport from the ER (Hancock, 2003). Enrichment at the plasma membrane is subsequently maintained by an energy-driven mechanism that involves PDE (Schmick et al., 2014).

PDE , a 17 kDa protein, was discovered as a subunit of phosphodiesterase 6 (PDE6) in photoreceptor cells, where it plays a role in binding to lipid tails of the PDE6 catalytic

subunits. A hydrophobic cavity in the immunoglobulin-like sandwich fold of PDE binds the farnesyl anchor at the C terminus of Ras and other cargo (Ismail et al., 2011) independent of the nucleotide state. PDE is allosterically induced to relinquish its cargo by binding of Arl2-GTP or Arl3-GTP (Hanzal-Bayer et al., 2002; Ismail et al., 2011). In complex with Arl2-GTP, residues of PDE's hydrophobic pocket are shifted toward the inside of the pocket and clash with the farnesyl group (closed conformation). When a substrate such as Ras is bound rather than Arl2-GTP, the hydrophobic pocket is open (open conformation) (Ismail et al., 2011). Reduced expression of PDE has been shown to mislocalise Kras and Hras (Chandra et al., 2012).

The inner leaflet of the plasma membrane is exposing negatively charged phospholipids to the cytoplasm which offer binding sites for lysines, e.g. those in the polybasic stretch of the HVR of Kras. Such an electrostatic interaction strengthens the weak, lipophilic association to the plasma membrane conferred by prenylation (Schmick et al., 2015). The pericentriolar recycling endosome (RE) (Chen et al., 2010), which recycles cargo-containing vesicles from the plasma membrane, features negatively charged phospholipids on its outer (cytoplasm-facing) membrane leaflet. Kras that is displaced from PDE by Arl2 activity on perinuclear membranes has a high probability of encountering RE membranes. Due to a much lower dissociation rate from negatively charged surfaces compared with other perinuclear membranes, Kras rapidly dissociates from uncharged membrane surfaces until it becomes trapped on the RE (Schmick et al., 2015).

Kras is constantly depleted from the plasma membrane by spontaneous dissociation and vesicular internalization of the plasma membrane through endocytosis, phagocytosis, and pinocytosis. The rate of plasma membrane vesiculation is five times higher than the level of spontaneous dissociation of Kras from membranes (Schmick et al., 2014).

Until it reaches membranes to associate with, e.g. the endomembranes, Kras diffuses through the cytosol with no membrane association due to the loss of charge that occurs when vesicles are formed (Yeung et al., 2006). It equilibrates to all endomembranes in a highly dynamic way, constantly moving between the membranes via its soluble fraction. Equilibration occurs relatively slowly due to the large surface area of the endomembranes in comparison to the plasma membrane (Schmick et al., 2015).

Kras can escape from the endomembranes as a result of a competition between its low affinity endomembrane binding and the solubilising activity of PDE (Schmick et al., 2014; Chandra et al., 2012). Solubilised Kras diffuses faster through the cell lumen. Subsequently an Arl-2

mediated localized release of Kras from PDE and trapping of Kras at the recycling endosome takes place. Arl2 releases cargo from PDE in the perinuclear area (Ismail et al., 2011). The interaction between the G-protein Arl2/3 and PDE (Ismail et al., 2011) leads to a GTP-dependent release of its cargo, which can then either associate with (endo-) membranes or be rebound by free PDE. The presence of Arl2-GTP increases the dissociation rate of Kras 10-fold (Ismail et al., 2011). The recycling endosome is a compartment with negatively charged membrane surfaces (Chen et al., 2010), which in comparison to endomembranes are bound preferentially by Kras due to its polybasic stretch (Schmick et al., 2014). From the RE Kras is shuttled back to the plasma membrane via directed vesicular transport (Figure 4; Schmick et al., 2014).

Hras and Nras localize to the plasma membrane and the Golgi apparatus, respectively due to being irreversibly farnesylated and reversibly palmitoylated, resulting in distinct cellular responses for each isoform (Lorentzen, 2010). Leakage from the plasma membrane is countered via an acylation cycle that helps to maintain the distribution of palmitoylated and depalmitoylated Hras and Nras (Figure 4; Rocks et al., 2005).

In both cases, the strong hydrophobic interaction of the palmitoylated Ras with the membranes is weakened by cytosolic acyl protein thioesterases (APTs). These enzymes remove the S-palmitoylation from Ras proteins but leave the farnesyl moiety (Dekker et al., 2010). Absence of electrostatic interactions and depalmitoylation destabilize the membrane association and thereby increase the cytosolic fraction of Hras and Nras to speed-up equilibration to all membranes. This is further enhanced by the passive sequestration of soluble farnesylated Ras by the solubilisation factor PDE, which facilitates Ras diffusion in the cytoplasm (Chandra et al., 2012; Hanzal-Bayer et al., 2002; Ismail et al., 2011). The mechanism of PDE-mediated solubilisation followed by Arl-2-mediated localized release works in both the Kras-cycle and the Hras/Nras-cycle. Palmitoylation by palmitoyl transferases (PATs), which are localized to the cytoplasmic face of the Golgi apparatus increases the membrane affinity of H- and Nras by more than 100-fold as compared to only farnesylated Ras. Post-translational palmitoylation of depalmitoylated H- and Nras thus provides the means of trapping these molecules at the Golgi (Figure 4).

Due to depalmitoylating activity of APT 1/2, Nras and Hras dissociate from the plasma membrane, mono-palmitoylated Nras being faster than Hras with its two palmitoylation sites. The number of palmitoylation sites also means that Nras net palmitoylation is less stable (Rocks et al., 2010; Schmick et al., 2015). Depalmitoylation of Nras on secretory vesicles by

thioesterases is an additional factor diminishing palmitate stability and thus the membrane affinity of the protein. After losing its palmitate Nras can be solubilised by PDE and be trapped at the Golgi apparatus again, resulting in clearer steady-state Golgi localization in comparison to Hras (Rocks et al., 2010).

From the recycling endosome and the Golgi apparatus directed vesicular transport facilitates trapping and enrichment of Ras at the plasma membrane, thereby closing the Ras spatial cycles (Rocks et al., 2005; Rocks et al., 2010; Vartak and Bastiaens, 2010; Schmick et al., 2014; Figure 4).

Ras homolog enriched in brain (Rheb) is another member of the Ras family which is farnesylated and interacts with PDE (Hanzal-Bayer et al., 2002; Chandra et al., 2012; Schmick et al., 2014). It is part of the PI3K-mTORC1 pathway regulated by amino acid availability, energy status, and oxygen levels. One of the mechanisms by which amino acids positively regulate mTORC1 involves activation of the Rag GTPases, which recruit mTORC1 to lysosomes where it co-localizes with Rheb. In the case of glucose deprivation or hypoxia 5 α AMP-activated protein kinase (AMPK) activation due to an increase in AMP: ATP ratios negatively regulates mTORC1. AMPK then phosphorylates TSC2, priming it for additional activating phosphorylations by glycogen synthase kinase 3 (GSK3) and . This results in inhibition of Rheb-mTORC1 signalling as the GAP function of TSC is activated. AMPK is also a direct inhibitor of mTORC1 signalling as it phosphorylates Raptor, which is an adapter protein forming a stoichiometric complex with mTOR to regulate cell growth in response to nutrient and insulin levels (Mendoza et al., 2011).

Rheb has neither a polybasic sequence nor an additional palmitoylation site which would trap it in a specific membrane compartment. Therefore Rheb equilibrates relatively quickly over all endomembranes from the perinuclear area once it is released from PDE (Figure 4; Schmick et al., 2015).

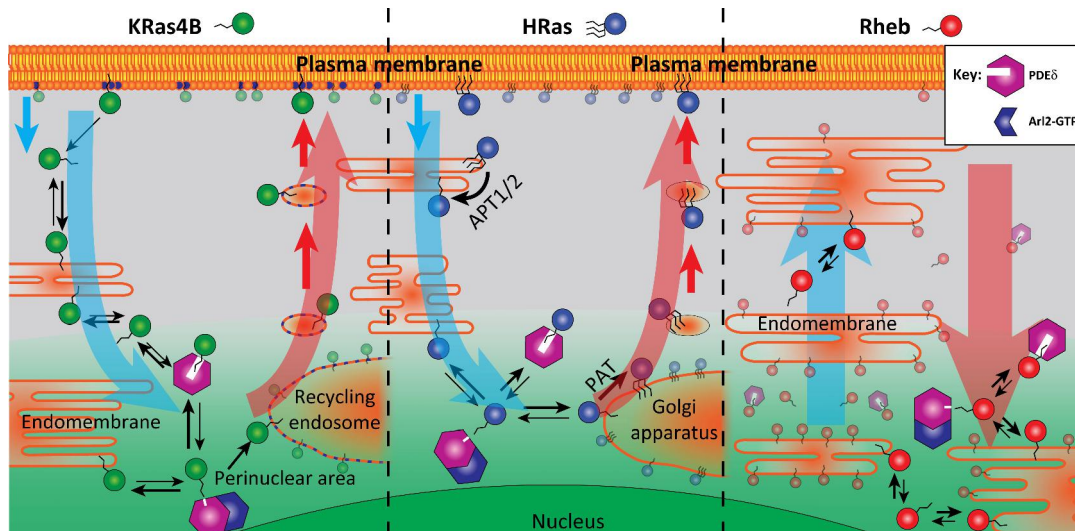


Figure 4: One delivery system to rule them all

Displacing farnesylated cargo from phosphodiesterase 6 (PDE δ) by Arl2 activity in the perinuclear area is responsible for enrichment of Kras4B (left) and Hras (middle) at the plasma membrane, as well as for perinuclear enrichment of Rheb (right).

Ras is displaced from membranes by vesiculation and spontaneous dissociation. Its dissociation into the cytosol is enhanced by a changed surface or lack of depalmitoylation by acyl protein thioesterase (APT) activity, where the solubilisation factor PDE δ enhances diffusional intracellular exploration. Farnesylated cargo can explore the perinuclear membranes for a trapping compartment as active disruption of the farnesyl-binding capacity of PDE δ by Arl2-GTP in the perinuclear area (green gradient) takes place. Palmitoylation by palmitoyl transferase (PAT) activity at the Golgi traps Hras by increasing its residence time on these membranes, as interaction with the negatively charged recycling endosome (RE) for Kras does. By directed vesicular export both Ras isoforms are displaced to the plasma membrane. Rheb is enriched in all perinuclear membranes by the PDE δ Arl2 delivery system and due to the lack of trapping on a vesicular transport compartment. The blue arrows denote the magnitude of entropic leakage from target membranes; red arrows represent the magnitude of the countering, energy-driven relocalisation processes. (Schmick et al., 2015)

3.1.4 Downstream effector signalling of Ras

During the 1980s a number of research groups reported several changes in cellular biochemistry that were caused by Ras proteins, but the precise mechanism underlying Ras δ function in cellular signalling remained to be determined. Over the years many studies have focused on finding the direct downstream signalling effectors that interact directly with Ras and mediate its various functions (Karnoub and Weinberg, 2008; Figure 5).

In 1993 the first interaction partner of Ras was identified, the Raf1 Ser/Thr kinase (Karnoub and Weinberg, 2008; Moodie et al., 1993; Warne et al., 1993; Zhang et al., 1993; Vojtek et al., 1993). Further characterization of Raf1 revealed that it signals through a pathway that

involves the mitogen-activated protein kinase (MAPK)/extracellular signal-regulated kinase (ERK) kinase (MEK), ERK1/2, and the E26-transcription factor proteins (ETS) (Wood et al., 1992; Leever and Marshall, 1992). In Ras biology MAPK signalling has been shown to be both sufficient and necessary for Ras-induced transformation of mammalian cell lines (Leever et al., 1994; Stokoe et al., 1994; Khosravi-Far et al., 1995; White et al., 1995; Karnoub and Weinberg, 2008). This signalling cascade became the prototype for a number of other pathways that signal from the plasma membrane towards the nucleus (Karnoub and Weinberg, 2008). The importance for aberrant Raf/MEK/ERK signalling in oncogenesis was established by the identification of B-Raf mutations in cancers such as melanoma or colon cancer that occur in non-overlapping frequencies with Ras mutations (Rajagopalan et al., 2002; Karnoub and Weinberg, 2008).

The p110 catalytic subunit of the class I phosphoinositide 3-kinases (PI3Ks) (Rodriguez-Viciana et al., 1994) and the guanine nucleotide-exchange factors for the Ras-like (RalA and RalB) small GTPases (Ral guanine nucleotide-dissociation stimulator (RalGDS) and RalGDS-like protein (RGL)) (Hofer et al., 1994; Kikuchi et al., 1994; Spaargaren and Bischoff, 1994) were identified as Ras effectors in 1994 (Karnoub and Weinberg, 2008). It was demonstrated that PI3K activity was required for Ras dependent transformation of NIH 3T3 cells (Rodriguez-Viciana et al., 1997). The signalling pathway of activated PI3K involves the Ser/Thr kinase AKT/protein kinase B and the transcription factor nuclear factor- κ B (NF- κ B), both of which have crucial roles in preventing anoikis and provide an explanation for the anti-apoptotic effects of Ras activation (Marte and Downward, 1997; Khwaja et al., 1997; Mayo et al., 1997; Karnoub and Weinberg, 2008). PI3K or Raf pathways alone were not sufficient to promote Ras transformation in human kidney epithelial cells, whereas activation of the RalGEF/Ral pathway did prove sufficient (Hamad et al., 2002). Another study showed prominent but distinct roles for the highly related RalA and RalB GTPases in countering apoptosis and regulating cellular proliferation (Chien and White, 2003; Karnoub and Weinberg, 2008).

Ras interacts with effectors like Raf or PI3K through the effector lobe, which is oriented toward the cytoplasm. The allosteric lobe on the other side interacts with the membrane and contains the Ras-GTP surface. GEFs like Sos or GAPs interact with Ras at the effector lobe and at the interface between the two lobes.

Other Ras effectors with diverse roles in cell physiology include phospholipase C- β (PLC β), T-cell lymphoma invasion and metastasis-1 (TIAM1), Ras interaction/interference protein-1

(RIN1), ALL (acute lymphoblastic leukaemia) 1 fused gene on chromosome 6 (AF-6) protein, and the Ras association domain-containing family (RASSF) proteins (Karnoub and Weinberg, 2008).

PLC is a direct effector of Ras (Kelley et al., 2001; Song et al., 2001) and its activation enables it to cleave PtdIns(4,5)P₂ into inositol-1,4,5- trisphosphate (Ins(1,4,5)P₃) and diacylglycerol (DAG), promoting the release of Ca²⁺ and the activation of PKC (Karnoub and Weinberg, 2008). PLC is also an upstream activator of the Ras/MAPK pathway as it contains a Cdc25 domain (Lopez et al., 2001).

The activity of the Ras effector TIAM1 has been shown to be required for Ras transformation (Malliri et al., 2002). AF-6 may participate in cytoskeletal activities downstream of Ras as it contains both microtubule- and actin-binding motifs (Ponting and Benjamin, 1996) and was shown to localize to adherens junctions and to associate with proteins that are involved in regulating cell polarity (such as ponsin and profilin) (Mandai et al., 1997). RIN1 and the RASSF proteins have reported tumour-suppressor activities and RIN1 was the first downstream effector of Ras that was shown to block Ras transformation (Han and Colicelli, 1995). RASSF proteins act as tumour suppressors although the detailed mechanism of action for RASSF proteins has not been fully discovered. RASSF kinases participate in a pathway that suppresses the activity of cyclin E and leads to cell cycle arrest and apoptosis as they associate with the mammalian sterile-20-like protein kinase-1 (MST1) and MST2 in *D. melanogaster*. Pro-apoptotic functions have been shown for RASSF1, RASSF2 and RASSF5 (Khokhlatchev et al., 2002; Vos et al., 2003; Vos et al., 2003a; Karnoub and Weinberg, 2008).

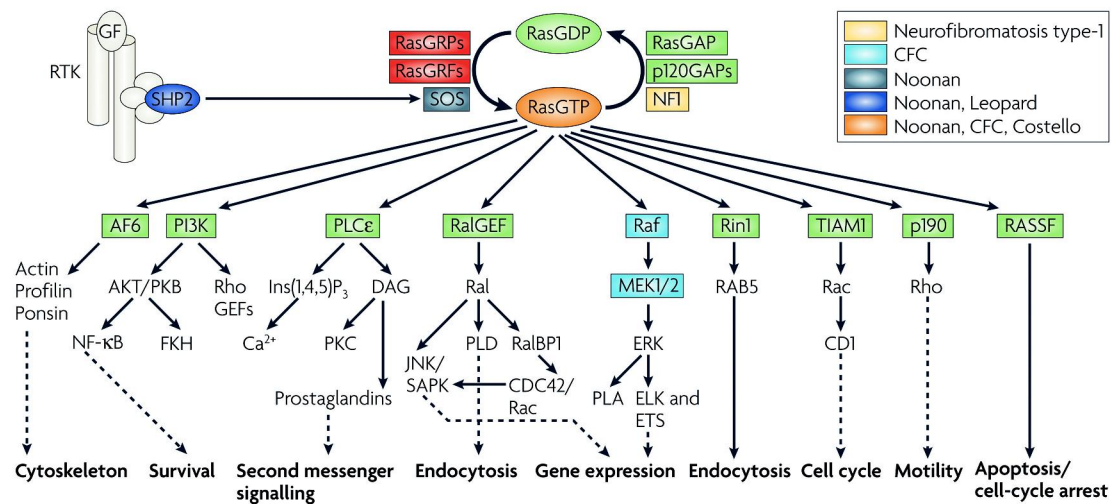


Figure 5: Ras signalling networks

Ras cycles between a GTP-bound state in which it interacts with downstream effector proteins, and a GDP-bound state in which it is inactive. A slow intrinsic GTPase activity cleaves off the γ -phosphate of active GTP bound Ras, leading to Ras functional inactivation and thus the termination of signalling. The activity of the proteins that activate Ras (GEFs) and deactivate Ras (GAPs) is strictly controlled by the cells. GAPs, such as p120GAP or neurofibromin (NF1), enhance the intrinsic GTPase activity and hence negatively regulate Ras protein function. Conversely, GEFs (also known as GTP-releasing proteins/factors, termed GRPs or GRFs), such as son of sevenless (Sos), catalyse nucleotide ejection and therefore facilitate GTP binding and protein activation. After stimulation of receptor Tyr kinase (RTK) by growth factors (GF) Ras is activated and recruited to the plasma membrane. Several signal-transduction cascades can be initiated by effector molecules that are engaged by activated Ras. Outputs shown represent the main thrusts of the indicated pathways. Ras activation can also occur in endomembrane compartments (endoplasmic reticulum and the Golgi). Activating mutations in the different components of the Ras/Raf/mitogen-activated protein kinase (MAPK) pathway are associated with the indicated developmental disorders.

AF-6, acute lymphoblastic leukaemia - 1 fused gene on chromosome 6; CD1, cadherin domain-1; CDC42, cell division cycle-42; ELK, ETS-like protein; ERK, extracellular signal regulated kinase; ETS, E26-transcription factor proteins; Ins(1,4,5)P₃, inositol-1,4,5-trisphosphate; JNK, Jun N-terminal kinase; MEK, mitogen-activated protein kinase/ERK kinase; NF- κ B, nuclear factor- κ B; PI3K, phosphoinositide 3-kinase; PKB/C, protein kinase B/C; PLA/C/D, phospholipase A/C/D; RalBP1, Ral-binding protein-1; RASSF, Ras association domain-containing family; Rin1, Ras interaction/interference protein-1; SAPK, stress-activated protein kinase; SHP2, Src-homology - 2 domain-containing protein Tyr phosphatase-2; TIAM1, T-cell lymphoma invasion and metastasis-1. (Karnoub and Weinberg, 2008)

In primary cells oncogenic Ras has been shown to induce senescence through activation of the p53/p21WAF1 and/or p16INK4A/Retinoblastoma (Rb) tumour-suppressor pathways (Serrano et al., 1997; Wei et al., 2003; Voorhoeve and Agami, 2003; Karnoub and Weinberg, 2008; Figure 6). Normal cells undergo cell-cycle arrest or senescence in response to hyperactive Ras signalling rather than unlimited proliferation or transformation. Moreover, the susceptibility of certain normal cells to Ras-mediated transformation seems to rely on prior inactivation of these tumour-suppressor pathways (Karnoub and Weinberg, 2008). Therefore, Ras activation in normal cells does not cause an initiation of tumourigenesis, but instead a halt in cell proliferation. This Ras induced senescence in normal cells can be explained by the oncogenic cooperation model proposed in 1983 (Land et al., 1983; Raley, 1983), as Ras-collaborating oncoproteins, like E1A, SV40 and E6/E7 are all well-known inactivators of the Rb and the p53 pathways (Karnoub and Weinberg, 2008).

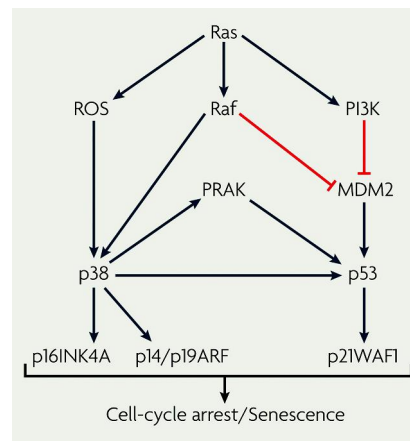


Figure 6: The tumour suppressor effect of Ras

Ras activation of p16 and p53 depend, in part, on the activation of the p38 mitogen-activated protein kinase (MAPK) pathway through unidentified mechanisms. Ras activation has been shown to cause elevated reactive oxygen species (ROS) levels, and ROS promote p38 activation. The Ras-induced Raf/MAPK pathway might feed into the p53 pathway by activating the p38-regulated/activated protein kinase (PRAK), which in turn phosphorylates and activates p53.

MDM2, murine double minute-2; PI3K, phosphoinositide 3-kinase; p14/19ARF, p14ARF in humans and p19ARF in mice. (Karnoub and Weinberg, 2008)

Whether cells become transformed or senescent in response to Ras activation is determined by p16, which appears to be the key factor in making this decision. High levels of Ras expression result in cell-cycle arrest due to an acute elevation of p16. However, moderate Ras activation allows Ras-induced transformation of cells as it does not induce an acute p16 response (Karnoub and Weinberg, 2008). It has been demonstrated in mice that in vivo

expression of oncogenic Kras at endogenous levels could cause cellular transformation (Tuveson et al., 2004; Johnson et al., 2001).

3.1.5 Kras

Kras is a protein consisting of 188/189 amino acids with a molecular mass of 21.6 kDa. It is the only isoform of the Ras family that is essential in mouse embryogenesis. Knockout of Kras is embryonic lethal at day 12-14, which is not the case for either Hras or Nras (Johnson et al., 1997).

Kras was first identified in the rat genome in 1981 (DeFeo et al., 1981) as a cellular homolog of the Kirsten transforming Ras sequence and was subsequently also found in the human and mouse genomes (Chang et al., 1982; Ellis et al., 1982). These studies revealed that Kras behaved similarly to the Src oncogene of Rous sarcoma virus (RSV), the origins of which were first reported in 1976 (Stehelin et al., 1976). Soon mutant alleles of Kras were discovered in human cancer cell lines including e.g. those of bladder and lung carcinoma (Der et al., 1982). These mutations did not arise from culturing the cancer cells in vitro - in 1984 mutant Kras alleles were found for the first time in lung cancer specimens (Santos et al., 1984; Nakano et al., 1984). Associations between particular types of human cancer and specific Ras oncogenes are known to exist (Karnoub and Weinberg, 2008).

Two copies of the Kras gene can be found in the human genome. One of them, Kras1, has been assigned to chromosome 6 (O'Brien et al., 1983) and is reported to be a pseudogene (McGrath et al., 1983); and the second, Kras2, resides on chromosome 12 (Sakaguchi et al., 1983). Kras also has two splice variants, Kras4A and Kras4B, arising from alternative mRNA splicing of exon 5 (fourth coding exon) of the Kras mRNA transcript (Carta et al., 2006; Pells et al., 1997). Exon 6 encodes the HVR at the C-terminus of Kras4B and remains untranslated in Kras4A. The two splice variants of Kras therefore differ only in four catalytic domain residues (151, 153, 165, and 166) and in their HVRs (Chakrabarti et al., 2016; Figure 7).

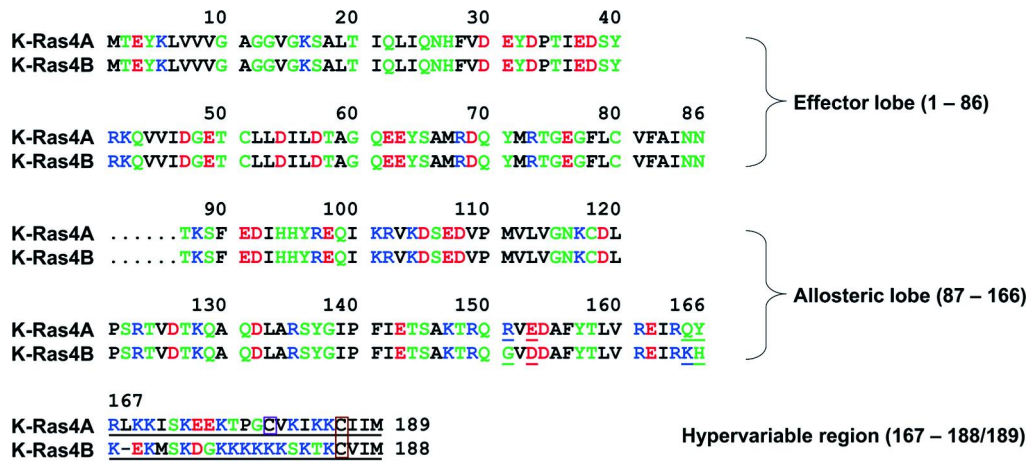


Figure 7: Multiple sequence alignment of the amino acids in the Kras4A and Kras4B proteins

In the sequence, hydrophobic, polar/glycine, positively charged, and negatively charged residues are coloured black, green, blue, and red, respectively. Underlined text indicates the non-identity of residues in the alignment. In the HVRs a purple box denotes the palmitoylated cysteine in Kras4A, and an orange-box indicates the farnesylated cysteines in Kras4A and Kras4B. (Chakrabarti et al., 2016)

Kras4A undergoes additional palmitoylation upstream of the CAAX motif whereas Kras4B shows no detectable palmitoylation (Hancock et al., 1989). In older studies it was hypothesized that Kras4A is a minor species in comparison to Kras4B (Jackson et al., 1994; Plowman et al., 2006; Normanno et al., 2009; Stone, 2011). However, a more recent study using splice variant-specific primers and antibodies could show that Kras4A and Kras4B mRNA transcript and protein are expressed at equal levels - or even higher levels of Kras4A can be found - in colorectal and bladder-derived tumour cell lines and in primary human colorectal adenocarcinoma tissues (Tsai et al., 2015; Chakrabarti et al., 2016). In colorectal cancers the ratio of Kras4A to 4B expression is commonly altered in favour of Kras4B, which may be due to a tumour-suppressive effect of the Kras4A isoform in colon adenomas that favours Kras4B expression (Luo et al., 2010). In cancer cells both splice variants are expressed (Plowman et al., 2006; Butz et al., 2004).

As the Kras4B gene product was the only Kras variant used in the present work it will henceforth be termed Kras.

3.1.6 Kras mutations and their impact in cancer

The Ras genes account for approximately 30% of all cancers in humans (Roberts and Der, 2007; Thumar et al., 2014). Kras is of particular interest, as its mutations account for nearly 86% of all Ras mediated cancers (van Hattum and Waldmann, 2014; Cox et al., 2014). In about 90% of pancreatic carcinomas and 40% to 50% of colorectal adenomas oncogenic

mutations leading to a permanently active Kras molecule can be found (Blum and Kluog, 2005; Blum et al., 2008; Vogelstein et al., 1988; Mitin et al., 2005).

Kras protein translation and expression is poor in comparison to e.g. Hras due to a high frequency of rare codons in the Kras DNA coding sequence (Lampson et al., 2013). As described earlier, high expression levels of activated Ras induce senescence rather than uncontrolled proliferation. But a cell with mutated Kras does not harbour the combination of an activated Ras protein with high expression of the mutated Ras protein due to Kras's low expression levels. Consequently, this cell will survive and other genetic events can take place in order to promote tumour progression (Hobbs et al., 2016).

In the case of Kras, the three mutation hotspots (G12, G13, Q61) show the following mutation frequency: Most mutations occur at G12 (83%), followed by G13 mutations (14%), while Q61 mutations are rare (2%). Between different cancer types the mutation frequency within Kras also exhibits significant differences. In colorectal adenocarcinoma (CRC) a relatively high frequency of G13 mutations can be found while in pancreatic ductal adenocarcinoma (PDAC) the dominating mutation is located at G12 and mutations of G13 and Q61 are exceptional. Therefore, it is likely that different Ras mutations may have different functional consequences and depending on the tissue of origin the properties that are crucial for their oncogenic functions vary (Hobbs et al., 2016). It has been shown that the Q61L mutation leads to reduced intrinsic hydrolysis and GAP sensitivity, as well as increased intrinsic nucleotide exchange while the G12V mutation leads to a loss of GAP sensitivity (Smith et al., 2013; Hobbs et al., 2016). In comparison to WT Ras the G13D mutant displays decreased GAP-mediated hydrolysis and an increased rate of intrinsic nucleotide exchange (Smith et al., 2013; Hobbs et al., 2016).

The mutations at different hotspots could be of great consequence for the clinical outcome and treatment of cancer patients. Initially, patients with Kras G12 or G13 mutations were excluded from anti-epidermal growth factor receptor (EGFR) therapy to treat CRC because EGFR is a receptor tyrosine kinase that is positioned upstream of Ras. The US Food and Drug Administration (FDA) reviewed this advice (Allegra et al., 2009) and a subsequent analysis has recommended that CRC patients with Kras G13 mutations would benefit from anti-EGFR therapy (Tejpar et al., 2012; Hobbs et al., 2016). However, another study concludes that CRC patients with any Kras mutation, including Q61 and A146, will not benefit from anti-EGFR therapy (Tran et al., 2015). There is thus still much work to be done to elucidate the

underlying mechanisms and thereby to determine in which cases anti-EGFR therapy is beneficial for patients and in which cases the relevant mutation status precludes any benefit.

The different amino acid substitutions at the mutation hotspots also appear to be of importance for cancer patient survival. For PDAC, different clinical outcomes for different Kras mutations have been described. It was demonstrated that Kras G12D and G12R mutations are a negative prognostic factor for patient survival (Ogura et al., 2013). Overall survival rates are increased when only Kras G12R mutations are present, whereas poor survival rates are associated with a mutation of Kras G12D (Hobbs et al., 2016). Improved survival could also be detected for patients with Kras Q61 mutations (Witkiewicz et al., 2015). Therefore, to determine the prognostic value of the mutation, it is necessary to consider cancer type, amino acid substitution and mutation site of each patient (Hobbs et al., 2016).

In PDAC the substitution found most frequently at codon G12 of Kras is G12D, followed by G12V. In contrast, in lung adenocarcinoma (LAC) the main substitution is G12C, which is rare in PDAC (3%) (Cox et al., 2014). The tissue-specific exposure to certain carcinogens could play a role in establishing these distinct frequencies and the different substitutions at one position may have different biological consequences, also in different Ras isoforms (Hobbs et al., 2016).

A model of progression has been established for the development of PDAC based on genomic analyses and molecular pathology studies. Kras mutations appear to contribute to its inception as activating mutations of Kras are found in most tumours of PDAC patients (>90%) (Kanda et al., 2012; Hwang et al., 2016). To accelerate the progression of PDAC other genetic alterations affecting CDKN2A, TP53 and SMAD4 cooperate with oncogenic Kras (Morris et al., 2010). In premalignant lesions associated with the pancreatic ducts, named pancreatic intraepithelial neoplasia (PanIN), the signature mutations of PDAC have been identified. PanIN exhibit alterations in their cellular architecture, such as mucinous cytoplasm, nuclear crowding and nuclear atypia (Hruban et al., 2001; Hwang et al., 2016). In mice, activation of oncogenic Kras in pancreatic epithelial cells is sufficient to initiate PDAC and PDAC progression can be accelerated by additional mutation of Trp53, Cdkn2a or Smad4, sharing many features of the human disease (Hingorani et al., 2005; Bardeesy et al., 2006).

Many human PDAC cell lines have been characterised in terms of molecular aberrations and cellular phenotype (Deer et al., 2010) and several pancreatic cell lines have been shown to be Kras-dependent in growth and survival (Singh et al., 2009). In some tumour types it could be

seen that acute inactivation of transforming oncogenes leads to cell-cycle arrest, differentiation or apoptosis. Therefore, it is sufficient to induce tumour regression in such cases by abrogating the function of individual oncogenic products. For cell lines gene expression signatures were established that can distinguish two groups of cells (Kras-dependent/ Kras-independent) after genes were identified that are specifically up regulated in Kras-dependent cells and are required for their viability (Singh et al., 2009). It has been possible to develop prognostic classifiers for patients and predictive biomarkers for drug response because the cell lines harbour a distinct set of mutations with corresponding transcription profiles (Hwang et al., 2016).

In the 1980s, it had already been found that most, if not all, malignant colorectal carcinomas arise from pre-existing benign tumours (adenomas) and that both hereditary and environmental factors contribute to the development of colorectal neoplasia by leading to genetic alterations (Fearon and Vogelstein, 1990). Even a small number of cells within a pocket of epithelial stem cells are capable of initiating the process of neoplasia by clonal expansion as it was found that adenomas arise from a single pocket in this way (Ponder and Wilkinson, 1986).

Thus, colon cancer develops in stages. After normal tissues have acquired certain mutations, they develop into hyperplastic epithelia and then into early adenomas. Early adenomas develop into intermediate and late adenomas, then into carcinomas with additional key gene mutations, activation of oncogenes, loss and gain of chromosomes, and/or chromosome amplifications (Fearon and Vogelstein, 1990). This development takes a long time, usually decades. The transition from colorectal carcinoma to a metastatic CRC can take another 2-3 years (Rao and Yamada, 2013).

Approximately 50% of colorectal carcinomas (Bos et al., 1987; Forrester et al., 1987) have been found to harbour (K) Ras gene mutations, which could also be found in adenomas > 1 cm in size but in fewer than 10% of adenomas less than 1 cm in size (Vogelstein et al., 1988; Farr et al., 1988). In a subset of colorectal tumours and adenomas with Ras gene mutations they may also be the initiating event. However, in most tumours they occur in cells of a pre-existing adenoma and are then responsible for the conversion of a small adenoma into a larger and more dysplastic one, through clonal expansion of the cell with the mutation (Fearon and Vogelstein, 1990).

In colorectal neoplasia a loss of specific chromosomal regions frequently occurs, usually involving only one of the two parental chromosomes present in normal cells. The gene

products encoded by the alleles that are lost are tumour suppressor genes and thus indirect suppression of neoplastic development is counteracted. This phenomenon of chromosomal losses in colorectal tumours was first detected in the early 1980s (Reichmann et al., 1981; Muleris et al., 1985).

In about 30% of colorectal adenomas and in 20%~50% of colorectal carcinomas allelic losses of chromosome 5q have been observed if the patients do not harbour polyposis (Vogelstein et al., 1988; Sasaki et al., 1989). This region contains the information for the APC gene. In cases where familial adenomatous polyposis was diagnosed and patients develop adenomas, allelic losses of chromosome 5q in the tumours are rare (Solomon et al., 1987; Vogelstein et al., 1988; Sasaki et al., 1989).

More than 75% of colorectal carcinomas, but hardly any adenomas at any stage, display loss of a large portion of chromosome 17p caused by chromosome loss or mitotic recombination (Vogelstein et al., 1988; Delattre et al., 1989). These 17p allelic losses can be associated with the progression of individual tumours from adenoma to carcinoma (Fearon et al., 1987; Vogelstein et al., 1988) which can be explained by the fact that the p53 tumour suppressor gene is encoded in that chromosomal region (Baker et al., 1989; Fearon and Vogelstein, 1990). In several CRC cases where loss of one 17p allele was present, mutations resulting in amino acid substitutions in p53 in the gene product of the remaining allele have been found (Baker et al., 1989; Nigro et al., 1989). The combination of loss of the wild type allele and point mutation of the other p53 gene appears to occur frequently in colorectal tumours (Fearon and Vogelstein, 1990).

Allelic loss of chromosome 18q can be found in more than 70% of colorectal carcinomas (Vogelstein et al., 1988, 1989; Delattre et al., 1989) and in almost 50% of late colorectal adenomas (Vogelstein et al., 1988). The tumour suppressor gene located in this region, termed Deleted in Colon Cancer (DCC), was identified in the early 1990s (Fearon et al., 1990) and encodes a protein with significant homology to the family of cell adhesion molecules (Fearon and Vogelstein, 1990). It appears to play a role in tumour development through alterations in normal cell-cell and/or cell-extracellular matrix interactions as it is normally expressed in the mucosa of the colon. However, in the majority of colorectal carcinomas its expression is either reduced or absent as a result of a loss of 18q or somatic mutations of the DCC gene (Fearon and Vogelstein, 1990).

A progressive development model of colon cancer and some of the key genetic changes associated with the stages of progression described above was proposed and presented in

1990 by Fearon and Vogelstein and given the name δ Vogelgramö (Fearon and Vogelstein, 1990). Here, the correlation between genetic/genomic changes and stages of colon cancer progression are depicted in a schematic way (Figure 8; Rao and Yamada, 2013).

In the early stages of colon tumour development, inactivation of the tumour suppressor Adenomatous polyposis coli (APC) is observed. Transition from early to intermediate adenoma is associated with activation of the Kras oncogene. When transition from intermediate to late adenoma occurs, genomic level changes, such as a loss of chromosome 18q together with a loss of the DCC gene, can be seen. At later stages, when the late adenoma becomes a carcinoma, a loss of tumour suppressor p53 and a gain of chromosome 8q can be observed. When a loss of chromosome 8p subsequently occurs, the tumour gains the ability to metastasize (Fearon and Vogelstein, 1990; Kinzler and Vogelstein, 1996; Grady, 2004; Rao and Yamada, 2013; Figure 8).

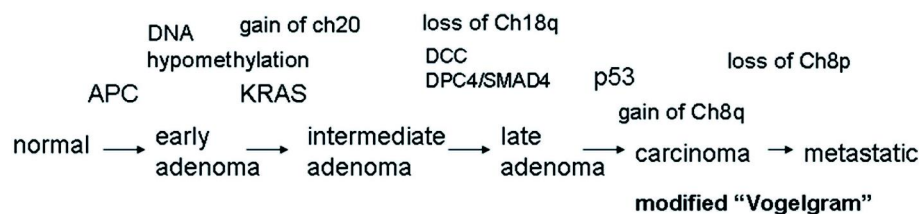


Figure 8: modified Vogelgram

The δ Vogelgramö (modified from the original in Fearon and Vogelstein, 1990). The original δ Vogelgramö (Fearon and Vogelstein, 1990) mapped loss of chromosome 5q, 12p, 18q, and 17p, and mutations on APC, Kras, DCC, and p53 in a sequential order of cancer progression. DNA hypermethylation was also mapped in the early adenoma stage. Gain of Chromosome 20, gain of chromosome 8q, loss of Chromosome 8p and mutation in DPC4/SMAD4 were added. (Rao and Yamada, 2013)

3.1.7 Inhibition of oncogenic Ras – The "undruggable" protein

Many efforts have been made to inhibit oncogenic Ras signalling due to its high potency as an oncogene and the frequent mutations occurring in various types of cancer. However, it has been proven to be almost impossible to target Ras proteins directly with small molecule inhibitors.

Ras proteins undergo isoform-specific lipophilic post-translational modifications, including irreversible farnesylation and reversible palmitoylation. In the past, attempts have been made to turn off oncogenic Ras signalling by inhibition of the farnesyl transferase through small molecules, the farnesyl transferase-inhibitors (FTIs), inhibiting the addition of the farnesyl-moiety to the C-terminus of Ras, which is necessary for its membrane affinity. However, in

the absence of farnesyltransferase activity Kras4b and Nras can be modified at the CAAX box motif by geranylgeranyltransferase-I-catalyzed addition of geranylgeranyl isoprenoid, and thus FTIs fail to effectively block the membrane association of the Ras isoforms most commonly mutated in cancer (Hobbs et al., 2016). Other approaches were targeting the prenylation and post-prenylation modifications as alternatives (Konstantinopoulos et al., 2007), but this led to toxic effects as the higher frequency of prenylation in membrane anchoring proteins necessitates higher active antitumor concentrations (Gysin et al., 2011). Inhibition of some postprenylation processing enzymes or of others like isoprenylcysteine carboxyl methyltransferase was not very successful either. The same is true for targeting the regulation of GDP/GTP exchange (Nussinov et al., 2013).

An alternative strategy focused on targeting components of the pathways downstream of Ras, e.g. Raf, MEK, Erk or PI3K. Drugs that target Raf kinase, such as PLX-4032, have not proved effective in tumours harbouring Ras mutations, though they do show some benefit in the treatment of melanoma caused by Braf mutations (Gysin et al., 2011). By turning off the Raf kinase with drugs, MAPK pathway activation can be triggered in some Ras mutants and the drug action is bypassed. Another strategy attempts to inhibit MEK in order to block the Ras-MAPK pathway. However, MEK inhibitors can uncouple a negative ERK feedback loop, activating PI3 kinase via EGFR and other tyrosine kinases. Consequently, multiple therapy combinations are required. The different drugs have to be combined to avoid alternative routes by drug resistant mutations and the protein targets within the pathways must be selected carefully to have minimal impact on normal cell function (Nussinov et al., 2013).

Colorectal carcinomas in particular are treated with antibodies that block the EGF receptor. This therapy is successful provided Kras is not oncogenically mutated as it is downstream of the receptor.

3.1.8 The principle of oncogene addiction

Cancers can be divided into oncogenic Kras-dependent and -independent (Singh et al., 2009). This Kras status is helpful in forming a prognosis for the therapy and survival of the patient.

In some tumour types it could be seen that acute inactivation of transforming oncogenes leads to cell-cycle arrest, differentiation or apoptosis. Therefore, it is sufficient to induce tumour regression in such cases by abrogating the function of individual oncogenic products. These observations can be explained by a concept proposed in 2000 by Bernard Weinstein termed 'oncogene addiction' (Weinstein, 2000). Essentially it is this: Inhibition of a specific

oncogene can be sufficient to stop the progress of the neoplastic phenotype because some tumours rely on one single dominant oncogene for growth and survival despite their different genetic lesions which are a typical feature of cancer (Torti and Trusolino, 2011).

To explain the mechanism of oncogene addiction three models which take the cancer specific properties of the cells into account have been proposed. These are the theories of genetic streamlining, oncogenic shock and synthetic lethality, each of which has been experimentally validated and all of which are useful in explaining different aspects of oncogene addiction (Torti and Trusolino, 2011; Figure 9).

Genetic streamlining

The genetic streamlining theory postulates that cancer cells inactivate non-essential pathways during tumour evolution as a consequence of constant selective pressure caused by the tumourigenic process and the tumour microenvironment. In this way, dominant, addictive pathways are not surrogated by compensatory signals. Upon abrogation of dominant signals, there is a collapse in cellular fitness as these cells can no longer cope with sudden changes in the composition of the surrounding stroma or inhibition of any pathway still active in the cancer cell. Consequently, the cells experience cell-cycle arrest or apoptosis. In cancer cells there is only a small number of functionally active, self-sufficient transducers present, whereas a relatively large number of inactive and functionally neutral pathways can be found as a consequence of chronic oncogenic signalling. The inactivation can take place at transcriptional and biochemical levels after genetic drift. The result is a limited subset of operational signalling nodes and the absence of buffering circuits, making the cells in oncogene addiction state vulnerable, particular if abrupt changes occur (Torti and Trusolino, 2011).

Oncogenic shock

The oncogenic shock model proposes that addictive oncoproteins, such as RTKs, are able to simultaneously trigger pro-survival and pro-apoptotic signals. Under normal conditions the pro-survival signals dominate over the pro-apoptotic outputs. However, if the addictive receptor is blocked (e.g. by drugs), the activity of the survival pathway will decline rapidly and the death-inducing signals will accordingly be dominant. These signals tend to last longer and this will eventually lead to apoptosis (Torti and Trusolino, 2011).

Synthetic lethality

Gene A is in a synthetically lethal relationship with gene B when loss of one or the other is still compatible with survival, but loss of gene products/ activity of both A and B is lethal for the cell (Kaelin, 2005). Inactivation of pathway A would have no effect on cell viability because of the existence of pathway B, which at some point converges on a common substrate or effector, thereby acting in a compensatory manner. If pathway B is also blocked, it is no longer able to compensate for the loss of pathway A and the common downstream biochemical function is lost. Consequently, the cancer cells will go into cell cycle arrest or apoptosis (Torti and Trusolino, 2011).

The concept of synthetic lethality can also be implemented for dominantly acting oncogenes, particularly for Kras, which is mutated in many human cancers and considered to be undruggable. To abrogate its tumour promoting activity, the inhibition of its putative synthetic lethal partners was considered. Many groups identified different synthetic lethal interactors of Kras (Torti and Trusolino, 2011). It was found that the serine/threonine kinase STK33 is selectively required in Kras mutated cancer cells of different tissues to maintain viability (Scholl et al, 2009). An additional finding was that inactivation of distinct proteins, like the tyrosine kinases SYK, RON, and integrin b6, could induce epithelial-mesenchymal transition and apoptosis in Kras-dependent cells (Singh et al, 2009; Torti and Trusolino, 2011).

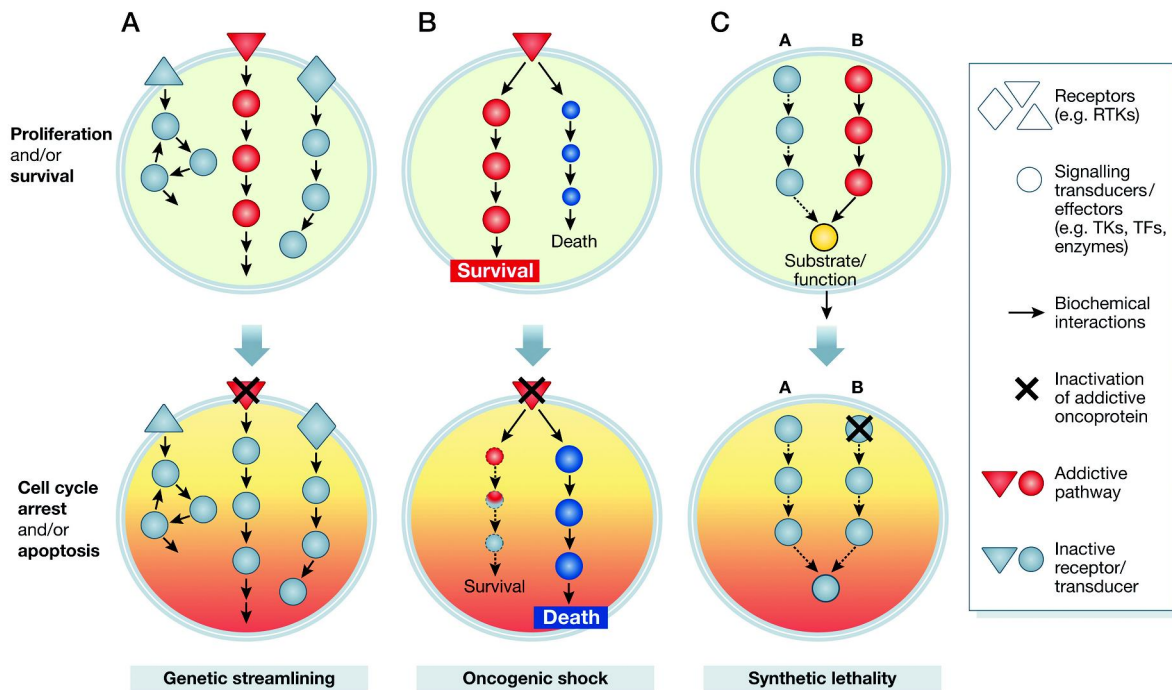


Figure 9: The three models of oncogene addiction

The ‘genetic streamlining’ theory (A) postulates that non-essential pathways (top, light grey) are inactivated during tumour evolution, so that dominant, addictive pathways (red) are not surrogated by compensatory signals.

In the ‘oncogenic shock’ model (B), addictive oncoproteins (e.g. RTKs, red triangle) simultaneously trigger pro-survival and pro-apoptotic signals (top, red and blue pathway, respectively). Blockade of the addictive receptor (dashed lines, bottom) subverts this balance in favour of death-inducing signals, which tend to last longer and lead to apoptotic death.

Two genes are considered to be in a synthetic lethal relationship (C) when loss of one or the other is still compatible with survival but loss of both is fatal. (Torti and Trusolino, 2011)

3.1.9 Another way to target Ras – small molecule PDE δ inhibitors

It may not be possible to target Ras directly with small molecule inhibitors but it has been demonstrated that PDE δ is important for maintaining the spatial organization of Ras family proteins (Chandra et al., 2012).

In 2013 a small molecule, Deltarasin, was identified. It has a benzimidazole-based lead structure and mimics a farnesyl moiety, which is used to bind to the farnesyl-binding pocket of PDE δ with high affinity. Therefore, this molecule has been shown to be a potent inhibitor of PDE δ and to lead to redistribution of Kras from the plasma membrane to endomembranes when applied to cells (Zimmermann et al., 2013). Through the use of fluorescence lifetime imaging microscopy (FLIM) assays, it was demonstrated that Deltarasin induces a loss of

interaction between PDE and Rheb. It also inhibits growth of a Kras-dependent pancreatic cancer cell line (PancTu1) in vitro and of subcutaneous human PancTu1 tumour cell xenografts transplanted into immunodeficient mice treated with the compound, but has no such effects in xenografts derived from Kras-independent cell lines (Zimmermann et al., 2013). Ras induced proliferation via MAPK pathway is thus impaired as the fraction of active Ras at the plasma membrane decreases (Zimmermann et al., 2013). A promising inhibitor to target Ras, Deltarasin has one drawback: there is only a small therapeutical window between onset of specific effect and onset of general cytotoxicity.

A second compound, named Deltazinone 1, was found one year later and also binds PDE with nanomolar affinity. Deltazinone 1 is based on a pyrazolopyridazinone scaffold and blocks the prenyl-binding pocket of PDE by binding to it competitively (Papke et al., 2016). Deltazinone 1 is less toxic for cells than Deltarasin, but when applied to mice it is metabolized within two hours, limiting its therapeutic application.

Both inhibitors block the binding pocket of PDE by mimicking farnesylated proteins, thereby preventing a proper cellular localization of Ras proteins.

3.2 Organoids as a new model system

Although they are generally used in preclinical cancer research, there is increasing evidence that 2D monolayers are not the most appropriate system to test the efficacy of drugs as they do not accurately reflect the biological complexity of a tumour. 2D cultures lack the complex stroma-cancer interactions that can be cell-cell and cell-matrix interactions. The architecture of the tissue and gradients in oxygenation, nutrition and pH are also missing, all of which are present in tumours in vivo. This is the most probable explanation for the fact that drugs which pass preclinical in vitro testing in 2D cultures later fail in patients (Zeeberg et al., 2016).

In the case of cancers like the pancreatic ductal adenocarcinoma (PDAC) the tumour's microenvironment is an important factor for metastatic spread, therapeutic resistance and carcinogenesis in general (Zeeberg et al., 2016).

Three-dimensional (3D) cultures have several advantages over 2D monolayers and could therefore constitute a better model as they more precisely reflect the bio-mechanical properties and structural design of the tumour (Zeeberg et al., 2016). Not only response of cells to growth factors and therapeutic treatment, but also the growth dynamics of the cells in general differ in 3D models in comparison to 2D models (Coleman et al., 2014).

Since the 1970s normal cells and their malignant counterparts can be kept in 3D culture using a semi-solid matrix including components like collagen, laminin and fibronectin so that epithelial cells can develop cell-matrix interactions simulating the basement membrane and polarized structures forming cell-cell contacts (Hwang et al., 2016). Comparison of the expression profiles of cells grown in 2D or 3D cultures revealed that cell-matrix interactions have a great impact on gene expression (Zschenker et al., 2012; Ghosh et al., 2005; Ridky et al., 2010; Hwang et al., 2016).

In the last decade an alternative in vitro 3D model for tissues has been developed. Termed organoids, these represent a relatively new cell culture model system that is closer to the in vivo situation than standard cell culture systems. Organoids are 3D multi-cellular structures that originate from self-renewing and organ-specific stem or progenitor cells that give rise to differentiated cells. This generates a cluster of different types of cells that is reminiscent of an organ in several aspects. Organoids can be derived from many organs and species and provide an accessible 3D system outside the organism in which cellular signalling can be studied in the presence of a near in vivo environmental niche (Jung et al., 2011; Barker et al., 2010; Huch et al., 2013; Sato et al., 2009; Sato et al., 2011). The homeostatic environment of the normal tissue stem cells is mimicked and the organoid cultures are able to self-renew while remaining genetically stable and being expanded long-term (Sato et al., 2011; Huch et al., 2015).

4 Objectives

The major goal of this project was to study the effect of small molecule PDE inhibitors on (K) Ras localization in space and time in order to confirm that PDE inhibition results in Ras relocalisation from the plasma membrane towards the endomembranes.

Therefore, this work investigates whether human cancer cells from different tumour origins or murine small intestine organoids are affected by the PDE inhibitor Deltarasin and a new PDE inhibitor called Deltazinone 1. The readout will be the localization of (K) Ras in space and time. In addition it will determine whether any differences between Kras-dependent and -independent cell lines in Ras localization after PDE inhibition exist. The overall goal is to ascertain whether PDE constitutes a valid target for inhibiting oncogenic Kras-dependent signalling through interference with Kras localization, and to confirm that PDE inhibition results in Ras relocalisation from the plasma membrane towards the endomembrane system.

5 Material

5.1 Cell lines used

A431 (ATCC® CRL-1555)

ATCC American tissue culture collection

DiFi

PancTu1

MDCK

Platinum E

5.2 Antibodies

5.2.1 Primary antibodies for Western Blots

antibody	host	dilution	company
Tubulin clone B-5-1-2	mouse, monoclonal	1:1:000	Sigma
Pan Ras EPR 3255	rabbit, monoclonal	1:1000	Abcam
GAPDH	mouse	1:1000	Calbiochem

Table 1: Primary antibodies for Western Blots

5.2.2 Secondary antibodies for Western Blots

antibody	host	dilution	company
rabbit IgG IRDye 680RD	goat	1:10000	LiCor
mouse IgG IRDye 800CW	goat	1:10000	LiCor

Table 2: Secondary antibodies for Western Blots

5.2.3 Primary antibodies for Immunofluorescence

antibody	host	dilution	company
Human lysozyme	rabbit, polyclonal	1:200	Dako
Pan Ras	mouse, monoclonal	1:200	Calbiochem
Pan Ras EPR 3255	rabbit, monoclonal	1:200	Abcam
Chromogranin A	rabbit polyclonal	1:100	Abcam
Villin	rabbit polyclonal	1:100	Pierce

Table 3: Antibodies for Immunofluorescence

5.2.4 Secondary antibodies for Immunofluorescence

antibody	host	dilution	company
mouse IgG Alexa Flour 488	rabbit	1:1000	Invitrogen
mouse IgG Alexa Flour 488	goat	1:1000	Invitrogen
rabbit IgG Alexa Flour 546	goat	1:1000	Invitrogen

Table 4: Secondary antibodies for Immunofluorescence

5.3 Materials and Media for cell culture

Blasticidin	Invitrogen
DMEM high glucose (#P04-03600)	PAN Biotech Inc.
DMEM high glucose without phenol red (#P04-01163)	PAN Biotech Inc.
DMEM high glucose without phenol red without HEPES (#P04-01158)	PAN Biotech Inc.
DMSO	Serva
DPBS (#P04-36500)	PAN Biotech Inc.

Fetal calf serum (FCS) (#P30-0402)	PAN Biotech Inc.
L-Glutamine 200 mM (#P04-80100)	PAN Biotech Inc.
Non-essential amino acids 100x (MEM NEAA) (#P08-32100)	PAN Biotech Inc.
Penicillin (10,000 U/ml)/Streptomycin (10 mg/ml) (#P06-07100)	PAN Biotech Inc.
Puromycin	Invitrogen
OptiMem	Invitrogen
Trypsin-EDTA solution (#P10-023100)	PAN Biotech Inc.
Bottles and dishes to culture cells	Sarstedt

5.4 Transfection

Effectene (#301427)	Qiagen
Fugene HD (#E2312)	Promega Corp.
Lipofectamine 2000 (#11668-019)	Invitrogen

5.5 Oligonucleotides

All oligonucleotides were purchased from MWG Eurofins as unmodified DNA Oligos.

5.5.1 Primer for LIC

- LIC Cre-pBABE fw

43bp; Tm: >75°C

5' CCA GTG TGG TGG TAC GTA CGC CAC CAT GGC CAA TTT ACT GAC C

- LIC Cre BABE rev

53bp; Tm: 74.1°C

5' GAC CAC TGT GCT GGC GAA TTT CAC AGA TCT TCT TCA GAA ATA
AGT TTT TGT CC

5.5.2 Primer for sequencing

- IRES_r
20bp ; Tm: 57.3°C
5'→3' CCT CAC ATT GCC AAA AGA CG
- IRES_f
20bp ; Tm: 57.3°C
5'→3' TGG CTC TCC TCA AGC GTA TT
- pBABE3'
21bp ; Tm: 57.9°C
5'→3' ACC CTA ACT GAC ACA CAT TCC
- pBABE5'
17bp ; Tm: 52.8°C
5'→3' CTT TAT CCA GCC CTC AC
- SV40proF
20bp ; Tm: 57.3°C
5'→3' TAT TTA TGC AGA GGC CGA GG
- pCAG-Cre-5714F
23bp ; Tm: 60.6°C
5'→3' GGC GAC ACG GAA ATG TTG AAT AC
- pCAG-Cre-725 re
19bp ; Tm: 58.8°C
5'→3' GTA ACG CGG TCA GTC AGA G
- pCAG_Cre 570-f
16bp ; Tm: 54.3°C
5'→3' CAG CCA ATC AGA GCG G

- pCAG_Cre1889 r
22bp ; Tm: 65.8°C
5'→3' CAA CTT GCA CCA TGC CGC CCA C
- pCAG_F_primer
20bp ; Tm: 57.3°C
5'→3' GCA ACG TGC TGG TTA TTG TG
- B_glob-pA_R
20bp ; Tm: 53.2°C
5'→3' TCT TTT TCC CTC TGC CAA AA
- M13_pUC_rev pr
23bp ; Tm: 58.9°C
5'→3' CCT GTG TGA AAT TGT TAT CCG CT
- Amp r primer
20bp ; Tm: 57.3°C
5'→3' ATA ATA CCG CGC CAC ATA GC
- pBR322ori F pri
20bp ; Tm: 57.3°C
5'→3' AAA GAT ACC AGG CGT TTC CC
- Cre 151 r
26bp ; Tm: 66.4°C
5'→3' CCG GCA AAC GGA CAG AAG CAT TTT CC
- Cre 851 F
22bp ; Tm: 65.8°C
5'→3' TGG CCT GGT CTG GAC ACA GTG C

- Primer Cre 70f
22bp ; Tm: 62.1°C
5'3' ATG GAC ATG TTC AGG GAT CGC C
- Primer Cre 670f
20bp ; Tm: 61.0°C
5'3' TCT GGT GTA GCT GAT GAT CCG AAT

5.5.3 Primer for genotyping

- 10136_59
20bp ; Tm: 57.3°C
5'3' GCA AAG GTC GCA TTT CCA TG
- 5812_1
18bp ; Tm: 56.0°C
5'3' TTA TTG ATC CGC GCC TGG
- 1281_1
20bp ; Tm: 59.4°C
5'3' GTG GCA CGG AAC TTC TAG TC
- 1281_2
20bp ; Tm: 55.3°C
5'3' CTT GTC AAG TAG CAG GAA GA
- 2240_31
20bp ; Tm: 59.4°C
5'3' ACG TCC AGA CAC AGC ATA GG
- 10137_62
22bp ; Tm: 60.3°C
5'3' ACA CAC TGT CTT CCT TAC CCT G

- 1260_1
20bp ; Tm: 59.4°C
5'3' GAG ACT CTG GCT ACT CAT CC
- 1260_2
21bp ; Tm: 63.7°C
5'3' CCT TCA GCA AGA GCT GGG GAC
- 10138_63
25bp ; Tm: 61.3°C
5'3' GTA CAT CTG TAG TCA CTG AAT TCG G
- 10138_64
21bp ; Tm: 59.8°C
5'3' AAG TAG TTG GGG ATG TCG TCG
- 10139_60
21bp ; Tm: 57.9°C
5'3' ACC CAA AAT TGC TCC TGT ACG
- 10139_67
21bp ; Tm: 61.8°C
5'3' CAG TAA CAG GAC CAC AAG GGC

5.6 Animal resources, organoid preparation and organoid culture

5.6.1 Mice

C57/BL6 NTac WT02 born 2nd week 2015, died 16th of June 2015

C57/BL6 Kras mTFP G12D Het F16 3L/R born 24th of November 2015, died 16th of June 2015

5.6.2 Material and Media for organoid culture

70µM cell strainer (#352350)	BD Falcon
Advanced D-MEM/F-12 (#12634028)	Life Technologies
B 27 (#17504044)	Life Technologies
Glutamax (#35050038)	Life Technologies
GSK3 inhibitor (#CHIR99021)	Sigma
Hepes (#15630056)	Life Technologies
Hexadimethrine bromide (Polybrene) (#107689)	Sigma Aldrich
Mouse EGF (#)	Peprtech
Mucasol® (#60442)	Merz Hygiene GmbH
Matrigel (#356231)	BD Corning
N-Acetyl-L-Cysteine (#A9165 ó 5g)	Sigma Aldrich
Nicotinamid (#N0636-100g)	Sigma Aldrich
Noggin conditioned medium	Sato and Clevers, 2013
Penicillin Streptomycin (#15140122)	Life Technologies
Rhokinase inhibitor (#Y-27632)	Hölzel biotech
R-Spondin conditioned medium	Sato and Clevers, 2013
Surgical instruments	Gebrüder Martin GmbH & Co. KG
TrypLE (#12604013)	Life Technologies
Recovery Solution (#354253)	BD Corning
Wnt3a conditioned medium	Sato and Clevers, 2013
24 and 48 well plates for suspension cells	Sarstedt
FEP Tube	Roth
Glass bottom dishes	Greiner
Super frost slides	Roth

5.7 Bacteria

XL10---Gold® Ultracompetent cells (#200314)

Agilent Technologies (amplified and provided by J. Luig and L. Rossmannek)

5.8 Plasmids

5.8.1 Eukaryotic Vectors

- pCAG Cre (5583)
- EGFP Cre (5780)
- pcDNA3.1 (1206)
- pcDNA3.1 Cre #7 (5621)

5.8.2 Viral Vectors

- pBABE puro (2227):
- pBABE puro Cre #8 (5861)
- pBABE puro Cre # 20 (5632)

5.9 Media for Bacteria

Lysogeny broth 1% (w/v) Tryptone; 0.5% (w/v) yeast extract; 1% NaCl; pH 7.0; autoclaved

LB-Agar Lysogeny broth with 1.5% (w/v) agar and 100 g/ml Ampicillin or 50 g/ml Kanamycin

SOC-Medium 2% (w/v) Tryptone; 0.5% (w/v) yeast extract; 10mM NaCl; 2.5mM KCl; 10mM MgSO₄; 10mM MgCl₂; 20mM Glucose

5.10 PFA preparation

5.10.1 4% PFA in PBS

To prepare 4 %PFA in PBS, 2 g PFA powder were diluted in 45 ml H₂O. To increase the pH 10 1 1 N NaOH were added. The mixture was heated up to 65°C for 10-20 min and mixed every 2 min. After complete salvation of the powder 5 ml of 10x PBS were added and the liquid was pressed through a sterile filter (pore size 45 μm). PFA was stored at 4°C or as frozen aliquots and protected from light to avoid decomposition of the polymer.

5.10.2 4% PFA in PME

To prepare 4 %PFA in PME, 2 g PFA powder were diluted in 50 ml PME buffer. The mixture was heated up to 65°C for 10-20 min and mixed every 2 min. After complete salvation of the powder PFA was stored as frozen aliquots and protected from light to avoid decomposition of the polymer. It is recommended to use it fresh!

5.11 Commercial Material and Kits

Roti Mount Aqua (#2848.2)	Roth
100mM dNTP Set (#10297-117)	Invitrogen™ Life Technologies
2-log DNA ladder (#N3200)	New England Biolabs Inc
5x T4 DNA Ligation Buffer (#46300-018)	Invitrogen™ Life Technologies
BigDye® Terminator sequencing kit (#4337455)	Invitrogen™ Life Technologies
Bovine serum albumin (BSA) (20 mg/ml) (#B9000)	New England Biolabs Inc.
Calf intestinal phosphatase (CIP) (10,000 U/ml) (#M0290)	New England Biolabs Inc.
CutSmart™ Buffer (#B7204)	New England Biolabs Inc.
DNA clean and concentrator™ kit (#D4004)	Zymo Research Corporation
Herculase II Fusion Enzyme (#600677)	Agilent Technologies Inc.
High-fidelity (HF®) restriction endonucleases	New England Biolabs Inc.
Jung Tissue Freezing Medium (#14020108926)	Leica Biosystems
NucleoBond® finalizer (#740519)	Macherey-Nagel
NucleoBond® Xtra Midi/Maxi EF Kit (#740422)	Macherey-Nagel

NucleoSEQ (#740523)	Macherey-Nagel
Restriction endonucleases	New England Biolabs Inc.
Roti®-Prep Plasmid Mini Kit (#HP29)	Carl Roth GmbH
T4 DNA Polymerase (#18005-025)	Invitrogen® Life Technologies
TE-EF and H2O-EF	Macherey-Nagel
Zymoclean™ Gel DNA Recovery Kit (#D4001)	Zymo Research Corporation
Quick DNA Universal KIT (#D4068)	Zymo Research Corporation
Eosin Solution 1% in H2O (#3137.1)	Roth
Hem alum solution acid acc. to Mayer (#T865.1)	Roth

5.12 Inhibitors

cOmplete, Mini, EDTA-free Protease

Inhibitor Cocktail Tablets (#04693159001)	Roche
Odyssey Infrared Imaging System blocking buffer (#927-40000)	LI-COR Biosciences GmbH
Phosphatase Inhibitor Cocktail 2 (#P5726)	Sigma-Aldrich®
Phosphatase Inhibitor Cocktail 3 (#P0044)	Sigma-Aldrich®
Protease Inhibitor Cocktail Tablets (#04693132001)	Roche Diagnostics

5.13 Standards

2-log DNA ladder (50µg/ml)	NEB (#N3200)
Protein-Standard	Bio-Rad Laboratories Inc Precision Plus Protein™ Dual Colour Prestained standard (#161-0374)

5.14 General chemicals

-Mercaptoethanol	SERVA Electrophoresis GmbH
Acetic acid conc.	
Acetone	Fluka

Ammonium persulfate (APS)	SERVA Electrophoresis GmbH
Ampicillin sodium salt	SERVA Electrophoresis GmbH
Bromophenolblue	Sigma-Aldrich®
BSA (bovine Serum albumin)	Applichem
Dimethyl sulfoxide (DMSO)	SERVA Electrophoresis GmbH
Dithiothreitol (DTT)	Fluka® Analytical
Ethanol (EtOH)	J.T.Baker
Ethylenediaminetetracetic acid (EDTA)	Fluka® Analytical
Glycerol	GERBU Biotechnik GmbH
Hoechst 33287 (10mg/ml)	Sigma
Isopropanol	J.T.Baker
Kanamycin sulfate	GERBU Biotechnik GmbH
Magnesium chloride (MgCl ₂)	Merck KG/J.T.Baker
Methanol (MeOH)	AppliChem GmbH
N,N,N',N'-Tetramethylene-diamine (TEMED)	Sigma-Aldrich®
Para-formaldehyde (PFA)	Serva
Sodium chloride (NaCl)	Fluka® Analytical
Sodium dodecyl sulfate (SDS)	SERVA Electrophoresis GmbH
Sodiumhydroxide (NaOH)	
Tris-base	Carl Roth GmbH
Tris-HCl	J.T.Baker
Triton X-100	SERVA Electrophoresis GmbH
Tween 20	SERVA Electrophoresis GmbH
UltraPure® Agarose (#16500-500)	Invitrogen® Life Technologies

Chemicals that are not listed were purchased from Applichem, Fermentas, Gibco, Merck, Roth or Sigma-Aldrich.

5.15 Buffer

10xDNA-sample buffer	0.1M EDTA, 50% glycerol, 0.1% (w/v) Orange G
RIPA-lysis buffer	50mM Tris pH7.5; 5mM Na ₂ EDTA, 0.1% (w/v) SDS; 0.5% (w/v) Sodium Deoxycholat; 1% (w/v) NP-40; 150mM NaCl
1xPBS	138mM NaCl; 2.7mM KCl; 10mM Na ₂ HPO ₄ ; 1.8mM KH ₂ PO ₄ ; pH7.4 (with HCl)
5xSDS-loading buffer	60mM Tris-HCl pH6.8; 2% (w/v) SDS; 25% (v/v) Glycerol; 0.1% (w/v) bromophenolblue; 14.4mM - mercaptoethanol
1xSDS-running buffer	192mM Glycine; 25mM Tris; 0,1% (w/v) SDS
Separating gel buffer	1.5M Tris-HCl (pH 8.8)
Stacking gel buffer	0.5M Tris-HCl (pH 6.8)
1xTAE buffer	40mM Tris/Acetate (pH7.5), 20mM NaOAc, 1mM EDTA
1xTBS	50mM Tris; 150mM NaCl; pH 7.4 (with HCL)
1xTBS-T	50mM Tris; 150mM NaCl; pH 7.4; 0.1% Tween 20
WB-Transfer buffer /Tank Blot	192mM Glycine; 25mM Tris; 20% (v/v) Methanol

5.16 Devices and expendables

ōVortex Genie 1ō touch mixer	Scientific Industries
1.5 mm 10-well combs	Bio-Rad Laboratories, Inc.
1.5 mm glass plate system for western blots	Bio-Rad Laboratories, Inc.
4-well LabTek® chambers No. 1.0	Nalge Nunc International
8-well LabTek® chambers No. 1.0	Nalge Nunc International
AutoFlow NU-4750 Water Jacket CO ₂ Incubator	Integra Biosciences
BioRad Power Pac HC	Bio-Rad Laboratories, Inc.
Cell scraper 16 cm 2-Pos.-blade (#83.1832)	Sarstedt AG und Co.

Centrifuge 5415R	Eppendorf
Centrifuge 5810R	Eppendorf
Centrifuge 5702R (Rotor A-4-38)	Eppendorf
Sorvall RC6+ (Rotor F13-14x50cy and Rotor SLA-1500)	Thermo Scientific
Concentrator plus	Eppendorf
Vapo.protect PCR machines / thermo cycler	Eppendorf
Cryostat CM 3050S	Leica Microsystems
Eppendorf safe lock tubes (0.5/1.5/2/5 ml)	Eppendorf
Falcon tubes (15/50 ml)	BD Falcon™
Heatable magnetic stirrer öIKMAG®RCTö	IKA®Labortechnik
Heating block öQBD4ö	Grant Instruments
Incubation box for western blots	Li-Cor® Biosciences
Incubator Shaker Series I26	New Brunswick Scientific
Innova 4000 Incubator Shaker	New Brunswick Scientific
MilliQ water, Millipore Advantage A	Millipore
Mini and Midi agarose gel chamber	Carl Roth GmbH
Molecular Imager Gel Doc XR	Bio-Rad Laboratories, Inc.
Nanodrop® ND-1000 spectrophotometer	Peqlab Biotechnologie GmbH
NUAIRE™ Cellgard class II biological safety cabinet	Integra Biosciences
Odyssey Infrared Imager	Li-Cor® Biosciences
Parafilm® Pechiney Plastic Packaging	
Pipetboy acu	Integra Biosciences
Research, Research Plus and Reference pipettes	Eppendorf
Safe ImagerĤ	InvitrogenĤ
Safegrip® nitril gloves	Süd-Laborbedarf GmbH

Sarstedt serological pipettes (5/10/25 ml)	Sarstedt
SDS-electrophoresis chamber - Mini-Protean System	Bio-Rad Laboratories, Inc.
Surgical disposable scalpel (No. 11, No.21)	Braun Melsungen AG
Thermomixer comfort	Eppendorf
Tissue culture plates	BD Falcon™
Whatman filter paper	Fisher Scientific

5.17 Microscopes

Leica TCS SP5	Leica Microsystems
Leica TCS SP8	Leica Microsystems
Leica DMIRB	Leica Microsystems

6 Methods

The exact composition of buffers and solutions can be found in part 5 of the thesis.

6.1 Culture of cell lines

Material:

- DMEM complete medium (10% FCS, 2mM L-glutamine, 1% NEAA)
- FCS (fetal calf serum)
- L-glutamine
- NEAA (non-essential amino acids)
- TE (Trypsin / EDTA)
- 1x PBS

All cell lines used are maintained in T75 culture flasks in DMEM (Dulbecco's modified Eagle medium) supplemented with 10 % FCS, 2 mM L-glutamine and 1 % NEAA at 37°C, 5 % CO₂ in a humidified incubator. Before cells become confluent they are detached from their culture dish, diluted and seeded into a new flask, culture dishes or LabTeks to perform experiments with them. Confluency might transform adherent cells that grow in general as a monolayer by growth inhibition and the system would therefore not be controllable and predictable anymore. First old growth medium is removed from the cells and they are washed with 1x PBS to get rid of old cells and serum leftovers. By adding TE and incubation for a few minutes at 37°C cells are detached from their culture dish afterwards. Trypsin is a digestion enzyme which none specifically recognizes positive amino acid residues (Arg, Lys). EDTA works as a chelator and complexes bivalent cations (Ca²⁺). Adhesion is strongly dependent on Ca²⁺ and TE therefore facilitates a proper detachment of the cells. Finally addition of fresh growth medium inactivates Trypsin. The detached cells are resuspended, counted if necessary and seed into new culture dishes in the desired amount.

6.2 Freezing and thawing cell lines

Material:

- cryo-medium (DMEM; 10% FBS; 10% DMSO)
- DMEM complete medium
- 1x PBS
- TE (Trypsin / EDTA)
- NALGENE® Cryo 1°C freezing box

Freezing cells:

In order to generate reproducible results for this work and future work it is necessary to keep backups from all cell lines which are used for cell culture work for long-term storage.

1 or 2 days before freezing them cells are seeded in T75 flasks. When they reach a confluency of 70% they are treated as if passaging them as described above, counted and collected by spinning down. The resulting cell pellet is resuspended in cryo-medium to a concentration of 2×10^6 cells/ml. Cryo-medium contains DMSO as a cryo-protectant to prevent intracellular ice crystal formation, hence enhancing cell viability during freezing and thawing processes. 500 μ l (10^6 cells) of the resulting cell suspension is applied per cryo vial, stored on ice and transferred to a freezing box. The vials are stored in the freezing box at -80°C for at least 1 day. Freezing boxes allow for controlled freezing rates of $1^\circ\text{C}/\text{min}$ and are stocked with sponges filled with isopropanol. For long-term storage the frozen aliquots are moved to a -150°C freezer.

Thawing cells:

Frozen vials are thawed as quickly as possible in a 37°C water bath to avoid toxic effects of DMSO on the cells. The thawed cell suspension is transferred to a falcon tube containing 10ml DMEM complete medium. After centrifugation (1200rpm, 6minutes) and removing the medium to eliminate DMSO the pellet is resuspended in fresh medium and transferred to an appropriate culture dish or flask with the appropriate amount of DMEM complete medium. The next day medium is exchanged and replaced with fresh DMEM complete medium to remove traces of DMSO.

6.3 Transfection of cell lines

Transfection is the process of bringing extrinsic DNA into eukaryotic cells. Transient transfections only last a few days if for example a plasmid is used that will not be integrated into the DNA of the transfected cell. If the transfection is permanent because the extrinsic DNA is integrated into the genome of the transfected cell the transfection is stable. For this work only transient transfections were done. Depending on the cell line different techniques can be used.

6.3.1 Transfection with Fugene

Material:

- Fugene
- DMEM complete medium
- Plasmid DNA

Transfection with Fugene is done with PlatE cells to bring Plasmids in that need to be packed into viral particles. The amount of DNA to Fugene chosen for transfection is 1:3.

For a 10cm dish 663.3µl DMEM complete medium and 30µl Fugene are applied in a 1.5ml Eppendorf cup. After 5 minutes incubation at room temperature 10µg Plasmid DNA is added and the mixture vortexed immediately. The transfection mix is incubated for 15 minutes at room temperature and afterwards drop-wise applied onto the cells in the dish. The dish is gently swirled to ensure uniform distribution of the transfection complexes. It is not necessary to change the medium after transfection but medium is changed the day after transfection.

6.3.2 Transfection with Effectene

Material:

- Effectene
- Enhancer
- Buffer EC
- DMEM complete medium
- Plasmid DNA

This method is used to transfect MDCK cells for Ras relocalisation studies. 4-well LabTeks with 2×10^4 cells/ml medium are transfected with 50µl of transfection mix per well. As

Effectene Reagent enables transfection in the presence of serum without lowering transfection efficiencies DMEM complete medium is used.

One day before transfection 2×10^4 cells per well in 1 ml DMEM complete medium are seeded in 4-well LabTeks. They are incubated under their normal growth conditions. The following day they should be 40-80% confluent. For transfection with Effectene Reagent in 60 mm dishes the recommended amount of DNA is 0.562 g. The typical ratio of DNA to Enhancer is 1 g DNA to 8 l Enhancer. In this work a ratio of 1µg DNA to 7.5µl Enhancer is used. The ratio of Effectene Reagent to DNAóEnhancer mixture determines the overall charge of the EffecteneóDNA complex. A slightly net positive charge is required for optimal binding of EffecteneóDNA complexes to negatively charged groups on the cell surface. It is recommended using a DNA: Effectene ratio of 1 g DNA to 25 l Effectene Reagent in 60 mm dishes as a starting point for optimization of transfection. The ratio used in this work is 1µg DNA to 20µl Effectene Reagent. Removal of transfection complexes is not necessary. The day of transfection 0.8µg DNA dissolved in TE buffer is diluted with the DNA-condensation buffer, Buffer EC to a total volume of 180 l. 6µl Enhancer is added and the solutions are mixed by vortexing for 1s. The mixture is incubated at room temperature for 5min and afterwards spun down for a few seconds to remove drops from the top of the tube. 16µl Effectene Transfection Reagent are added to the DNA-Enhancer mixture and mixed by pipetting up and down 10 times. The samples are incubated for 10 min at room temperature (15ó25°C) to allow transfection-complex formation. The transfection complexes are added drop-wise onto the cells in the LabTeks. The LabTeks are gently swirled to ensure uniform distribution of the transfection complexes.

6.3.3 Transfection with Lipofectamine 2000

Material:

- Lipofectamine 2000 (Invitrogen)
- OptiMem (Sigma)
- DMEM complete medium
- Plasmid DNA

All transient transfections in Panc-TUI cells are performed with Lipofectamine 2000. Cells are seeded in 4-well Labtek chambers (2×10^4 cells in 1 ml medium per well) in DMEM complete medium one day before they are transfected. For transfection 480 l OptiMem are mixed with 4 g Plasmid DNA in a 1.5ml Eppendorf tube. In a second tube, 480 l OptiMem

and 9.6 μ l Lipofectamine are applied. Both tubes are incubated for 5 min at room temperature, pooled and further incubated for 20 min at room temperature to allow transfection-complex formation. 120 μ l are applied to each well of the 4-well Labtek chamber.

6.4 Preparation of small intestine organoids

Material:

- mouse
- surgical instruments
- 1x PBS
- Petri dishes
- Falcon Tubes
- Syringes and needles
- cover slip (haemocytometer)
- aluminium foil
- 5mM EDTA in PBS
- 70 μ m sieve (BD Falcon)
- Organoid normal medium (adv DMEM/F12-ENR = +EGF+Noggin+RspoI)
- 24-well-plates for suspension cells
- Matrigel
- Rho Kinase Inhibitor

The mouse the organoids are to be prepared from is killed by cervical dislocation while still in the animal facility and immediately brought to the laboratory. Its limbs are fixated with tape to a metal stand and the fur of the belly is sterilized with 70% ethanol. The dead mouse is cut open and the stomach pushed a bit upwards with forceps. The first cut is made between stomach exit and beginning of the small intestine. Now the small intestine is pulled out with forceps and a second cut is made just before the colon starts. The small intestine is directly flushed with 20 ml (or more) ice-cold PBS to clean it from faeces and put in a petri dish filled with PBS on ice. While holding it with forceps fat and pancreatic tissue are removed to avoid contaminations with pancreatic ducts. The small intestine is flushed with ice-cold PBS in a syringe. After cutting it in 5 cm long pieces one piece at a time is put on aluminium foil together with a bit PBS. While holding it with forceps it is cut open with one cut in order to have a straight line. With a cover slip (from haemocytometer as they are thicker and have rounder edges) the Villi are scratched off 3 to 5 times and the small intestine is opened to

have a flat layer. The opened and Villi-free small intestine is transferred into a 50 ml Falcon tube with 20 ml ice-cold PBS and shaken thoroughly. PBS is renewed and the small intestine is washed in this way at least 6 times to get rid of the Villi until there is almost no foam anymore. It is transferred into 20 ml of ice-cold 5mM EDTA in PBS and rotated 30 minutes on a wheel at 4°C in the cold room to digest the tissue and release the crypts. During incubation on the wheel the scraped Villi are checked under the microscope and a 50 ml Falcon tube is prepared with a 70µm sieve which is pre-wet with ice-cold PBS. One drop of the suspension is checked under the microscope before filtration to compare with. The intestine with released crypts is filtered through the sieve. Villi will stay in the sieve and crypts will go through. There should not be more than 10% villi in the crypt fraction (flow through). In case not enough crypts came off the intestine is kept for a second digestion and filter round. Another drop of suspension is checked under the microscope, this time after filtration. There should be enrichment in crypts and only few Villi. To pellet the crypts, but not single cells, the suspension is centrifuged at 700 rpm for 5 min at 4°C (Eppendorf 5810R). After aspiration of the supernatant the pellet is resuspended in 1 ml normal organoid medium and seed in two dilutions (undiluted and 1:5). Per well of a pre-warmed 24-well plate for suspension cells two matrigel drops of 20 to 25µl each are seed. For seeding in 1.5ml tubes 80µl matrigel and 40µl cell suspension are mixed by carefully pipetting up and down. This amount is sufficient for putting 6 drops in 3 wells. The plate is afterwards put upwards down in an incubator at 37°C for 5 to 10 minutes that the matrigel can solidify. 500 µl medium are added to each well, containing Rho kinase Inhibitor for the first week to prevent cell death through anoikis in dissociated stem cells. Medium is changed after 3 days and organoids are passaged the first time after 7 to 14 days. After the first passage it is changed to normal medium.

6.5 Culture of small intestine organoids

Material:

- Advanced DMEM F12 (2 mM Glutamax, 10 mM HEPES, 100 U/ml Penicillin, 100 µg/ml Streptomycin) Basal culture medium
- Pasteur Pipettes
- FBS
- 24-well-plates for suspension cells
- Falcon tubes or 5 ml Eppendorf tubes
- Matrigel basement membrane matrix, growth factor reduced (GFR), phenol red-free

- N-Acetylcysteine, 500× stock (Sigma-Aldrich): 81.5 mg/mL in distilled water (500 mM)
- B27 supplement, 50x (Life Technologies)
- 0.1% BSA in PBS: 0.1% (w/v) BSA in PBS, sterile filtered with 0.22 mm filter
- Murine recombinant EGF, 10,000x stock, 500 mg/mL in 0.1% BSA/PBS (PeproTech)
- Noggin conditioned medium, approx. 10x stock, ~1µg/mL Noggin
- Rspo1 conditioned medium, approx. 10x stock, ~10 mg/mL Rspo1
- Complete crypt culture medium: Basal culture medium with B27 supplement (1×), and 1 mM N-acetylcysteine, 50 ng/mL EGF, 100 ng/mL Noggin, 1 mg/mL R-spondin

Small intestine organoids can be passaged the first time 7-14 days after seeding and are subsequently passaged from that on every 5-7 days. After preparation of all media that are needed, fire-polishing and FBS-coating of Pasteur pipettes the culture medium is removed and 1 ml ice-cold basal medium is put per well instead. The Matrigel is gently broken up by pipetting with a p1000 pipette and the organoids are resuspended in basal culture medium in this way. For washing the organoid suspension is transferred to a 15 ml tube or to a 5 ml Eppendorf tube. 9 ml / 4 ml ice-cold basal medium are added and the organoids are centrifuged at 700 rpm at 4°C for 2 minutes (1500 rpm for single cells). After centrifugation a pellet consisting of living organoids will be visible with a bigger almost transparent matrigel layer on top containing dead cells. The supernatant is removed to a degree that approximately 2 ml will be left in the tube which includes the Matrigel pellet. The organoids are disrupted using a fire-polished Pasteur pipette (decreased diameter) by thoroughly pipetting up and down for 6 to 10 times. This will dissociate the organoids by mechanically breaking them into smaller pieces and to get rid of released dead cells and single cells they are washed again with 8 ml / 3 ml ice-cold basal culture medium. To dissolve the matrigel the tube is inverted 3 to 5 times before centrifugation at 1200 rpm for 5 minutes at 4°C. The supernatant is removed nearly completely and the pellet remaining in the tube has a volume of approximately 15-20 µl. The organoids are mixed with fresh matrigel and seeded on a fresh 24-well plate. For passaging 1 well of an old plate 1 to 6 the pellet is mixed with 240 µl matrigel and divided to 6 wells on the new plate, 2 drops per well. The 24-well-plate is turned around and put in an incubator at 37°C for 5 minutes that the matrigel can solidify. By applying this hanging drop method the organoids will localize to the periphery of the Matrigel drop and not stick

near the bottom of the plate. 500 µl complete medium are added per well and the organoids are incubated at 37°C for 5 to 7 days. Medium is changed after 3 days.

6.6 Freezing and thawing organoids

Material:

- Advanced DMEM F12 (2 mM Glutamax, 10 mM HEPES, 100 U/ml Penicillin, 100 µg/ml Streptomycin) Basal culture medium
- cryo-medium (Complete crypt culture medium; 20% FBS; 10% DMSO)
- 24-well-plates for suspension cells
- Matrigel basement membrane matrix, growth factor reduced (GFR), phenol red-free
- N-Acetylcysteine, 500× stock (Sigma-Aldrich): 81.5 mg/mL in distilled water (500 mM)
- B27 supplement, 50x (Life Technologies)
- Murine recombinant EGF, 10,000x stock, 500 mg/mL in 0.1% BSA/PBS (PeproTech)
- Noggin conditioned medium, approx. 10x stock, ~1µg/mL Noggin
- Rspo1 conditioned medium, approx. 10x stock, ~10 mg/mL Rspo1
- Complete crypt culture medium: Basal culture medium with B27 supplement (1×), and 1 mM N-acetylcysteine, 50 ng/mL EGF, 100 ng/mL Noggin, 1 mg/mL R-spondin
- Cryo vials
- NALGENE® Cryo 1°C freezing box

Freezing organoids:

In order to generate reproducible results for this work and future work it is necessary to keep backups from all organoids which are used for long-term storage.

After preparation of all media that are needed the culture medium is removed and 1 ml ice-cold basal medium is put per well instead. The Matrigel is gently broken up by pipetting with a p1000 pipette and the organoids are resuspended in basal culture medium in this way. For washing the organoid suspension of the number of wells (typically 4 to 6 wells) that are to be frozen is transferred to a 15 ml tube. Up to 9 ml ice-cold basal medium are added (total volume 14 ml) and the organoids are centrifuged at 700 rpm at 4°C for 2 minutes. After centrifugation a pellet consisting of living organoids will be visible with a bigger almost

transparent matrigel layer on top containing dead cells. The supernatant is removed to a degree that approximately 2 ml will be left in the tube which includes the Matrigel pellet. The organoids are a little bit disrupted using a p1000 pipette by pipetting up and down. This will dissociate the organoids by mechanically breaking them into smaller pieces and to get rid of released dead cells and single cells they are washed again with 8 ml ice-cold basal culture medium. To dissolve the matrigel the tube is inverted 3 to 5 times before centrifugation at 1200 rpm for 5 minutes at 4°C. The supernatant is removed nearly completely and the pellet remaining in the tube is dissolved in cryo medium. Per well of organoids that was used 1 ml of medium is added to the falcon tube. The organoid suspension is put into Cryo Vials and they are subsequently transferred into a NALGENE® Cryo 1°C freezing box to be stored for 2 days at -80°C. For long-term storage the frozen aliquots are moved to a -150°C freezer.

Thawing organoids:

Frozen vials are thawed as quickly as possible in a 37°C water bath to avoid toxic effects of DMSO on the cells. The thawed organoid suspension is transferred to a 15 ml falcon tube containing 10 ml basal culture medium. After centrifugation (700rpm, 5 minutes, 4°C) and removing the medium to eliminate DMSO the pellet is resuspended again in 10 ml fresh basal culture medium and centrifugation is repeated. After removal of the supernatant 100-200 µl matrigel are added and the organoids are seeded on a pre-warmed 24-well plate and incubated for 5 minutes at 37°C in the incubator. When the matrigel is solid 500 µl complete crypt culture medium are added to each well.

6.7 Retroviral infection of organoids

By retroviral transduction gene over expression and knockdown can be achieved in organoids. The technique can also be used in combination with chemical and biological inhibitors or activators or applied to organoids derived from pre-established mutant mouse lines (Koo et al., 2013). This protocol explains in single steps retrovirus production, organoid cell preparation, infection of the organoids and drug selection after infection.

Material:

- Advanced DMEM F12 (2 mM Glutamax, 10 mM HEPES, 100 U/ml Penicillin, 100 µg/ml Streptomycin) Basal culture medium
- Small intestine organoids
- 24-well-plates for suspension cells
- 48-well-plates for suspension cells

- Matrigel basement membrane matrix, growth factor reduced (GFR), phenol red-free
- N-Acetylcysteine, 500× stock (Sigma-Aldrich): 81.5 mg/mL in distilled water (500 mM)
- B27 supplement, 50x (Life Technologies)
- Murine recombinant EGF, 10,000x stock, 500 mg/mL in 0.1% BSA/PBS (PeproTech)
- Noggin conditioned medium, approx. 10x stock, ~1µg/mL Noggin
- RspoI conditioned medium, approx. 10x stock, ~10 mg/mL RspoI
- Complete crypt culture medium: Basal culture medium with B27 supplement (1×), and 1 mM N-acetylcysteine, 50 ng/mL EGF, 100 ng/mL Noggin, 1 mg/mL R-spondin
- ENRWntNic medium (Complete crypt culture medium with 50% Wnt3a conditioned medium and 10mM nicotinamide)
- 5 µM CHIR99021 (Sigma) (GSK3b inhibitor)
- Fugene
- DMEM complete medium
- Plasmid DNA (retroviral DNA construct)
- 1 µg/ml Puromycin
- 10 µg/ml Blasticidin
- Infection medium with and without polybrene (20 ml ENRWntNic medium with 20 µl 10 mM Y-27632 (Sigma) and 20 µl 8 mg/ml polybrene, always prepared freshly)
- TrypLE (Invitrogen)
- 150-mm culture dishes
- Refrigerated centrifuge with microtiter plate carrier
- Micro centrifuge
- Rho Kinase Inhibitor (Y-27632, Sigma, 10 mM Stock (1000x))
- 1 mM nicotinamide (Sigma, cat. no. N0636)
- polybrene (stock 8 mg/ml)

Before infection

To convert small intestine organoids from a budding to a cystic structure, at least 3 days before starting the infection the medium in a 24-well plate is changed from complete crypt culture medium to ENR-Wnt-Nic medium. This step is essential to keep stem cells of small-

intestinal organoids alive during the infection procedure. GSK3 inhibitor CHIR99021 (Sigma, 5 μ M) is added to the medium as well to promote stronger Wnt/ β -catenin signalling and help obtaining the cystic structure.

Virus production

For each infection one 150-mm dish of the retroviral packaging cell line (Platinum-E cells) is prepared by seeding 4.5×10^6 cells with 20 ml of DMEM complete medium containing selective antibiotics. Platinum-E cells maintain their viral envelop protein expression under Puromycin (1 μ g/ml) and Blasticidin (10 μ g/ml) selection. When cells are 70% to 80% confluent (after 2 days) medium is changed to DMEM complete medium without antibiotics and Fugene transfection is performed (see 6.3.1). Medium is changed the next day to 40 ml DMEM complete medium and after 2 days the medium which is now containing viral particles is collected. For that it is first filtered through a 0.45 mm strainer to get rid of cell particles and kept in a 50 ml Falcon tube. The viral particles are pelleted by centrifugation at 8000 x g at 4°C for 12 to 16 hours. The medium is discarded and the pellet resuspended with 250 μ l of infection medium containing polybrene. The infection medium contains Y-27632 (Rho Kinase inhibitor, 10 μ M) and polybrene (8 μ g/ml) to prevent cell death by anoikis and to facilitate interaction of viral particles and cells, respectively.

Preparing single cells from organoids for infection

The culture medium is removed and 1 ml ice-cold basal medium is put per well instead. The Matrigel is gently broken up by pipetting with a p1000 pipette and the organoids are resuspended in basal culture medium in this way. For washing the organoid suspension is transferred to a 15 ml tube. 9 ml ice-cold basal medium are added and the organoids are centrifuged at 700 rpm at 4°C for 2 minutes (1500 rpm for single cells). Afterwards the supernatant is removed to a degree that approximately 2 ml will be left in the tube which includes the Matrigel pellet. The organoids are disrupted using a fire-polished Pasteur pipette (decreased diameter) by thoroughly pipetting up and down for 6 to 10 times. This will dissociate the organoids by mechanically breaking them into smaller pieces and to get rid of released dead cells and single cells they are washed again with 8 ml ice-cold basal culture medium. To dissolve the matrigel the tube is inverted 3 to 5 times before centrifugation at 1200 rpm for 5 minutes at 4°C. The supernatant is removed nearly completely and 1 ml TrypLE is added to the pellet remaining in the tube. After vortexing it the tube is incubated at 37°C for 5 minutes and afterwards vortexed again. Centrifugation at 1100rpm at 4°C for 5 minutes is followed by removing the supernatant as completely as possible.

Infection

The cells of the organoid cell pellet are combined with 250 μ l of viral suspension, mixed by pipetting several times and transferred to a 48- well plate. The plate is sealed with parafilm and centrifuged at 600 x g for 60 minutes at 32°C. This step is called spinoculation and significantly enhances the number of infected cells. The parafilm wrapping is discarded and the plate incubated for 6 hr in a tissue culture incubator. To achieve a high percentage of infection this step is critical. Short incubation causes poor infection while long incubation (e.g., overnight) results in poor survival of organoids. Organoids are transferred in a 5 ml Eppendorf tube and centrifuged at 900 x g for 5 minutes at 4°C. The infection medium is discarded and organoids are resuspended with 100 μ l of matrigel. They are seeded in 2 wells of a 24-well plate which is afterwards turned around and put in an incubator at 37°C for 5 minutes that the matrigel can solidify. 500 μ l infection medium without polybrene are added per well and the organoids are incubated at 37°C for 5 to 7 days. Medium is changed after 3 days.

After infection

After 2 to 3 days drug selection can be started, e.g. with Puromycin (1 μ g/ml). When drug-resistant organoids grow out, the culture is split and medium changed to normal organoid medium supplemented with the appropriate antibiotics. Maintaining the drug selection ensures viral transgene expression. Small intestinal organoids need 1 to 2 weeks of culture to revert back to budding structures.

6.8 Whole cell lysates

6.8.1 Mammalian cells

Material:

- RIPA-Lysis buffer (150mM NaCl)
- 1x PBS
- Complete Mini EDTA-free protease inhibitor (Roche)
- Phosphatase inhibitor cocktail 2&3

Whole cell lysates from mammalian cells cultured in dishes are prepared for protein analysis (Western Blot). 6-well plates are usually sufficient to have enough cells for lysis and afterwards enough protein for analysis. After removal of the growth medium cells are washed two times with 1xPBS. Per well 500 μ l 1xPBS is added and cells are scraped with a plastic

cell-scraper and transferred to a falcon tube. Centrifugation at 1200rpm for 10 minutes at 4°C follows and the PBS is removed. The pellet is resuspended in an appropriate amount of 1x RIPA buffer supplemented with 1 tablet Complete Mini EDTA-free protease inhibitor and 100 μ l phosphatase inhibitor cocktail 2 and 3 and the mixture transferred to a 1.5ml Eppendorf tube. For lysis the cells are incubated with the buffer for 30 minutes at 4°C on the wheel. Samples are spun down at 13,000 rpm for 10 minutes at 4°C and the supernatant is collected in fresh tubes.

The total protein concentration can afterwards be determined by Bradford assay (see chapter 6.13). For calibration a BSA (bovine serum albumin) standard curve is recorded.

6.8.2 Organoids

Material:

- RIPA-Lysisbuffer (150mM NaCl)
- 1x PBS
- Recovery Solution
- Complete Mini EDTA-free protease inhibitor (Roche)
- Phosphataseinhibitorcocktail 2&3

Whole cell lysates from organoids are prepared for protein analysis (Western Blot, see part 6.10) or cells are collected for DNA preparation (see part 6.14). 2 wells containing 4 drops of matrigel with organoids are usually sufficient to have enough material for lysis and afterwards enough protein/DNA for analysis. After removal of the growth medium the organoids in matrigel drops are washed two times with 1xPBS. Per well 1 ml 1xPBS is added and removed. Afterwards 1 ml Recovery Solution is added and together with the matrigel transferred to a 5 ml Eppendorf tube. While incubating 45 minutes on ice the matrigel is dissolved. The suspension is centrifuged at 4°C at 900 x g for 5 minutes and the supernatant removed. For whole cell lysates the pellet is resuspended in an appropriate amount of 1x RIPA buffer supplemented with 1 tablet Complete Mini EDTA-free protease inhibitor and 100 μ l phosphatase inhibitor cocktail 2 and 3 and the mixture transferred to a 1.5ml Eppendorf tube. The suspension is pushed through a fine needle with a small syringe for 15 times. Samples are spun down at 13,000 rpm for 10 minutes at 4°C and the supernatant is collected in fresh tubes. The total protein concentration can afterwards be determined by Bradford assay (see chapter 6.13). For calibration a BSA (bovine serum albumin) standard curve is recorded.

For DNA extraction 100 μ l 1x PBS are added to the sample instead of RIPA buffer and DNA preparation is performed (see 6.14).

6.9 SDS-PAGE

Material:

- 1xSDS-running buffer
- 5xSDS-sample buffer
- Acrylamide/Bis 30%
- 0.5M Tris pH 6,8
- 1.5M Tris pH 8,8
- SDS (w/v) 10% (Sodium dodecyl sulphate)
- APS (w/v) 10% (Ammonium persulphate) ó start polymerization
- TEMED (Tetra methyl ethylene diamine) ó stabilization of radicals
- Isopropanol 100%

SDS-PAGE is a method to separate proteins according to their size by electrophoresis. Acrylamide gels are used as sorting media having the function of a strainer where small proteins migrate longer distances than large ones in the same time span. The distance of migration is proportional to the pore size of the polymerized acrylamide gel. The gel is produced with radical polymerization from acrylamide with N, N'-Methylen bis(acrylamide) as cross-linker using TEMED to stabilize the radicals and APS to start the polymerization. Different percentages of acrylamide can be used for better separation and resolution of characteristic band sizes, depending on the molecular weight of the protein. Discontinuous gels are used in all experiments, consisting of a stacking and separation gel.

SDS is an anionic detergent which should shield the charge of proteins. It stoichiometrically binds proteins (1 SDS molecule per 2 amino acids) and also breaks their hydrogen and disulfide bonds therefore causing an unfolding resulting in negatively charged complexes which can be separated only by size. At sample preparation SDS is added in excess and samples are heated to 95°C to break secondary and tertiary structures of the proteins. To break disulfide bonds the sample buffer contains 2-mercaptoethanol (-mercaptoethanol), a reducing thiol group. When subjected to an electrical field the uniformly charged SDS-protein complexes migrate towards the anode.

Procedure of the SDS-PAGE is done according to the manufacturer's manual. Separating gels (Tris pH 8.8) are poured first and covered with 100% isopropanol to avoid drying of the gel air interface and to ensure an even surface. After polymerization and removal of the isopropanol the stacking gels (Tris pH 6.8) are poured on top, followed by immediate insertion of a comb to have sample pockets in the gel after polymerization. Gels can be wrapped in foil and stored under humidified ddH₂O conditions at 4°C or directly used for electrophoresis. The combs are removed from the gels and they are inserted into BioRad Gel chambers (TetraCell), filled with 1x running buffer. The sample pockets are cleaned with running buffer and afterwards samples are loaded in their respective pocket. For size determination of separated proteins, 3.5 l (Dual-Colour BioRad) standard, containing different bands of known molecular weight are loaded in at least one well/gel. Electrophoresis is performed with constant voltage of 80 V until samples leave the stacking gel, followed by an increase to 110 V for 1.5 h until leaving the separation gel. Further analysis of the proteins is done by Western Blot (see part 6.10)

6.10 Western Blot – Tank Blot method

Material:

- Tank Blot buffer
- Methanol
- Whatman paper
- Polyvinylidene difluoride (PVDF) Membran

By Western Blotting proteins sorted by size via SDS-PAGE (6.9) are transferred to a membrane that is applied to the gel using an electrical field applied vertically to the gel. Proteins stick to the surface of the membrane because of hydrophobic interactions keeping the pattern of the separation after size. SDS is removed from the samples while doing Western Blot; therefore proteins can go back to their secondary and tertiary structure. Proteins sticking to a membrane can be identified via Immunodetection (6.11).

Before it can be used the hydrophilic PVDF-Membrane is activated with methanol. Procedure of the Western Blot is done according to the manufacturer's manual using the Mini-Protean System (BioRad). The blot is assembled in the following sequence (cathode to anode):

- sponge
- 2 pieces Whatman paper
- Gel
- membrane
- 2 pieces Whatman paper
- sponge

Transfer of protein takes place in a blot chamber filled with Tank blot buffer at 100V for 60 minutes.

6.11 Immunodetection

Material:

- Licor Blocking Buffer (Li-Cor® Biosciences)
- 0.1% Tween 20 in TBS
- Primary antibody (see material: 5.2.1)
- IR-coupled secondary antibody (see material: 5.2.2)

To visualize proteins bound to Western Blot membranes immunodetection can be used. A specific primary antibody binds epitopes of the protein of interest and is itself recognized by a secondary antibody which can be used for detection of the whole complex. Secondary antibodies used in this work are IR-coupled and can directly be detected with the Odyssey Imaging System (Licor, Lincoln, Nebraska USA).

Following protein transfer, the PVDF membrane is transferred to a Li-Cor® incubation box and blocked with LiCor blocking buffer for 1 h at room temperature on a shaker to saturate unspecific binding sites. Afterwards the membranes are incubated overnight at 4 °C with primary antibodies diluted in 2 ml LiCor blocking buffer while being sealed in a plastic bag. On the following day, the blots are washed 3 times with 0.1% Tween 20 in TBS for 5 min and then incubated with the appropriate secondary antibodies, diluted 1:10000 in LiCor blocking buffer on a shaker at room temperature. Finally, blots are washed 3 times, 5 min each with 0.1% Tween 20 in TBS and specific bands are detected with the Odyssey Imaging System.

6.12 Antibody stripping of Western Blot membranes

Material:

- NewBlot PVDF stripping solution
- 1x TBS / 0.1% Tween
- LiCor blocking buffer

To detach antibodies from Western Blot membranes after an immunodetection antibody stripping is performed with NewBlot PVDF stripping solution according to the manufacturer's manual. Membranes are incubated in 1x working solution for 20 minutes at room temperature and after washing steps with 1x TBS / 0.1% Tween the membrane can be re-blocked with LiCor blocking buffer.

6.13 Bradford assay

Material:

- Bradford reagent
- BSA-Standard (logarithmic row, from 10 $\mu\text{g}/\mu\text{l}$ to 0.1 $\mu\text{g}/\mu\text{l}$)
- Aqua bidest (a.b. / ddH₂O)

The Bradford assay is a colorimetric protein determination assay, based on the absorbance shift of Coomassie Brilliant Blue G-250 dye in presence of protein. Coomassie Brilliant Blue G-250 forms complexes with cationic and hydrophobic side chains of proteins in acidic solution and is therefore stabilized in its blue, anionic form. In its unbound, cationic form it is red and the amount of blue complex formed in a sample is equivalent to its protein concentration. The maximal absorbance of the blue form is at 595nm and can be measured with a spectrometer.

Protein standards are prepared by serial dilution of BSA in ddH₂O. A BSA row containing concentrations of 10 $\mu\text{g}/\mu\text{l}$, 5 $\mu\text{g}/\mu\text{l}$, 2 $\mu\text{g}/\mu\text{l}$, 1 $\mu\text{g}/\mu\text{l}$, 0.5 $\mu\text{g}/\mu\text{l}$, 0.4 $\mu\text{g}/\mu\text{l}$, 0.2 $\mu\text{g}/\mu\text{l}$ and 0.1 $\mu\text{g}/\mu\text{l}$ is prepared and kept at -20°C if not needed.

4 μl of each BSA concentration are put in a well of a 96-well plate and mixed with 250 μl Bradford reagent. Samples are diluted 1 to 2 with ddH₂O and afterwards 4 μl of the dilution are put in a well of a 96-well plate and mixed with 250 μl Bradford reagent. For all standards and samples two values are estimated. After 10 minutes incubation at room temperature the

absorbance values are obtained at 595 nm in a photometer and plotted against the standard protein concentration.

6.14 DNA preparation using Quick-DNA™ Universal Kit

Material:

- Pellet of organoid cells
- Quick-DNA™ Universal Kit (Zymo Research #D4068)
- 1x PBS

The Quick-DNA™ Universal Kit is used to isolate total genomic DNA from organoids that is needed for genotyping. The protocol is performed according to the manufacturer's standard protocol for mammalian cells. 100 µl 1x PBS are added to a pellet of organoid cells (obtained as in section 6.8.2) and proteinase K digestion is performed for 10 minutes at 55°C. Afterwards the sample is mixed with genomic binding buffer and loaded onto a Zymo-Spin™ IIC-XL Column. After several washing steps to clean the sample the DNA is eluted with 50 µl DNA elution buffer (10 mM Tris-HCl, pH 8.5, 0.1 mM EDTA).

6.15 Determination of DNA concentration with NanoDrop Spectral photometer

To determine concentration and quality of isolated DNA e.g. after plasmid preparations a NanoDrop spectrometer is used. In principle, the absorption of the sample at 260nm which is the maximal absorption of nucleic acids is measured in a volume of 1µl. As a reference a blank 1µl elution buffer is used. The absorption at 260nm of the sample is a measure for its DNA concentration. The quality of the sample can be determined by measuring the ratio 260/280 nm as well as 260/230 nm ratio.

6.16 Bacterial culture

Material:

- LB medium
- LB agar with the appropriate antibiotic
- Chemical competent bacteria: E.coli XL10 gold
- antibiotics: Ampicillin or Kanamycin (100µg/ml or 50µg/ml)
depending on the plasmid

Liquid cultures of *Escherichia coli* XL 10 Gold are grown in LB medium with the appropriate antibiotic at 37°C in an incubator at 180 rpm shaking. Bacteria can also be plated on LB agar plates with the appropriate antibiotic (selection marker) and incubated at 37°C to obtain single colonies.

For mini-prep (see 6.20) and pre-culturing single colonies are picked from agar plates and inoculated in 5 ml LB medium. Pre-cultures for midi prep (see 6.19) are transferred to 150 ml medium and incubated over night at 37°C and 180 rpm shaking.

6.17 Transformation of bacteria

Material:

- LB medium
- LB agar with the appropriate antibiotic
- Chemical competent bacteria: *E.coli* XL10 gold
- antibiotics: Ampicillin or Kanamycin (100µg/ml or 50µg/ml)
depending on the plasmid

Transformation is a method to bring recombinant DNA in bacteria for amplification.

For each transformation one aliquot bacteria containing 100µl cells is thawed on ice. They are gently mixed with 3.5 µl DTT (2.25 mM) and either divided into 25µl portions in case of retransformation or transformed completely by mixing them with ~1 µl DNA. Bacteria are incubated on ice for 30 minutes followed by a heat-shock for 45 seconds at 42°C and immediate incubation on ice for 2 minutes. 100 µl (25 µl portions) or 400 µl (complete aliquot) SOC medium is added and the transformation mixture is incubated at 37°C for 1 h while shaking. During this time successfully transformed bacteria develop the plasmid-encoded antibiotic resistance that is later needed for selection. 10 µl are plated on LB agar plates containing the selection marker and incubated overnight in case of retransformation. In case of ligation product transformations, all bacteria are completely plated to enhance the number of positive colonies

6.18 Polymerase Chain Reaction (PCR) methods

Polymerase Chain Reaction (PCR) was developed in the early 1980s (Mullis, 1986) and is based on thermal cycling. It can be used for amplification of a particular DNA sequence and therefore offers a broad application spectrum e.g. for cloning, sequencing, gene analysis, forensic science, genetic fingerprints and paternity testing.

In general, the thermal cycles of a PCR are as follows

- Denaturation 95 °C, 1-4 min.
 - Denaturation 95 °C, 50 sec.
 - Primer-Annealing xx °C, 50 sec.
 - Elongation 60 °C, 60 sec. x kb (Plasmid)
 - Elongation 60 °C, 7-10 min.
 - storage 4 °C
- } x 18-35 cycles

dsDNA is in a first step denatured by heat (95°C), resulting in a single stranded template, followed by the annealing process of two oligonucleotide primers, that are designed in a way they flank the region of interest. The annealing temperature (melting temperature T_m) of the primers to the ssDNA has to be adjusted for every primer pair and depends on their length and G-C content. Its range usually varies between 45 and 65°C but can differ from that.

It can be calculated according to the following formula:

$$T_m = [2 \cdot (nA + nT) + 4 \cdot (nG + nC)]^\circ C - 5^\circ C$$

The template strand is copied by elongation of the primers by a heat-stable DNA polymerase (e.g. Taq polymerase) that binds to and elongates them by consumption of dNTPs. The DNA sequence is doubled in every cycle and cycle repetition leads to an exponential amplification of the template between the primer pair.

6.18.1 Ligation independent cloning

Ligation independent cloning is a method to clone DNA constructs being nearly completely independent of restriction sites and ligation. The Vector has to be opened with only one restriction enzyme. It is also possible to exchange bigger regions of the original vector. The insert is produced by PCR. Primers are designed in a way that they have 20 base pairs overlap with the vector after it has been opened via restriction enzyme digest. PCR product and linearised vector are cleaned (see 6.25) and elution is performed with only 15 µl buffer. To create 5' overhangs Vector and PCR product are incubated with 0.2 µl T4 DNA Polymerase (NEB, 3u/µl) in buffer 2 + BSA in 20 µl volume for 1 hour at 22°C. The enzyme is inactivated by heat at 75°C for 20 minutes afterwards. For annealing of vector and insert 50 ng Vector are mixed with insert in relation 1:1, 1:2 together with 2µl 5x T4 ligase buffer, ad 10 µl H₂O and incubated 30 minutes at 37°C. 5µl are transformed in 100µl XL10 Gold bacteria while the leftover can be stored at -20°C and used for transformation at a later time point.

6.18.2 Genotyping PCR (Organoids)

Material:

- Genomic DNA
- dNTP-Mix (10 mM each dNTP)
- Platinum Taq DNA Polymerase (Invitrogen)
- 10x PCR Buffer, minus Mg
- 50 mM MgCl₂
- Primer (forward and backward, 10 µM each)
- Aqua bidest, sterile

To control for the correct genotype and recombination genotyping of the organoids genomic DNA is performed. The PCR reaction is done with Platinum Taq Polymerase according to the standard protocol given by Invitrogen. Primers were designed and tested by Taconic during the process of exchanging one wild type Kras allele for mTFP-KrasG12D.

Typical reaction:

- 2 µl (~80 ng) DNA
- 1 µl of dNTP-Mix (10 mM)
- 5 µl PCR buffer (10x)
- 2 µl MgCl₂ (50 mM)
- 1.5 µl each primer (in case of loxP) or 1 µl each primer
- 0.2 µl PlatinumTaq DNA Polymerase (1 unit)
- Adjusted with Aqua bidest to 50 µl

Program for performing a genotyping PCR:

- Denaturation 94 °C, 5 minutes
 - Denaturation 94 °C, 30 seconds
 - Annealing 60 °C, 30 seconds
 - Elongation 72 °C, 60 seconds
 - Elongation 72 °C, 10 minutes
 - storage 4 °C
- } x 35 cycles

The PCR products can be directly analyzed by agarose gel electrophoresis (see 6.21) after adding DNA sample buffer.

6.19 DNA preparation M&N Midi kit

Material:

- E.coli XL 10 gold, grown over night
- M&N Midi kit (Endotoxin-free NucleoBond® Xtra)
- Isopropanol

150-300 ml cultures of E.coli transformed with the desired plasmid are handled according to the manufacturer's protocol for high-copy plasmids, except low-copy plasmids. By centrifugation for 20 min at 5000 x g, 4 °C in a standard tabletop centrifuge with a swinging

bucket rotor a bacterial wet pellet is obtained. After precipitation plasmid DNA is loaded to NucleoBond® finalizers according to the user's manual. DNA is eluted with TE (endotoxin-free). The outer layer of the second (outer) membrane of Gram-negative bacteria like E.coli consists of amphiphilic lip polysaccharides (LPS) also called endotoxins. They are released during cell growth in small amounts and in very large quantities upon cell death and lysis and thus also during plasmid preparation. Free LPS molecules can induce inflammatory reactions of the mammalian immune system. To achieve high transfection rates and ensure viability of transfected cells endotoxins should be removed during plasmid preparation.

6.20 DNA preparation using Roti®-Prep Plasmid Mini Kit

Material:

- E.coli XL 10 gold, grown over night
- Roti®-Prep Plasmid Mini Kit

2-4 ml cultures of E.coli transformed with the desired plasmid are handled according to the manufacturer's standard protocol. Cells are harvested at 8000 x g in a conventional table top microcentrifuge and acidic lysis and neutralization are performed afterwards in order to obtain purified plasmid DNA which is in a last step eluted in 30µl elution buffer.

6.21 Agarose Gelelectrophoresis

Material:

- Agarose
- TAE
- Red Safe
- DNA sample buffer
- DNA standard (NEB, 2-log DNA ladder)

Agarose gel electrophoresis is used to separate DNA fragments by size. The principle is similar to SDS-PAGE (see 6.9) that is applied for proteins but here agarose-containing gels are used. These have the advantage of a defined pore size according to the percentage of agarose content an electrical field is used for separation; the negatively charged DNA migrates towards the anode and smaller fragments migrate faster, resulting in a separation by fragment size. To determine the correct size of a certain DNA fragment, a DNA standard is used for comparison. To cast a gel the appropriate amount of agarose (0.8-2%) is melted in 1x

TAE buffer. The size of the DNA fragments to be separated determines the agarose concentration used: 2 % for 0.1-3 kb, 1 % for 0.5-8 kb and 0.8 % for 1-10 kb. To visualize dsDNA RedSafe is added (5 μ l in 100 ml 1x TAE with agarose). RedSafe intercalates into dsDNA and can be visualized using a conventional UV-table. It is excited by UV light (309 nm), but as well by 419 nm and its emission can be detected at 537 nm (orange/red). The mixture is afterwards poured into a gel cast with comb. Agarose forms a stable hydrogel when it is cooled down to room temperature. Electrophoresis is carried out at 100-120 V, constant, depending on the size of the gel, for 30-40 min in 1x-TAE buffer. After gel electrophoresis images of the DNA separation are taken using the molecular imager Gel Doc XR (Bio-Rad).

6.22 Purification of DNA from Agarose gels

Material:

- Agarose gel with separated DNA fragments
- Zymo gel extraction kit

To isolate and purify DNA fragments from agarose gels (up to 10 μ g DNA from 70 bp to 10 kb) the Zymo gel extraction kit for isolation of DNA fragments is used according to the manufacturer's protocol. First, the DNA fragment of interest is excised from the agarose gel, weighed and afterwards dissolved in 2 volumes ADB buffer for 5-10 minutes at 50 °C. Columns with silica membranes facilitate DNA-binding under high salt conditions and allow for washing steps to clean from small DNA fragments (<50bp), agarose and proteins. Purified DNA is eluted with 6-10 μ l H₂O or EB.

6.23 Restriction digest

Material:

- DNA
- Restriction enzyme specific to DNA sequence
- Buffer compatible with enzyme (10x stock)
- Aqua bidest.

Restriction endonucleases type II bind to palindromic dsDNA sequences (restriction sites) that are specific for each enzyme and catalyze the hydrolysis of phosphodiester bonds (3' to 5') in each strand, resulting in a double strand break with either sticky or smooth ends. That feature can be used for preparative techniques such as linearization of Vectors to bring in

DNA fragments via ligation or for analytical techniques such as checking DNA for the presence of a certain sequence or investigation of the fragment pattern after agarose gel electrophoresis.

The dsDNA to be investigated is incubated with the appropriate restriction enzyme in the most suitable buffer diluted in aqua bidest for 2 h at 37°C for complete digestion. If possible, restriction enzymes are heat-inactivated at 67°C for 30 minutes after digestion. For analytical purposes digestions are performed in 20 µl, for preparative purposes in 50 µl volume.

6.24 Dephosphorylation of 5'-phosphorylated DNA

Material:

- digested Plasmid-DNA
- Enzyme CIAP (calf intestine alkaline phosphatase) (NEB)

To prevent self-ligation of vector DNA without incorporation of the insert during ligation 5' phosphorylated ends are dephosphorylated by alkaline phosphatase (CIAP) after restriction digest. 1 U CIAP is added to each restriction digest of the desired vector backbone and incubated for 1 h at 37°C.

6.25 PCR product purification

Material:

- QIAquick PCR Purification Kit
- Zymo DNA clean and concentrator kit

The QIAquick® PCR purification kit is used for purification of DNA fragments according to the manufacturer's protocol. Only DNA fragments between 100bp and 10kb can be bound to the column and are therefore cleaned from Primers (after PCR) or smaller fragments (after restriction digest).

The Zymo DNA clean and concentrator kit follows the same approach like the gel extraction kit for DNA fragment purification (see 6.22). DNA is dissolved in high salt buffer and afterwards bound to a silica-membrane in a column. Before DNA elution in 6-10 µl H₂O or EB contaminating small DNA fragments (<50 bp), proteins and salt are washed off in two washing steps, according to the manufacturer's protocol.

6.26 Ligation

Material:

- T4-DNA-Ligase
- T4-DNA-Ligase buffer
- DNA fragments that are to be ligated
- Aqua bidest

T4-DNA-Ligase catalyzes the ATP-driven phosphodiester bond formation between 3'OH and 5'phosphate group of linear DNA fragments if they are blunt ends or they are complementary to each other in case of sticky ends. With ligation DNA fragments can be inserted into linearised vectors. 50-100 ng cut and dephosphorylated vector is mixed with 3-5x molar excess of cut insert DNA.

The required amount of insert can be calculated as follows:

$$Insert[ng] = \frac{molar_excess \cdot vector[ng] \cdot size(insert)[bp]}{size(vector)[bp]}$$

After addition of 1 μ l of T4-DNA-ligase and 4 μ l ligation buffer the volume of each sample is adjusted to 20 μ l with Aqua bidest. After incubation at 16°C for 6 hours the enzyme is inactivated by heating the sample to 65°C for 10 minutes. The preparation can be used as such for transformation of chemical competent bacteria (see 6.17).

6.27 Sequencing using BigDye® Terminator kit

Material:

- ready reaction premix
- BigDye® termination buffer
- sequencing primer (10 pmol/ μ l)
- DNA
- NucleoSEQ spin columns (Macherey-Nagel)
- Aqua bidest

Most sequencing methods are based on Sanger's dideoxy chain terminating method using 2',3'-dideoxy-nucleotides (ddNTPs) which cannot form phosphodiester bonds (missing an OH-bond). The BigDye Kit applies fluorescently labelled ddNTPs leading to DNA strand termination after one of them is incorporated during synthesis. With capillary gel electrophoresis the labelled nucleotides are detected afterwards (in-house facility).

Typical sequencing reaction:

- 500 ng DNA
- 2 µl of ready reaction premix
- 3 µl BigDye® termination buffer
- 0.5 µl sequencing primer (10 pmol/ µl)
- Adjusted with Aqua bidest to 20 µl

PCR cycle for sequencing reaction:

- Denaturation 96 °C, 1 min.
 - Denaturation 96 °C, 10 sec.
 - Primer-Annealing 50 °C, 5 sec.
 - Elongation 60 °C, 4 min.
 - storage 8 °C
- } x 25 cycles

After PCR impurities like salts, primers and excess ddNTPs are removed using NucleoSEQ spin columns, hydrated with 600 µl Aqua bidest for at least 30 minutes prior to use, according to the manufacturer's manual. Cleaned PCR product is transferred to a 0.5 ml Eppendorf tube and dried in a speed vacuum centrifuge at 60°C for 30 minutes and afterwards send for in-house analysis.

6.28 Preparation of Cryoslices using a Cryostat

Material:

- Aluminium foil
- Liquid nitrogen
- Cryo slides
- Pellet of organoids in recovery solution
- 1x PBS
- forceps
- cryo medium (Leica)
- brush
- plastic bags (for storage only, same as used for western blot incubation)

To prepare cryo slices with a large number of organoids per slice samples have to be prepared the following way. To freeze the sample a vessel is needed. This is build from aluminium foil by wrapping it around a thumb or a big pen making sure to not have it too buckled. Organoids are prepared the same way as for staining (see 6.29.3) but not fixed. After the matrigel is completely dissolved and the pellet of organoids is covered with PBS cryo medium can be added. It will sink down towards the pellet. Meanwhile cryo medium is filled into an aluminium vessel (not more than half) and it is set into liquid nitrogen for a few seconds. The outer part will become solid and the inner part will stay liquid. This inner part is removed using a p1000 pipette. Into the originated hole the organoids (together with cryo medium) are put using a p200 pipette (long tips, cut off). Fresh cryo medium is placed carefully on top and the vessel is set into liquid nitrogen again (use forceps). Once the sample is completely frozen the aluminium foil is removed and the sample stored in a sealed plastic bag at -80°C prior to usage. Once the sample is brought into position in the Cryostat it is cut at 6 nm at -20°C chamber temperature and slices are brought onto slides with help of a brush if necessary.

6.29 Immunofluorescence

6.29.1 Cells

Material:

- Methanol (ice-cold) or 4% PFA and 0.2% Triton X100 in TBS
- 1xPBS
- 1xTBS
- TBS/0.1% Tween20
- Licor Buffer
- Antibody anti Ras, Calb. Mouse, pan-AB, 1:200
- Alexa 488 goat anti mouse 1:1000 or Alexa 488 donkey anti mouse 1:1000
- Deltarasin
- DMSO
- DMEM complete medium
- 8-well LabTeks

Per well of an 8-well LabTek 1×10^4 cells are seeded in DMEM complete medium. The following day cells are treated with Deltarasin or DMSO in the desired amount, usually for 24 hours. After 2 washing steps with 1xPBS cells are fixed with ice-cold Methanol or PFA. As PFA does not permeabilise the cells, after washing again with TBS, a second incubation with triton x 100 in TBS is required. To block non-specific binding sites the cells are incubated for 1.5 hours in Licor buffer at room temperature. Afterwards the cells are incubated with the primary antibody, e.g. anti Ras pan antibody, 1:200 diluted in Licor Buffer for 2 hours. After washing 3 times in TBS/0.1% Tween to remove unspecific antibody binding the secondary antibody labelled with fluorescent dye is applied diluted 1:1000 in Licor Buffer and incubated for 1.5 hours in a dark box shaking. Cells are washed 5 times with TBS/0.1% Tween and stored in the same buffer at 4°C in the dark until investigation with the Leica SP5.

6.29.2 Organoids on slides

Material:

- Organoids in slices, frozen, on slides
- 4% PFA and 0.5% Triton X100 in PME
- 1xPBS
- 1xTBS

- PME (50mM PIPES, 2,5mM MgCl₂, 5mM EDTA; pH 7 with NaOH)
- TBS/0.1% Tween20
- IF Buffer (PBS/1%BSA/0,2% Triton/0,05% Tween) or more BSA 5% or 10%
- Antibody anti Ras, Abcam, pan-AB, 1:200 (rabbit), anti ChromoA 1:100 (rabbit), anti Villin 1:200 or 1:500 (rabbit)
- Alexa 546 goat anti rabbit 1:1000 or Alexa 546 donkey anti rabbit 1:1000
- PAP Pen
- Hoechst 33258 (10mg/ml)
- Slow fade gold (S36936)
- Nail polish

Each slice on the slides is circled with PAP pen before starting fixation with 4% PFA in PME. Slices are incubated with PFA for 10 minutes and afterwards washed two times with 1x TBS. As PFA does not permeabilise the cells, after washing again with TBS, a second incubation for 10 minutes with triton x 100 in PME is required and the slices are washed afterwards three times with TBS/0,1% Tween. To block non-specific binding sites the slices are incubated for 1 hour in IF Buffer at room temperature in a wet chamber. Afterwards the organoids are incubated with the first antibody at 4°C over night in IF Buffer in a wet chamber. After washing 5 times in TBS/0.1% Tween the secondary antibody labelled with fluorescent dye is applied diluted 1:1000 in IF Buffer and incubated for 1 hour. For Hoechst staining the dye is diluted in 1x PBS (final concentration 1µg/ml) and incubated 5 minutes at room temperature with the slices. Organoids are washed 5 times with TBS/0.1% Tween, mounted with slow fade gold, sealed with nail polish and stored at room temperature in the dark until investigation with the Leica SP5 or Leica SP8.

6.29.3 Organoids in SPIM

Material:

- Organoids in normal growth medium
- Recovery Solution
- 4% PFA and 0.5% Triton X100 in PME
- 1xPBS
- 1xPBS / 1% BSA
- PME (50mM PIPES, 2.5mM MgCl₂, 5mM EDTA; pH 7 with NaOH)
- IF Buffer (PBS/1%BSA/0.2% Triton/0.05% Tween) or more BSA 5% or 10%

- Antibody anti Ras, Abcam, pan-AB, 1:200 (rabbit), anti ChromoA 1:100 (rabbit), anti Villin 1:200 or 1:500 (rabbit)
- Alexa 546 goat anti rabbit 1:1000 or Alexa 546 donkey anti rabbit 1:1000
- Hoechst 33258 (10mg/ml)
- Low melting point agar (1% in H₂O)
- glass bottom dishes, Greiner, 627861
- Transferpettor and matching tubes

2 wells containing 4 drops of matrigel with organoids are usually sufficient to have enough material for staining and afterwards enough preparing samples for investigation with SPIM. After removal of the growth medium the organoids in matrigel drops are washed two times with 1xPBS. Per well 1 ml 1xPBS is added and removed. Afterwards 1 ml Recovery Solution is added and together with the matrigel transferred to a 5 ml Eppendorf tube. While incubating 45 minutes on ice the matrigel is dissolved. The suspension is centrifuged at 4°C at 100 x g for 5 minutes and the supernatant removed. Organoids are incubated with PFA for 20 minutes and afterwards washed two times with 1x PBS/1%BSA. As PFA does not permeabilize the cells, after washing again with PBS/BSA, a second incubation for 20 minutes with triton x 100 in PME is required and the organoids are washed afterwards three times with PBS/BSA. To block non-specific binding sites the organoids are incubated for 1 hour in IF Buffer at room temperature. Afterwards they are incubated with the first antibody at 4°C over night in IF Buffer. After washing 5 times in PBS/BSA the secondary antibody is applied diluted 1:1000 in IF Buffer and incubated for 1 hour. For Hoechst staining 1µg/ml of the dye diluted in 1x PBS is used and incubated 5 minutes at room temperature with the cells. Organoids are washed 5 times with PBS/BSA and prepared for investigation with SPIM with the Leica SP8. To do so organoids from the samples are embedded in low melting point agarose with the transferpettor and stored at 4°C until they are used. They are transferred to the middle of a glass bottom dish via transferpettor and carefully embedded with low melting point agar. Once the agar is solid samples are put at 4°C in the dark until they are investigated.

6.30 Life cell imaging experiments

6.30.1 In cells

Material:

- MDCK cells or PancTuI cells
- DNA: mCitrine Hras G12V and mCherry Kras WT
- Effectene KIT or Lipofectamine 2000 for transfection
- Deltarasin
- DMSO
- DMEM complete medium
- Imaging medium without HEPES
- 4-well LabTeks

Per well of a 4-well LabTek 2×10^4 cells are seeded in DMEM complete medium. The next day cells are transfected with mCitrine Hras G12V (0.3 μ g DNA per 4 wells) and mCherry Kras WT (0.4 μ g DNA per 4 wells) using Effectene (MDCK) or mCherry Kras WT (4 μ g DNA per 4 wells) using Lipofectamine 2000 (PancTuI). Medium is exchanged by 900 μ l fresh growth medium or imaging medium before investigation with the microscope the following day. Once one or more cells of interest are found Deltarasin or DMSO diluted in 100 μ l growth medium/imaging medium are added and observation is continued for 1 hour.

6.30.2 In organoids with SPIM

Material:

- Organoids in normal growth medium (with mTFP KrasG12D switched on)
- glass bottom dishes, Greiner, 627861
- Advanced DMEM F12 (2 mM Glutamax, 10 mM HEPES, 100 U/ml Penicillin, 100 μ g/ml Streptomycin) Basal culture medium
- Pasteur Pipettes
- FBS
- Falcon tubes or 5 ml Eppendorf tubes
- Matrigel basement membrane matrix, growth factor reduced (GFR), phenol red-free
- N-Acetylcysteine, 500 \times stock (Sigma-Aldrich): 81.5 mg/mL in distilled water (500 mM)
- B27 supplement, 50 \times (Life Technologies)

- Murine recombinant EGF, 10,000x stock, 500 mg/mL in 0.1% BSA/PBS (PeproTech)
- Noggin conditioned medium, approx. 10x stock, ~1µg/mL Noggin
- RspoI conditioned medium, approx. 10x stock, ~10 mg/mL RspoI
- Complete crypt culture medium: Basal culture medium with B27 supplement (1×), and 1 mM N-acetylcysteine, 50 ng/mL EGF, 100 ng/mL Noggin, 1 mg/mL R-spondin
- Imaging medium with HEPES
- Deltarasin
- DMSO
- FEP tube
- Double sided sticky tape
- 70% EtOH
- 1.5mm drill and drilling machine
- Scissors

In a first step the glass bottom dish containing half a FEP tube with 1.5mm holes in it are prepared. To do so holes are drilled into the tube in a way that each 2 cm of the tube 2 holes can be found. Afterwards the tube is cut in 2 cm long pieces that are bisected lengthwise. The pieces are attached to the bottom of the glass bottom dish using double sided sticky tape. To sterilise the dish it is filled with 70% EtOH and incubated for 30 minutes. The EtOH is removed and the dish left for drying. Meanwhile media for the organoids are prepared.

After preparation of all media that are needed, fire-polishing and FBS-coating of Pasteur pipettes the culture medium of one well of organoids is removed and 1 ml ice-cold basal medium is put instead. The Matrigel is gently broken up by pipetting with a p1000 pipette and the organoids are resuspended in basal culture medium in this way. For washing the organoid suspension is transferred to a 5 ml Eppendorf tube. 4 ml ice-cold basal medium are added and the organoids are centrifuged at 700 rpm at 4°C for 2 minutes. After centrifugation a pellet consisting of living organoids is visible with a bigger almost transparent matrigel layer on top containing dead cells. The supernatant is removed to a degree that approximately 2 ml will be left in the tube which includes the Matrigel pellet. The organoids are disrupted using a fire-polished Pasteur pipette (decreased diameter) by thoroughly pipetting up and down for 6 to 10 times. This will dissociate the organoids by mechanically breaking them into smaller pieces and to get rid of released dead cells and single cells they are washed again with 3 ml ice-cold

basal culture medium. To dissolve the matrigel the tube is inverted 3 to 5 times before centrifugation at 1200 rpm for 5 minutes at 4°C. The supernatant is removed nearly completely and the pellet remaining in the tube has a volume of approximately 15-20 µl. The organoids are mixed with 100 µl fresh matrigel and seeded on top of the FEP tube where the holes are for better attachment. The dish is turned around and put in an incubator at 37°C for 5 minutes that the matrigel can solidify. By applying this hanging drop method the organoids will localize to the periphery of the Matrigel drop and not stick near the bottom of the tube. 5 ml complete medium are added per dish and the organoids are incubated at 37°C until investigation the following day.

The next day growth medium is removed and exchanged by 8 ml imaging medium while the dish is already inside the incubation chamber of the microscope. After calibration, setting up a stack for an interesting region to be investigated over time and taking a first set of images 1 ml medium is exchanged by 1 ml medium containing the desired amount of Deltarasin or DMSO. Observation of the organoid is continued for 2-3 hours while one stack of images is taken in 5 minutes (first hour) or in 10 minutes (after first hour).

7 Results

7.1 Comparison of the localization of different over expressed Ras isoforms upon Deltarasin and Deltazinone 1 treatment in MDCK cells

As Kras relocates from the plasma membrane to endomembranes after Deltarasin treatment in cells (Zimmermann et al., 2013; Iwig and Kuriyan 2013), I was interested in determining whether the same is true for Hras. It was to be expected that both Ras isoforms behave in a similar manner, but it was unclear whether the spatial and temporal localization of Hras would mirror the previously revealed profile of Kras.

To investigate this, I performed live cell imaging experiments with MDCK cells transfected with mCitrine HrasG12V and mCherry Kras^{WT} and in a first approach treated them with 5 μ M Deltarasin. The experiments showed that Kras and Hras delocalized in a similar manner upon Deltarasin treatment (figure 10, upper part and 11A).

Deltazinone 1 was also tested for its ability to relocate Kras and Hras from the plasma membrane. To do this, the experiment was repeated using 20 μ M Deltazinone 1 instead of 5 μ M Deltarasin (see figure 10, lower part). A dose of 20 μ M was chosen as previous Real Time Cell Analysis (RTCA) studies performed by Holger Vogel confirmed growth inhibitory effects of Deltazinone 1 at this concentration in a set of other cell lines. While mCitrine HrasG12V relocated partially upon Deltazinone 1 administration, mCherry Kras^{WT} did not (figure 10, lower part).

Quantification of the amount of fluorescent Ras inside the cells at different time points revealed the temporal profile of Ras relocation in MDCK cells upon treatment with the different compounds (Figure 11). When cells were treated with Deltarasin (Figure 11A), Kras and Hras exhibit a similar temporal profile of relocation. The most relocation appears to occur between 0 and 30 minutes after treatment (steep curve). Between 30 and 60 minutes after drug administration the effect starts ceasing, the curves begin to flatten out. However, Ras relocation constantly takes place as the curves are constantly increasing and it is not finished at the end point of the experiment.

Upon treatment with Deltazinone 1 (Figure 11B) Kras and Hras exhibit different temporal profiles of relocation. For Hras, the curve stays relatively flat during the first 15 to 30 minutes of the experiment, with almost no relocation taking place. Between 30 and 45 minutes after drug administration the curve increases, corresponding to an increase in relocation. For the last 15 minutes of the experiment (45 to 60 minutes after drug

administration), the curve flattens out as relocalization still occurs but to a lesser extent. In contrast, Kras fails to relocalize upon treatment with Deltazinone 1. This indicates that Deltarasin and Deltazinone 1 do not share exactly the same working mechanism and therefore may affect different pathways in addition to inhibiting PDE .

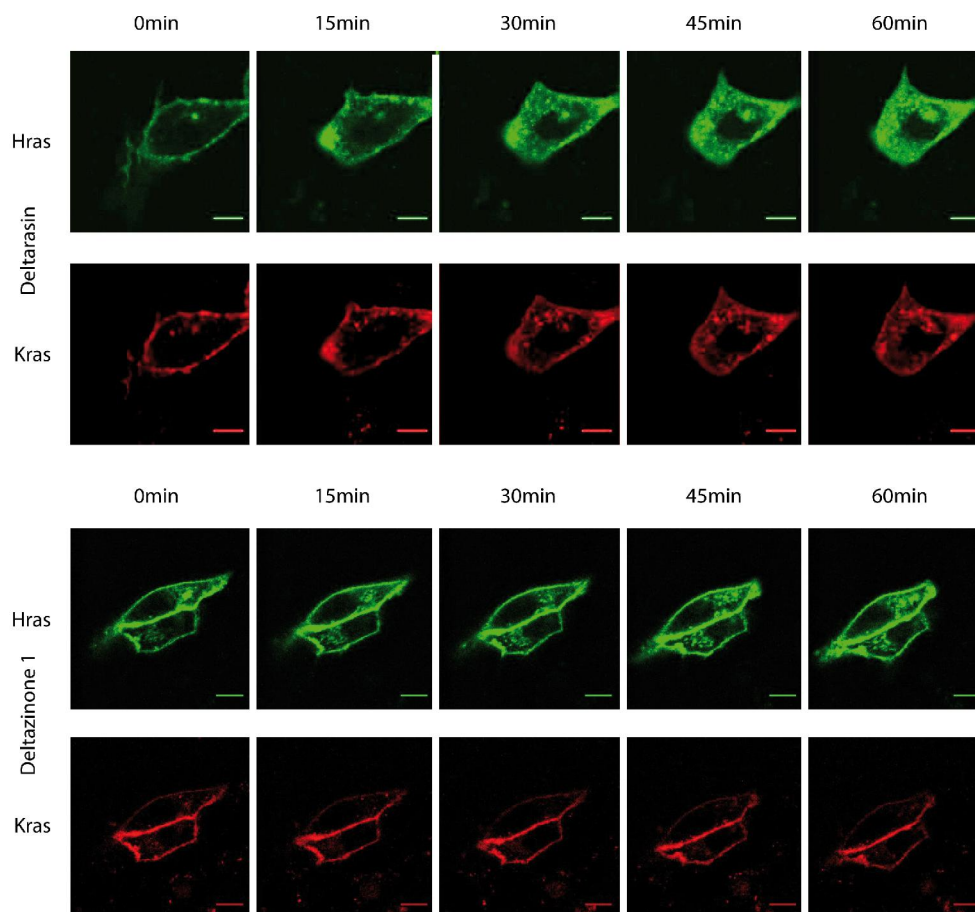


Figure 10: Localization of different Ras isoforms upon Deltarasin or Deltazinone 1 treatment

MDCK cells were transfected with mCitrine HrasG12V and mCherry KrasWT. One day after transfection the cells were treated with 5 μ M Deltarasin (upper part) or 20 μ M Deltazinone 1 (lower part) and constantly observed with the microscope. Pictures were taken every three minutes for 1 hour. The experiment was repeated 7 times for Deltarasin. It was first performed as proof of principle with both Ras isoforms for Deltazinone 1. Six additional experiments were conducted with cells that were transfected only with the mCherry KrasWT construct and treated with Deltazinone 1.

Hras is shown in green; Kras in red; scale bars 10 μ m

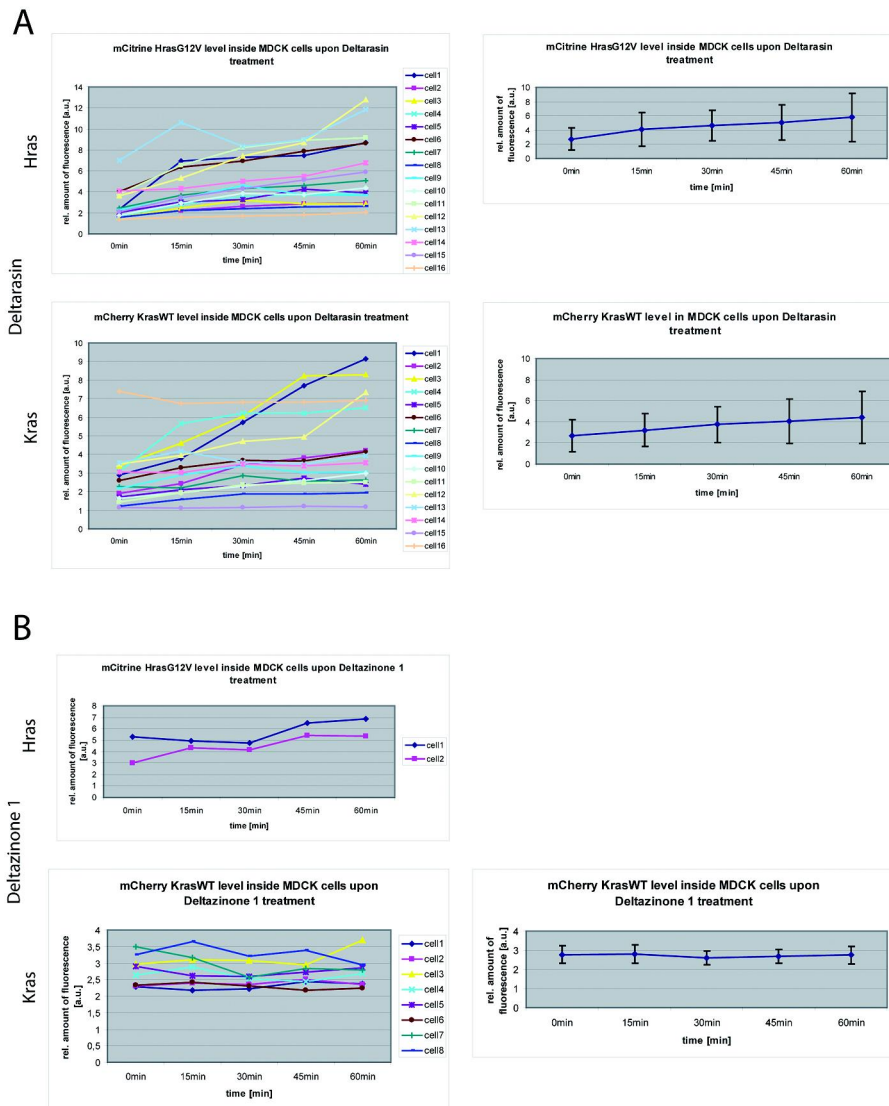


Figure 11: Quantification of the effects of Deltarasin or Deltazinone 1 treatment on different Ras isoforms in MDCK cells

MDCK cells were transfected with mCitrine HrasG12V and mCherry KrasWT. One day after transfection the cells were treated with 5 μ M Deltarasin (A) or 20 μ M Deltazinone 1 (B) and constantly observed with the microscope. Pictures were taken every three minutes for 1 hour. The experiment was repeated 7 times for Deltarasin. It was performed first as proof of principle with both Ras isoforms for Deltazinone 1. Six additional experiments were conducted with cells that were transfected only with the mCherry KrasWT construct and treated with Deltazinone 1. For 5 time points cells were masked leaving the plasma membrane unmasked. The masks were used to measure just the cytosol of the cells by multiplication of the mask with the original image and subsequently measuring the area of each cell that was previously marked. This was performed for all cells at the different time points and the results were plotted in a diagram. An average value was also calculated for each experiment and plotted separately together with its standard deviation.

7.2 Comparison of the effect of Deltarasin and Deltazinone 1 treatment on localization of endogenous Ras in A431 cells

To further characterize and compare the effects of Deltarasin and Deltazinone 1, the relocalization of endogenous Ras upon administration of Deltarasin and Deltazinone 1 was examined in A431WT cells using immunofluorescence. Cells were treated with different doses of each drug or DMSO as a control to compare their effects on Ras relocalization. While cell death occurs in A431 cells after treatment with 5 μ M Deltarasin, there was no evidence of cell death after Deltazinone 1 treatment. However, treatment with Deltazinone 1 appeared to reduce cell growth, even at high doses. This is consistent with the findings of Holger Vogel based on the RTCA experiments he conducted.

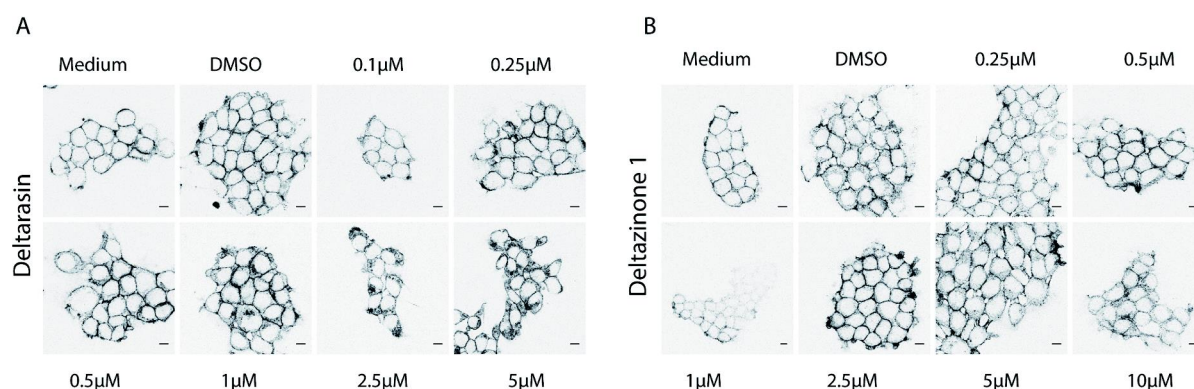


Figure 12: Localization of endogenous Ras in A431 cells upon Deltarasin or Deltazinone 1 treatment

Cells were treated with the indicated dose of Deltarasin (A) or Deltazinone 1 (B). As a control cells were left untreated (Medium) or treated with the DMSO contained in the highest drug concentration. After 24h they were fixed with methanol and stained with a panRas antibody. The experiment was performed twice. The second time higher doses of Deltazinone 1 (up to 50 μ M) were included (data not shown). Pictures of 4 regions of interest were taken in each well of the labtek chambers. Scale bars: 10 μ m

While Ras localizes to the plasma membrane in the DMSO control, cells treated with Deltarasin show a higher endomembranous fraction of Ras protein in a dose dependent manner (figure 12A). At a dose of 2.5 μ M Deltarasin relocalization can clearly be observed. Slight effects are visible at doses of 0.5 and 1 μ M of the compound but they cannot be distinguished from the mild relocalization effect also observed in the DMSO control. Nevertheless, the staining clearly shows that Deltarasin mislocalizes endogenous Ras in A431 cells. In contrast, cells treated with Deltazinone 1 (figure 12B) display behaviour similar to the DMSO control. All DMSO controls show a small amount of relocalization (compare

DMSO to Medium in figure 12A and 12B). The amount of DMSO in the control matches the amount of DMSO present within the highest concentration of the compound in each panel (0.05% in case of Deltarasin and 0.1% in case of Deltazinone 1). This DMSO-effect impedes interpretation of the results because effects of Deltazinone 1 could be missed.

The experiment was performed twice. The second time, higher doses of Deltazinone 1 (up to 50 μM) were included but the outcome did not differ from that observed with 10 μM Deltazinone 1 (data not shown). Based on these experiments, it was not possible to draw a clear conclusion about the capability of Deltazinone 1 relocalizing Ras because the DMSO controls bear such a similarity to the actual samples containing Deltazinone 1. However, with this experiment it was possible to demonstrate for the first time that Deltarasin mislocalizes endogenous Ras in a cancer cell line.

7.3 Deltarasin relocalizes Ras in colorectal cancer cells

Other cell lines were also tested to ascertain whether endogenous Ras exhibited the same behaviour as that found in A431 cells (figure 12). Therefore, experiments were conducted to determine whether Deltarasin could mislocalize Ras in cells of a Kras-independent colorectal cancer (CRC) line with high EGFR levels (DiFi, see Olive et al., 1993). DiFi cells were treated with different doses of Deltarasin or DMSO as a control and immunofluorescence experiments with a panRas antibody were performed. Upon treatment with 5 μM Deltarasin a clear effect on Ras localization was observed (figure 13A). Endogenous Ras relocalized from the plasma membrane towards the endomembranes as previously observed in A431 cells (figure 12). A similar experiment performed with MDCK cells (data not shown) displayed comparable results.

The experiment was repeated three times in total. For statistical analysis only two experiments were included as the number of cells were 10 times higher than in the third experiment (~ 100 in comparison to ~ 10) and this experiment also did not fulfil one condition (untreated cells). In all three cases, the trend is the same. Not only can a dose dependent relocalization effect of Deltarasin on endogenous Ras be observed, but this effect is statistically significant (see figure 13B). After treatment with 2.5 μM Deltarasin for 24 hours, around 80% of the cells exhibit this effect. After addition of 5 μM of the drug, most cells are dead and are no longer in a condition to be analysed. However, those that can be found display relocalization of endogenous Ras (see also figure 13A).

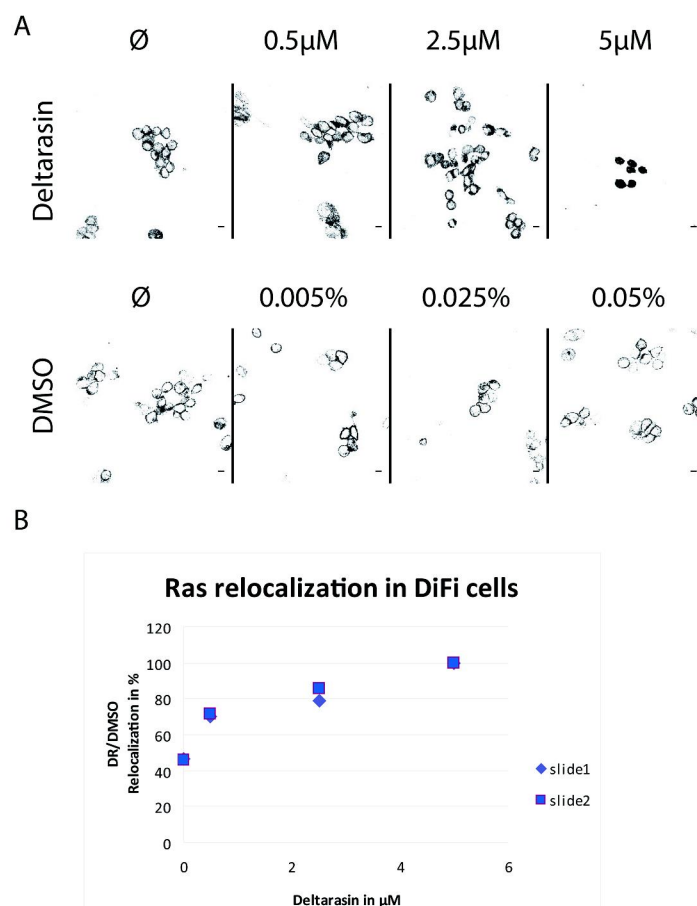


Figure 13: Localization of endogenous Ras in DiFi cells upon Deltarasin treatment

- A: DiFi cells were treated with 0.5 μ M, 2.5 μ M or 5 μ M Deltarasin, with a corresponding percentage of DMSO or left untreated. After 24 hours they were fixed with 4% PFA and stained with a panRas antibody in a 1:200 dilution in salmon sperm solution. The secondary antibody Alexa 488 rabbit anti mouse was used in a 1:1000 dilution in salmon sperm solution; scale bars: 10 μ m
- B: To quantify the results cells from all images that were taken were counted and grouped depending on their relocalization status and the amount of compound or DMSO that was used. Cell numbers obtained for cells that were treated with Deltarasin were divided by the number of cells of their corresponding DMSO control and the results were multiplied by 10 to obtain numbers high enough for calculation of the Chi square test. Chi square tests were performed to test for significance. P values obtained are \ll 0.05. The DMSO corrected cell numbers for the same amount of compound (relocalization, no relocalization, total number) were used to determine the percentage of cells that show relocalization by dividing the cell number of interest by the total number of cells. The results were plotted in a diagram.

The experiment was performed three times in total. For statistical analysis only two experiments were used due to larger cell numbers (<100 compared to ~10) and to a missing control (cells without adding compound).

7.4 Comparison of the effect of Deltarasin and Deltazinone 1 treatment on Localization of mCherry KrasWT in PancTuI cells

Recently, it has been shown that the interaction of Ras and PDE in Kras-dependent pancreatic ductal adenocarcinoma cells is disrupted after Deltarasin administration (Zimmermann et al., 2013). The cell lines used in the previous experiments (MDCK, A431, DiFi) were independent of Kras and came from varying backgrounds. To investigate whether Kras dependency could be an important factor - perhaps determining whether a compound is capable of relocating Kras - the cell system was changed.

PancTuI cells are a pancreatic ductal adenocarcinoma cell line. They are Kras-dependent and they harbour one mutant Kras G12V allele. In RTCA experiments, PancTuI cells die upon treatment with 5 μ M Deltarasin and also react to 10 μ M Deltazinone 1. However, Deltazinone 1 does not appear to induce death (cytotoxicity) but rather has a cytostatic effect, resulting in growth arrest (Papke et al., 2016).

To directly monitor the effects of the compounds on Ras localization I performed live cell imaging experiments with PancTuI cells transfected with mCherry KrasWT and treated them with 5 μ M or 6 μ M Deltarasin. It was already known that PancTuI cells react to Deltarasin treatment with a relocation of Kras from the plasma membrane to the endomembranes (Zimmermann et al., 2013). This part of the experiment therefore served as a positive control for comparison with the other inhibitor.

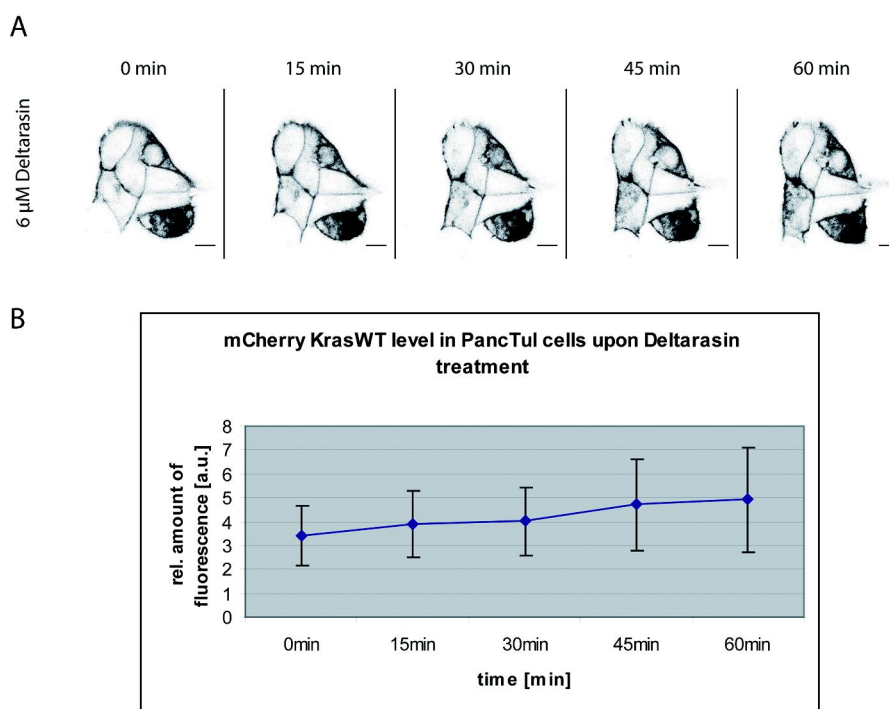


Figure 14: mCherry KrasWT relocalization in PancTuI cells upon treatment with Deltarasin

PancTuI cells were transfected with mCherry KrasWT. One day after transfection the cells were treated with 6 μ M Deltarasin and constantly observed under the microscope (A). One image was taken in three minutes. For further analysis the cells of interest were masked leaving the plasma membrane unmasked. The masks were used to measure only the cytosol of the cells by multiplication of the mask with the original image and measuring afterwards the intensity level of the area of each cell that was previously masked (amount of fluorescent Kras). The amount of fluorescence in each cell for five time points of the full length of the experiments was determined; the average value of all cells analyzed was calculated for each time point and plotted in a diagram together with its standard deviation (B).

The experiment was repeated 5 times with either 5 μ M or 6 μ M Deltarasin. 28 cells were analyzed in total; scale bars: 10 μ m

Figure 14 displays one example of PancTuI transfected with mCherry KrasWT after treatment with 6 μ M Deltarasin. Cells are responding to Deltarasin treatment. The amount of fluorescence in the cytosol of the cells increases with time showing that the fluorescent Ras moves towards the endomembranes. Relocalization starts between 0 and 15 minutes after treatment. Between 15 and 30 minutes after drug administration the effect stagnates. Subsequently cells again show clear effects, with a relatively strong increase in relocalization between 30 minutes and 45 after administration of the drug and a continued increase during the last 15 minutes monitored (figure 14B).

In order to compare both inhibitors, transfected cells were also treated with 20 μ M or 24 μ M Deltazinone 1 (see figure 15 for an example with 24 μ M Deltazinone 1).

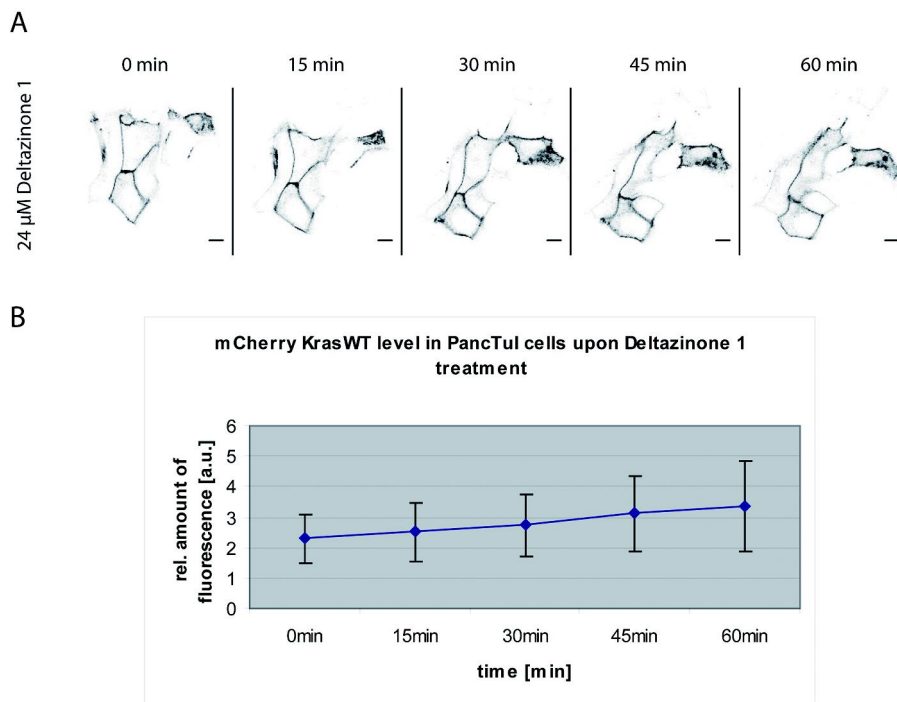


Figure 15: mCherry KrasWT relocation in PancTuI cells upon treatment with Deltazinone 1

PancTuI cells were transfected with mCherry KrasWT. One day after transfection the cells were treated with 24 μ M Deltazinone 1 and constantly observed with the microscope (A). One image was taken in three minutes. For further analysis the cells of interest were masked leaving the plasma membrane unmasked. The masks were used to measure only the cytosol of the cells by multiplication of the mask with the original image and measuring afterwards the intensity level of the area of each cell that was previously masked (amount of fluorescent Kras). The amount of fluorescence of each cell for five time points of the entire time of the experiments was determined; the average value of all cells analyzed was calculated for each time point and plotted in a diagram together with its standard deviation (B).

This experiment was repeated 4 times with doses of 20 μ M or 24 μ M of Deltazinone 1. 35 cells were analyzed in total; scale bars: 10 μ m

In this live-cell imaging experiment it could be seen that Deltazinone 1 indeed has an effect on the localization of the transfected KrasWT protein, albeit a weaker effect than that observed after Deltarasin administration (compare figure 14 and figure 15). Cells respond to treatment with Deltazinone 1, though the amount of fluorescence inside the cell does not increase as it does after Deltarasin treatment (compare figure 14B and figure 15B). The amount of fluorescence in the cytosol of the cells increased with time, demonstrating that the fluorescent Ras moves towards the endomembranes. Relocalization starts between 0 and 15 minutes after treatment. It continues in a linear fashion between 15 and 45 minutes after drug administration. During the last 15 minutes of monitoring the curve flattens out, meaning less

Kras relocates during that time. However, Kras is relocating during the entire period of the experiment and is not finished at its end point (figure 15B).

As a control transfected cells were treated with the highest amount of DMSO present in the experiments (figure 16).

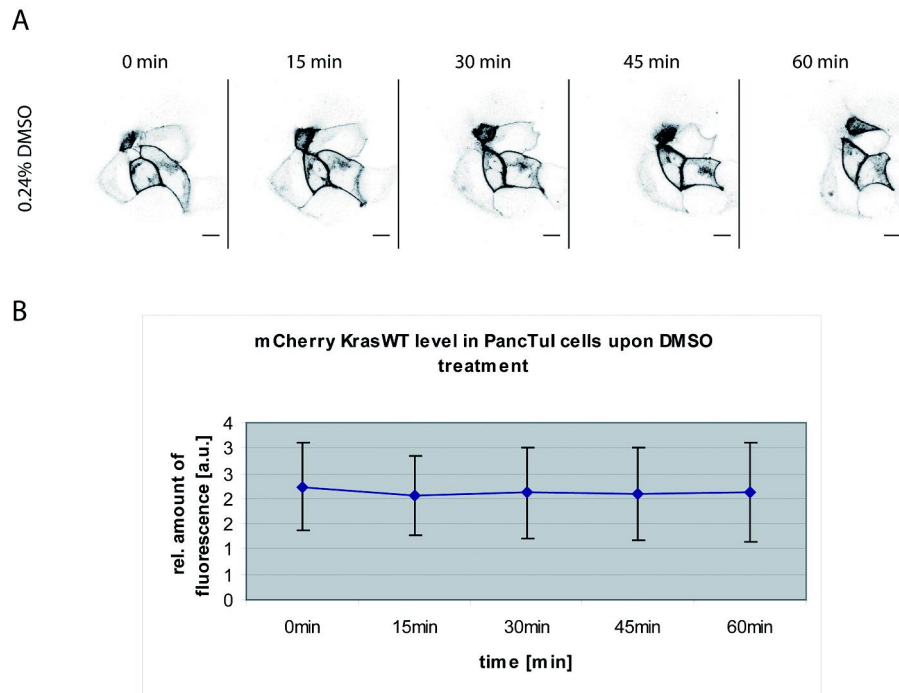


Figure 16: mCherry KrasWT relocation in PancTu1 cells upon treatment with DMSO

PancTu1 cells were transfected with mCherry KrasWT. One day after transfection the cells were treated with 0.24% DMSO and constantly observed with the microscope (A). One image was taken in three minutes. For further analysis the cells of interest were masked leaving the plasma membrane unmasked. The masks were used to measure only the cytosol of the cells by multiplication of the mask with the original image and measuring afterwards the intensity level of the area of each cell that was previously masked (amount of fluorescent Kras). The amount of fluorescence of each cell for five time points of the entire time of the experiments was determined; the average value of all cells analyzed was calculated for each time point and plotted in a diagram together with its standard deviation (B).

This experiment was repeated 3 times with doses of 0.2% or 0.24% DMSO. 11 cells were analyzed in total; scale bars 10 μm

Here, it can be seen that DMSO, even in the highest dose that was used in the complete set of experiments, has little effect on Kras localization in PancTu1 cells (figure 16). The curve that shows the average of all cells measured stays relatively flat meaning that Kras does not relocate in PancTu1 cells upon treatment with DMSO.

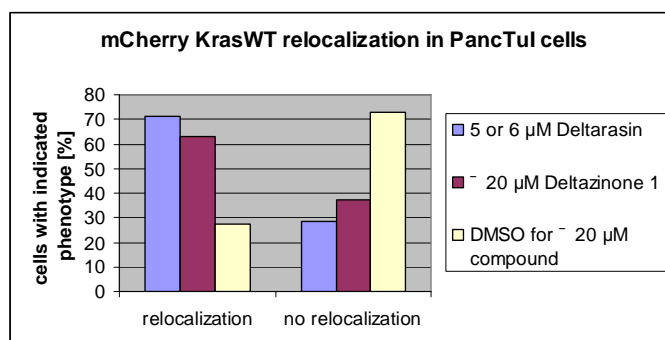


Figure 17: mCherry KrasWT relocalization in PancTuI cells

All cells that were analyzed (see also figure 14-16) were divided into 2 groups (relocalization/no relocalization) and the percentage of cells in each group was calculated. The results were plotted in a bar diagram.

28 cells taken from 5 experiments were analyzed for Deltarasin, 35 cells taken from 4 experiments were included for Deltazinone 1 and 11 cells taken from 3 experiments were used for the DMSO control.

All PancTuI cells that were analyzed in the previous experiments for relocalization effects of the compounds on mCherry KrasWT (figure 14-16) were divided according to their status of relocalization into two groups and subsequently the percentage of cells in each group was calculated. Afterwards the results were plotted in a bar diagram (figure 17). More than 70% of the cells exhibit relocalization of the fluorescent Kras when treated with Deltarasin. In Kras dependent PancTuI cells it is also possible to relocalize Kras with Deltazinone 1, provided the dose of the compound is high enough ($\times 20 \mu\text{M}$ Deltazinone 1 is required). More than 60% of the cells analyzed display relocalization. DMSO has only a mild impact (between 20% and 30% relocalization). The results are therefore not due to solvent effects and can be considered real.

Having established that two small molecule inhibitors for PDE mislocalize Kras verifiable, I was interested to determine whether Kras relocalization could also be caused in a model system closer to the in vivo situation than standard cell culture systems. Therefore, the system was changed to an organoid culture, a relatively new cell culture model system that approximates the in vivo situation more effectively than standard cell culture systems. Organoids are 3D multi-cellular structures originating from self-renewing and organ-specific stem or progenitor cells which give rise to differentiated cells. They have the great advantage of providing an accessible 3D system outside the organism in which cellular signalling can be studied in the presence of a near in vivo environmental niche. My aim was to investigate the phenotypic effects of the expression of endogenous levels of oncogenic KrasG12D in small

intestine organoids and to determine the manner in which they are affected by Deltarasin application.

7.5 Characterization of small intestine organoids

The organoids that were used for further experiments were isolated from two groups of mice. In the first group, one WT Kras allele was exchanged with mTFP-KrasG12D (hereafter δ Kras mice), the expression of which can be switched on using Cre recombinase. The second group were WT mice with the same genetic background (C57/B16) as the first group. To confirm the small intestinal origin of the organoids, they were sliced and placed on glass slides. After fixation with 4% PFA, immunofluorescence experiments with antibodies for different cell types of the small intestine were performed. Different types of cells populate the intestinal epithelium. Enterocytes (i.e. absorptive cells) and goblet cells (i.e. mucosecreting cells) are the most abundant cells. Scattered throughout the epithelium are other secretory cell types, such as enteroendocrine cells, which produce a diverse array of hormones. At the base of the crypt, the paneth cells reside. They secrete antimicrobial substances and nurture the ISCs (intestinal stem cells) living next to them in the crypt base (Clevers and Batlle, 2013).

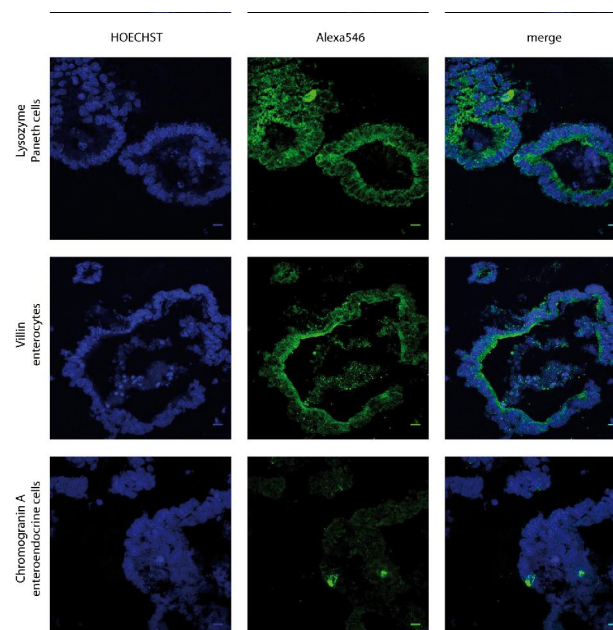


Figure 18: Detection of different marker cell types in small intestinal organoids

Organoids were embedded in a tissue freezing medium and frozen in liquid nitrogen. Afterwards they were cut into 6 μ m thick slices and placed on glass slides. After fixation with 4% PFA they were incubated with different antibodies overnight at 4°C. Antibodies were visualized using secondary antibodies coupled with Alexa546. Nuclei were stained with Hoechst dye.

Each staining was performed at least twice using the same conditions; scale bars 10 μ m.

Paneth cells, enterocytes and enteroendocrine cells were detected by immunofluorescence and are proof of the small intestinal origin of the organoids. The results also show that within the organoids differentiation of stem cells into small intestine-specific cells functions reproducibly (figure 18). Stainings for goblet cells and stem cells were unsuccessful although several antibodies and conditions for each of them were tested.

7.6 Infection with Cre recombinase leads to DNA recombination and expression of mTFP-KrasG12D protein in small intestine organoids

Small intestine organoids were isolated from WT mice serving as controls or from Kras mice (ΔKras organoids), where one WT Kras allele is exchanged by mTFP-KrasG12D and the expression of this can be switched on using Cre recombinase (figure 19).

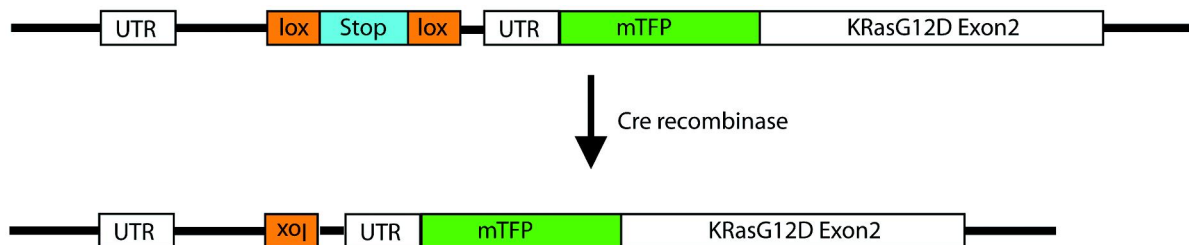


Figure 19: Switching mTFP-KrasG12D on via Cre-mediated recombination

Schematic representation of the mutated chromosome 6: the WT Kras allele was exchanged by mTFP-KrasG12D together with a lox-stop-lox site cloned in front (upper part). The resulting chromosome 6 when the stop site is excised after Cre recombination misses one of the loxP sites as well (lower part).

The stop codon (blue) prevents expression of the mutated gene. Once Cre recombinase is brought in it cuts at loxP sites (orange) - in this case before and after the stop codon - leading to recombination and therefore loss of the stop signal. The gene located after the stop signal can now be transcribed.

After successful recombination of Kras organoids, three kinds of organoids are available for experiments: WT organoids that harbour two WT alleles, Kras organoids harbouring both one WT allele and one allele that has not recombined, and Kras organoids infected with Cre recombinase that harbour one WT allele and one allele that has recombined and expresses the mutant mTFP-KrasG12D protein.

7.6.1 Cre-mediated DNA recombination in organoids to switch mTFP-KrasG12D expression on

In order to switch mTFP-KrasG12D expression on, single cells of Kras organoids were infected with retroviral particles produced by PlatE cells after transfection of those with pBABE-Cre. In addition to the Cre sequence, the viral particles contain a sequence for puromycin resistance. Thus, infected organoids were selected with puromycin to ensure Cre recombinase expression. Single organoids were picked at an early passage after infection by highly diluting the sample and their colonies were subsequently tested for mTFP expression to generate a culture of organoids where recombination could be assured. In a first step the organoids were monitored for traces of mTFP-expression using the wide field microscope. To confirm the results protein samples of organoids were prepared to be analyzed by Western Blot (see also figure 22) to monitor mTFP-KrasG12D protein levels and genomic DNA of the organoids was in parallel investigated by PCR for changes due to DNA recombination. The samples for the investigations were taken during passaging of the organoids, therefore the colonies were preserved.

First samples were taken two days after infection to examine changes at the DNA level due to DNA recombination (figure 20, upper part). After recombination, one of the loxP sites will be excised while the other loxP site will be flipped in orientation. The stop site in between them will also be excised. Therefore, the section of DNA on the mutated chromosome between the first exon (bearing an untranslated region, UTR) and the second exon (containing an UTR and the mTFP-KrasG12D mutation) will be shorter after recombination (figure 11, upper part). After extraction of DNA of the different organoids there are four characteristic DNA markers that can be monitored. First, the presence of the proximal loxP site; second, whether the distal loxP site has flipped; third, whether the sequence for mTFP is present in mutant organoids; and fourth, the distance between first and second UTR (in front of the mTFP sequence in mutant organoids). Following extraction of genomic DNA of the infected sample as well as of non-infected WT and Kras organoids, a panel of 4 different PCR combinations was performed (figure 20, lower part).

A first set of primers was used to identify the proximal loxP site in Kras organoids. A control band that would be present in all kinds of organoids was additionally amplified (figure 20, lox). The primers to identify the loxP site bind in the intron area in front of the proximal loxP site and directly after this site in the region containing the stop signal (figure 20, upper part). If all cells of an organoid are infected with Cre recombinase and recombination has also taken

place in all cells, the band identifying the loxP site (428 bp) should disappear as one binding site of the primers gets lost together with the loxP site and the stop signal (figure 20, upper part). The band should also not be detected in WT organoids as their DNA does not contain the lox-stop-lox site. The gel picture (figure 20, lox) shows precisely the results predicted. No band of a size of 428 bp is found in WT organoids, but a band of that size is evident in Kras organoids, showing that they possess the loxP site. After infection with Cre recombinase, the 428 bp band is no longer present in Kras organoids, but when infected with an empty vector control, the band remains. The control band (335 bp) to ensure the PCR is working effectively is present in all samples and amplifies the CD79b wild type allele (nt 17715045-17714730) on Chromosome 11.

Another combination of primers was employed to demonstrate the presence of the knock in allele in Kras organoids. A control band that would be present in all kinds of organoids was additionally amplified (figure 20, KI). The primers to detect the knock in allele bind within the region containing the stop sequence near the distal loxP site and in the intron area between the distal loxP site and exon2 (figure 20, upper part). After Cre recombination, it is to be expected that the band for the knock in allele (388 bp) will disappear if recombination has taken place in all cells of the organoids investigated. This is due to the fact that the distal loxP site remains, albeit flipped in orientation and the stop site in between the loxP sites will disappear and so does the binding site for one of the primers. The band should also not be detected in WT organoids as they do not possess the lox-stop-lox sequence and therefore one of the binding sites for the primers is missing. Again, the gel picture shows precisely the predicted results (figure 20, KI). No band of a size of 388 bp is found in WT organoids and a band of that size is present in Kras organoids, meaning they have the KI allele. After infection with Cre recombinase, the 388 bp band in Kras organoids disappears, but when infected with an empty vector control the band remains. The control band (585 bp) to ensure the PCR is working effectively is present in all samples and amplifies the CD79b wild type allele (nt 17714036-17714620) on Chromosome 11.

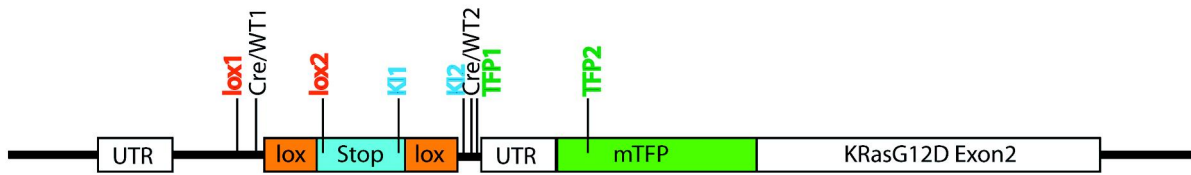
The presence of the mTFP coding sequence was verified by PCR using a different set of primers (figure 20, TFP). They bind in the intron area in front of exon2 and in the coding sequence for mTFP, which should be present in all organoids derived from Kras mice but not in WT organoids (figure 20, upper part). Consequently, a band showing the presence of the mTFP sequence (412 bp) was found in all organoids derived from Kras mice, whether they were infected with Cre recombinase, empty vector or not infected at all, showing that the

mutant Kras allele was present (figure 20, TFP). The control band (585 bp) to ensure the PCR was working effectively was found in all samples and amplifies the CD79b wild type allele (nt 17714036-17714620) on Chromosome 11.

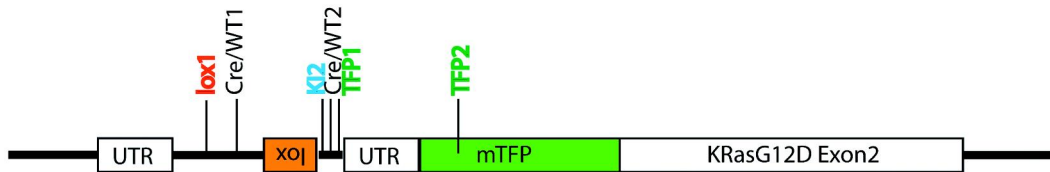
Another set of primers allowed me to distinguish between the WT allele and the Kras allele after recombination (figure 20, Cre/WT). The primers bind in the intron area between exon1 (first UTR) and exon2 (second UTR) and flank the lox-stop-lox element in mutant organoids (figure 20, upper part). Thus, the distance between the first and second UTR (in front of the mTFP sequence in mutant organoids) is monitored. After recombination has taken place, one of the loxP sites will no longer be present and the stop site that was located in between the two loxP sites will also disappear. Therefore, the section of DNA between the first UTR and the second UTR will be shorter than previously on the mutated chromosome (figure 20, upper part). The PCR setup is chosen in such a way that amplification can take place if the fragment size does not exceed 350 bp. WT DNA therefore always gives a band (267 bp) as it has the smallest fragment size. It serves as an internal control because all organoids that are used have a heterozygous background containing a WT allele. After infection with Cre recombinase, an additional band was observed (Kras + Cre) demonstrating that recombination took place (321 bp). In Kras organoids not infected with Cre recombinase the fragment on the mutant chromosome that has to be amplified is too large. Although both binding sites for the primers are present the PCR conditions were chosen in a way that it does not result in any product. The gel picture shows precisely the results predicted (figure 20, Cre/WT). There is no band of a size of 321 bp seen in WT organoids and no band of a size of 321 bp found in Kras organoids, but both possess a band of a size of 267 bp for the WT allele. After infection with Cre recombinase, the 321 bp band appears in Kras organoids, but when infected with an empty vector control no band of a size of 321 bp is detected. Only the control band (267 bp) for the WT allele can be found.

Overall the results of this experiment show that Cre-mediated DNA recombination of Kras organoids in order to switch on mTFP-KrasG12D expression was successful.

Kras conditional KI allele



Kras constitutive KI allele → after Cre recombination



WT

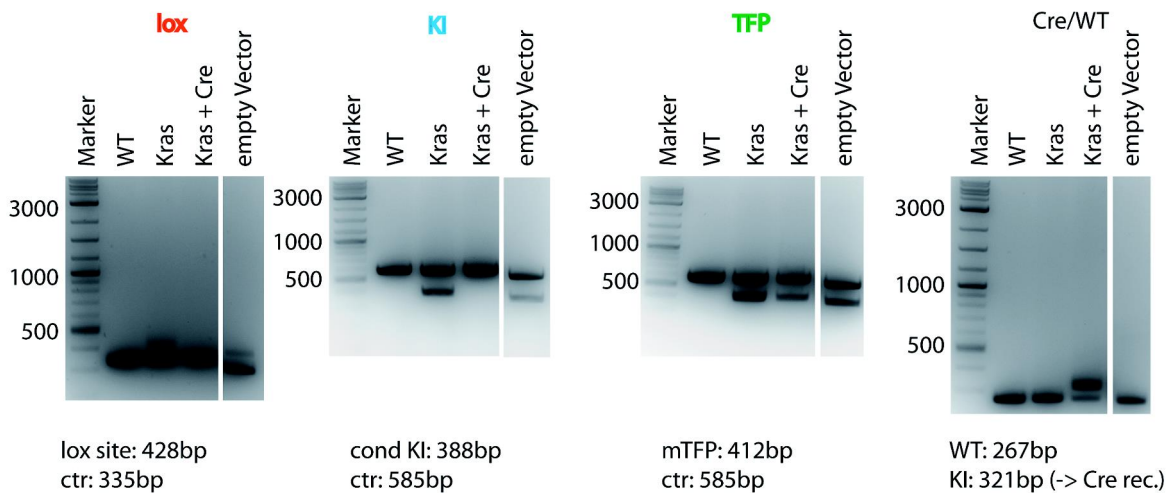
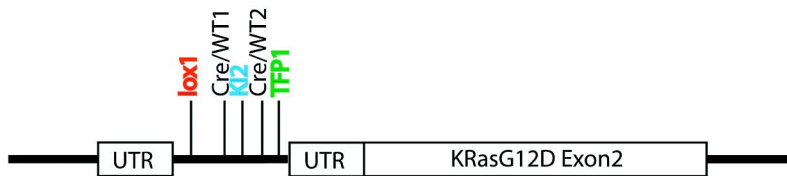


Figure 20: Genotyping of organoids

Upper part: Schematic representation of potential states of mouse Chromosome 6 and the binding sites of the primers (KI allele = knock in allele)

Lower part: PCR results obtained after investigation of genomic DNA of WT and Kras organoids and Kras organoids infected with Cre recombinase or infected with an empty vector control

Performed six times, empty Vector control included the last two times.

7.6.2 mTFP Kras expression in organoids

In order to demonstrate the existence of mTFP-KrasG12D protein in a population of organoids Western Blot experiments were performed (figure 21A). An additional band around 50 kDa appeared in the lane containing protein samples of Kras organoids after staining the blot membrane for all Ras isoforms. This is the region where mTFP-Kras is expected to be detected in Western Blots. The additional band for mTFP-KrasG12D was observed even without infection with Cre recombinase (lane δ Kras δ). 1 week after infection the signal was slightly elevated (figure 21B). GAPDH served as a loading control. The stop signal appears to leak as it does not completely shut the expression of mutant mTFP-KrasG12D down, explaining the band in the lane where organoids without infection with Cre recombinase were investigated. The signal intensity did not increase to a great extent (lane δ Kras + Cre δ), although recombination was verified for all organoids that were investigated in the sample (compare figure 20 δ Kras + Cre δ) as the lysates for control of DNA recombination and mTFP-KrasG12D protein levels were taken and investigated in parallel.

However, Western Blots only illustrate the condition in a population of organoids/cells. Single cells cannot be investigated by this method. If large differences occur between the cells/organoids of one sample a medium value will be observed in Western Blot, giving the impression of nothing or not much happening in the sample which may not be true. Thus, it may not be the best method to examine a system containing different cell types.

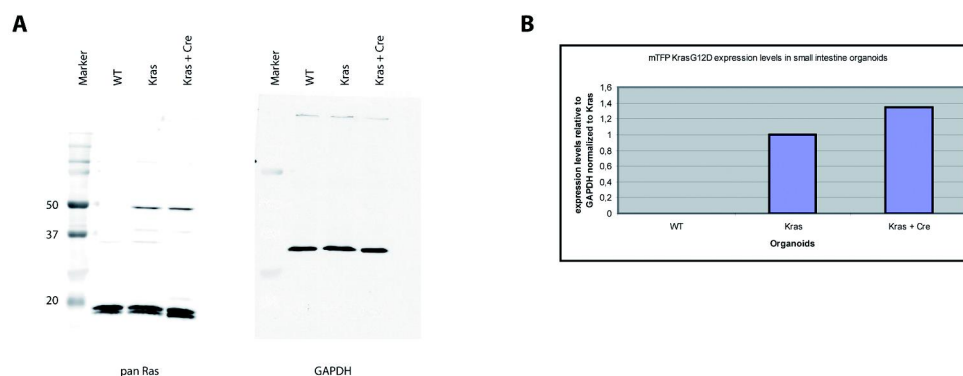


Figure 21: mTFP-KrasG12D in organoids

Western Blot (A) and its quantification (B) to detect mTFP-KrasG12D protein in organoids (WT, Kras control and Kras organoids 1 week after infection with Cre recombinase, GAPDH as loading control). 20 μ g protein loaded per lane. 1st antibody rabbit anti panRas 1:1000 and mouse anti GAPDH 1:1000 in Licor Buffer, 2nd antibody anti rabbit IR680 1:10000 and anti mouse IR800 1:10000 in Licor Buffer

Western Blots were performed three times with lysates taken once in two weeks.

The data of three independent Western Blot experiments were taken for quantification. It was investigated whether mTFP-KrasG12D protein levels in Kras organoids increased after Cre-mediated recombination (figure 22). All experiments were normalized to the expression levels of mTFP-KrasG12D in untreated Kras organoids. Thus, that condition lacks an error bar. In WT organoids mostly background was measured and nearly no signal could be detected. This was expected and the error bar is therefore relatively small. Kras organoids infected with Cre recombinase (Kras + Cre) display an increase in signal compared to Kras organoids that were untreated (Kras). T tests (2 sided and paired) were performed to test the results for significance. The values obtained were 2.27×10^{-5} for WT and Kras and 0.05 for Kras and Kras + Cre. The results are significant.

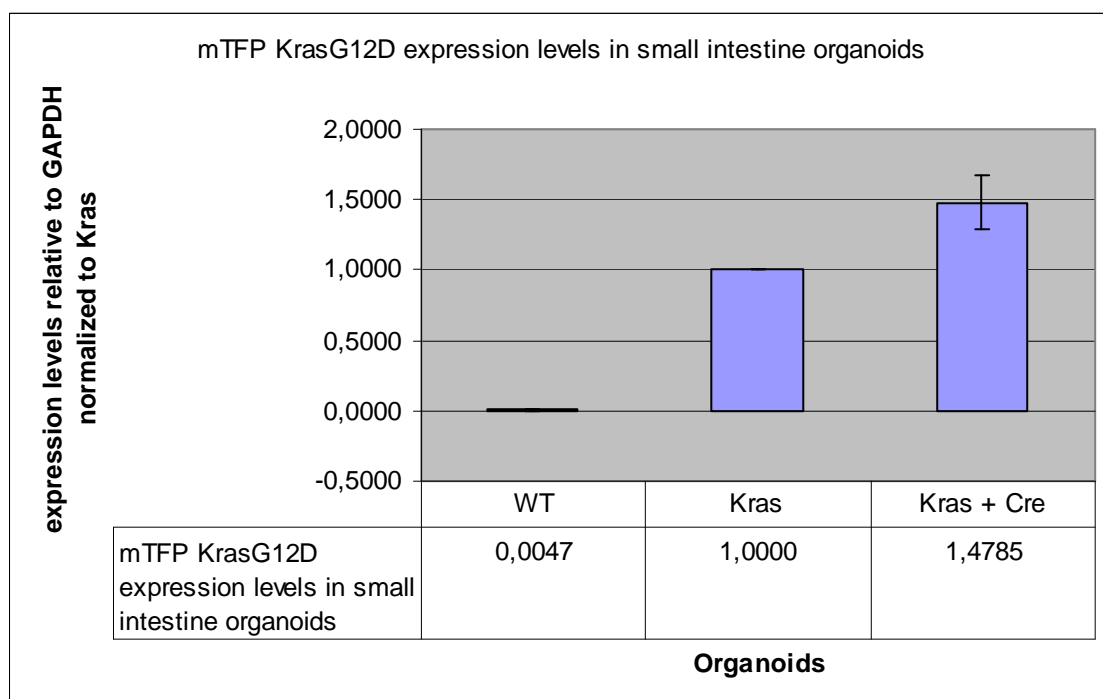


Figure 22: Quantification of mTFP-KrasG12D levels in organoids

Western Blot quantification of mTFP-KrasG12D protein levels in organoids (WT, Kras control and Kras organoids after infection with Cre recombinase, GAPDH as loading control) calculated of three independent experiments.

T tests (2 sided and paired) were performed in order to find out if the results were significant. The values obtained were 2.27×10^{-5} for WT and Kras and 0.05 for Kras and Kras + Cre.

The diverse organoids were investigated applying different microscopic approaches to demonstrate all of them displayed a normal morphology and to detect possible differences in expression levels of mTFP-KrasG12D between organoids or single cells of those after recombination (figure 23 and figure 24).

When investigated with wide field microscopy all groups of organoids demonstrated typical budding structures in the transmission light channel. Only after Cre-mediated recombination organoids displayed a discrete signal located at the plasma membrane in the TFP channel, while in WT and untreated Kras organoids none or slight background fluorescence could be detected in that channel (figure 23, wide field). Different patterns of mTFP expression (see also figure 22 and 24) were found during analysis of the organoids, which was the reason for constant monitoring of them. This ensured that the DNA level of recombination was complete and that different cultures were not erroneously mixed. In morphology no distinctions could be made between the three groups and they grew with the same speed.

Single Plane Illumination Microscopy (SPIM) was applied to investigate complete organoids the nuclei of which were stained with Hoechst dye and that were immunostained with a panRas antibody, labelled with a secondary antibody coupled with Alexa 546. Additionally, mTFP levels could directly be investigated with the setup (figure 23, digital light sheet).

The immunostaining for panRas was successful (for all organoids that were investigated) and most Ras could be detected at the plasma membranes of the organoids cells. TFP signal and Alexa 546 signal, which labelled panRas, overlapped in Kras organoids after recombination (figure 23). In WT and Kras organoids there was nearly no signal in TFP channel to be detected. These findings already gave another hint that the fluorescence signal in the TFP channel detected in mTFP-Kras organoids arose mainly from mTFP-KrasG12D expression rather than from background fluorescence (figure 23, digital light sheet).

The overview in SPIM and 3D reconstructions (data not shown) also confirmed the correct morphology of the small intestine organoids.

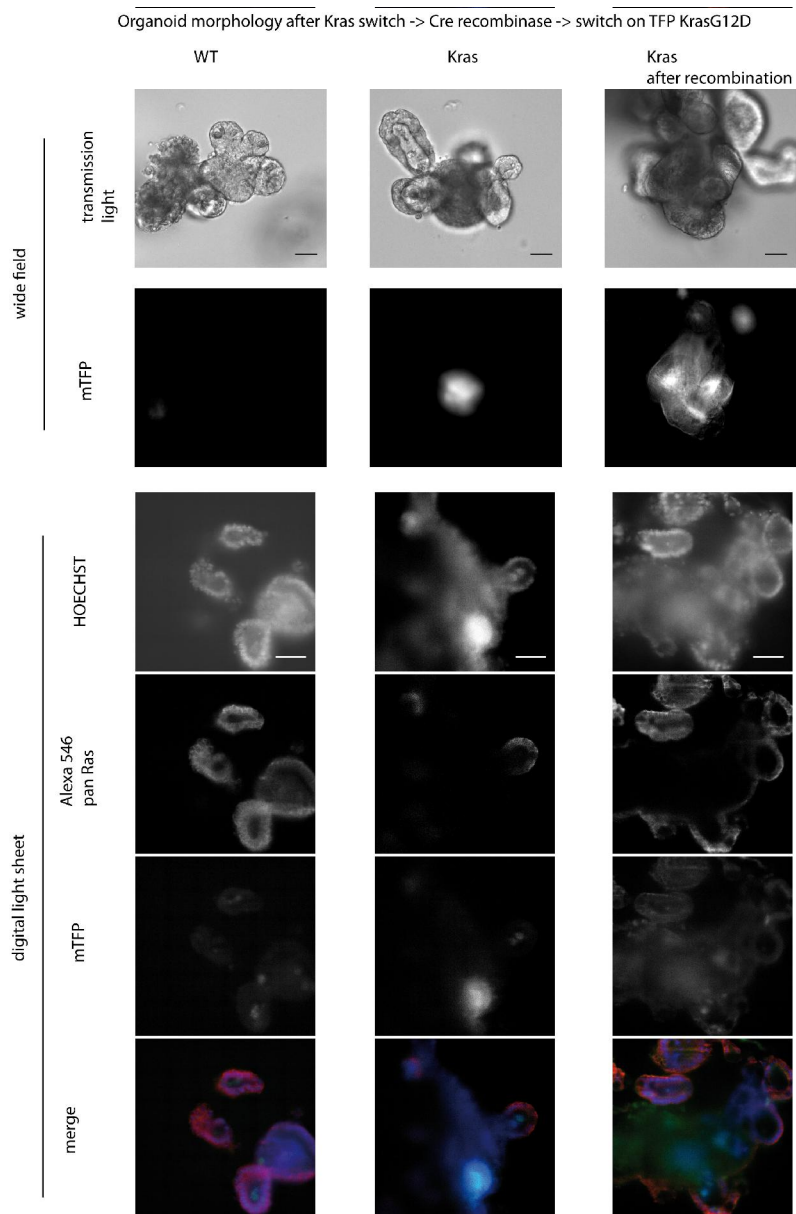


Figure 23: mTFP-Kras G12D and panRas in organoids

Wide field: living WT, Kras and Kras organoids after infection with Cre recombinase are investigated with the Leica DMRIB. The experiment was performed two times, each time three to five different organoids were monitored; scale bars 50 μm

Digital light sheet: complete organoids were fixed with 4% PFA and stained over night with a panRas antibody. All staining steps were performed in PBS with 5% BSA, 0.02% TritonX100 and 0.05% Tween20. The first antibody was used in a 1:200 dilution; the secondary antibody was Alexa546 goat anti rabbit and used in a 1:1000 dilution. Hoechst staining was performed in PBS with 0.1 $\mu\text{g/ml}$ Hoechst dye. For SPIM the Leica SP8 was used with a 25fold magnification objective. Before investigation samples were embedded in 1% low melting point agarose in glass bottom dishes. The experiment was performed two times, a complete set of data with all conditions was acquired only the second time; scale bars 50 μm

In order to characterise the exact localization of mTFP-KrasG12D and the Ras proteins stained with the panRas antibody 400x400 pixel from pictures in highest resolution used in figure 23 (WT, Kras after recombination) and from another picture of the Kras stack (Kras) that had been used for figure 23 were taken and analyzed in high magnification (figure 24).

In all cases the signal for the panRas antibody could mostly be detected at the plasma membranes and co-localized with the mTFP-KrasG12D signal in Kras organoids after recombination (figure 24). In WT and Kras organoids no such TFP signal was found. Therefore, the fluorescence signal at the plasma membrane in the TFP channel detected in mTFP-Kras organoids arose from mTFP-KrasG12D expression.

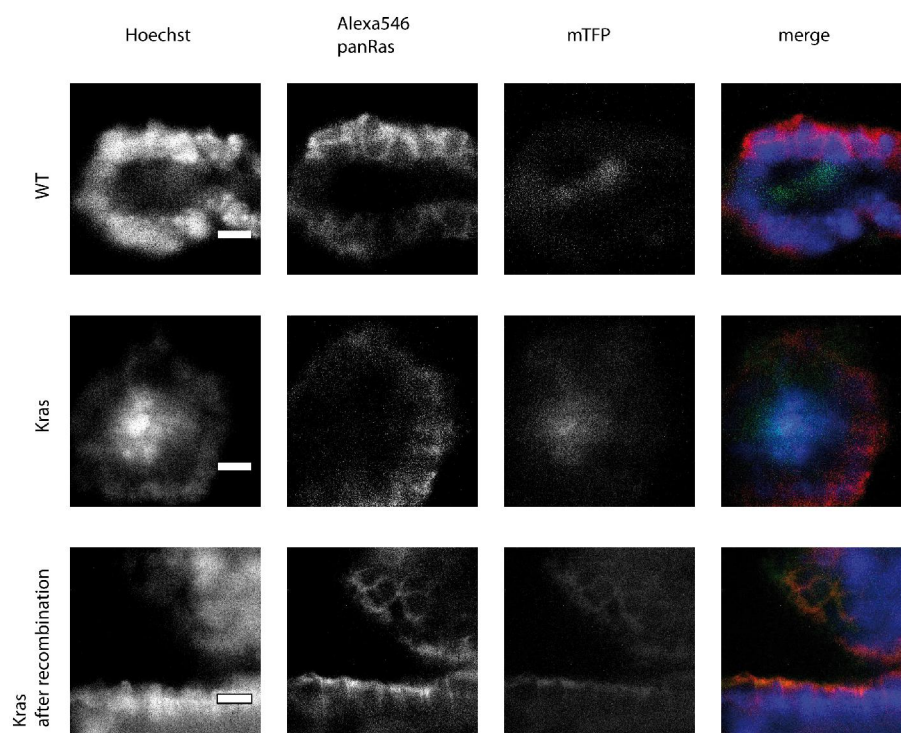


Figure 24: mTFP-Kras G12D and panRas in organoids in high magnification and resolution

Complete organoids were fixed with 4% PFA and stained over night with a panRas antibody. All staining steps were performed in PBS with 5% BSA, 0.02% TritonX100 and 0.05% Tween20. The first antibody was used in a 1:200 dilution; the secondary antibody was Alexa546 goat anti rabbit and used in a 1:1000 dilution. Hoechst staining was performed in PBS with 0.1µg/ml Hoechst dye. For SPIM the Leica SP8 was used with a 25fold magnification objective. Before investigation samples were embedded in 1% low melting point agarose in glass bottom dishes.

400x400 pixel taken from pictures used in figure 23 (WT, Kras after recombination) and one other picture of the Kras stack used for figure 23 in highest resolution to get a part of the image that can be analyzed in high magnification; scale bars 10 µm.

7.7 Deltarasin causes mTFP-KrasG12D relocalization in small intestine organoids

After demonstrating that mTFP-KrasG12D was present in the organoids following Cre-mediated DNA recombination and located correctly at the plasma membrane of the single cells I was interested in investigating whether it could be mislocalized subsequent to exposing the organoids to Deltarasin. To do so, I performed live cell imaging experiments with organoids displaying a good expression of mTFP-KrasG12D using the SPIM setup. This was an entirely new method for the whole institute and therefore had to be established first. Not only had the dose of Deltarasin needed been unknown but also the conditions how to perform the experiment. Organoids are a multicellular system and require certain growth conditions. As observed before in experiments with 2D cell culture in such a system cells might protect their neighbours because cells of cancer cell lines did not react to treatment with any of the compounds once they were too close to confluency (Holger Vogel and Dina Truxius, personal communication).

Doses of 7.5 μM Deltarasin, 10 μM Deltarasin and 15 μM Deltarasin and respective DMSO controls were used to find out how much of the compound would be sufficient to relocalize mTFP-KrasG12D from the plasma membrane towards the endomembranes. mTFP-KrasG12D could be relocalized with all amounts of Deltarasin that were used in a dose dependent manner. Subsequent to addition of the drug relocalization started to be visible after 10 to 15 minutes for 10 μM Deltarasin and after 5 minutes for 15 μM Deltarasin respectively (data not shown). However, the drawback in both cases was the strong effects the DMSO controls had on Ras localization. The DMSO control for 15 μM Deltarasin displayed behaviour similar to the sample containing the compound. In case of the DMSO control matching 10 μM Deltarasin there were differences in relocalization times but the control behaved way too much like the sample containing Deltarasin to draw any clear conclusions. Results where DMSO control and Deltarasin samples displayed a different behaviour, at least for more than 60 minutes, could be obtained with 7.5 μM of the drug (figure 25). 20 minutes after Deltarasin administration first relocalization effects were observed. 40 to 60 minutes after addition of the compound relocalization became more pronounced while the DMSO control displayed no relocalization during the entire timeframe between 0 minutes and 60 minutes. From 90 minutes onwards the organoids which were treated with either Deltarasin or DMSO displayed shrinkage. Relocalization was observed in Deltarasin treated samples and also in DMSO treated samples by that time. At 120 minutes and later time points sample and control looked alike (figure 25).

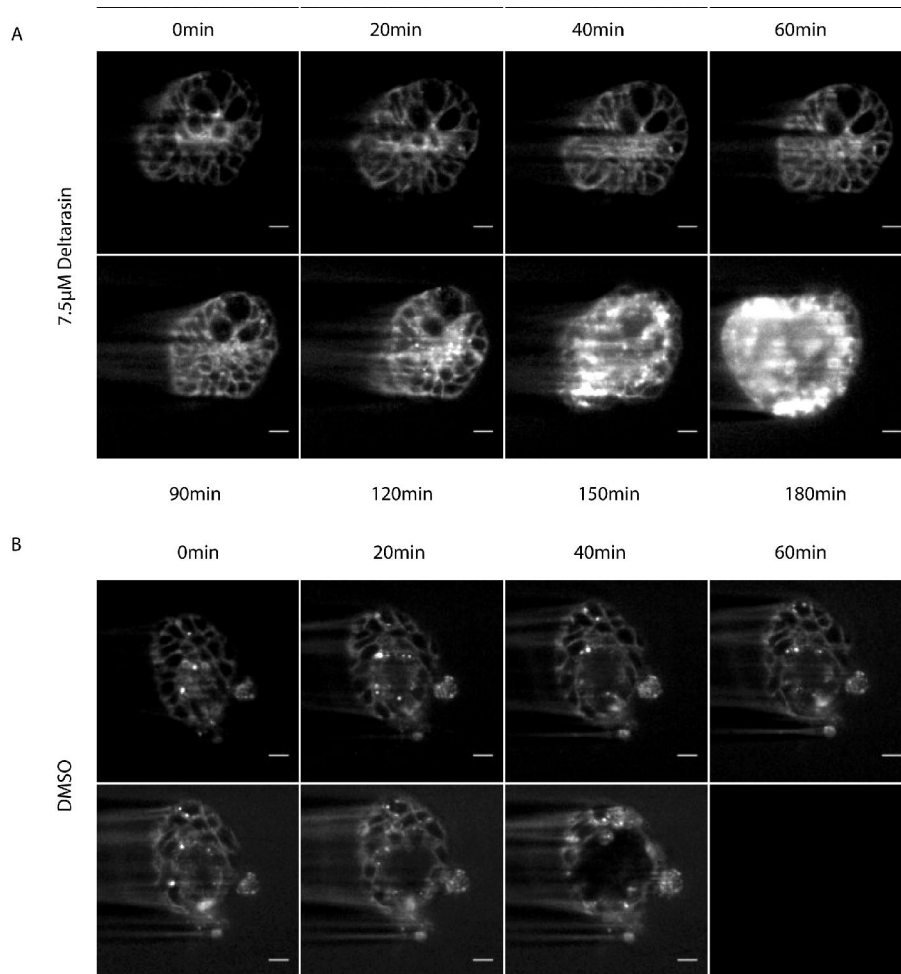


Figure 25: Relocalization of mTFP-Kras G12D in small intestine Organoids upon Deltarasin administration

Organoids that displayed recombination and Kras expression were seeded onto FEP tubes in glass bottom dishes. One day later medium was exchanged by imaging medium (contains HEPES) cells were treated with 7.5 M Deltarasin or DMSO and constantly observed with the Leica SP8 in DLS mode using a 25fold magnification Objective. One stack of pictures was taken in five minutes during the first hour of investigation. Afterwards one stack of pictures was taken in ten minutes. The organoids were observed for 2.5h or 3h; scale bars 10 μm.

This experiment was performed 4 times with 7.5 μM Deltarasin, 3 times with 10μM Deltarasin and 1 time with 15μM Deltarasin. The higher doses were used to find out the amount of Deltarasin that is needed to relocalize mTFP-Kras G12D in Organoids in this particular kind of experiment (data not shown).

In order to see the exact localization of mTFP-KrasG12D 200x200 pixel from pictures in highest resolution used in figure 25 were taken to be analyzed in high magnification (figure 26).

20 minutes after treatment with Deltarasin relocalization of mTFP-KrasG12D was observed and the effect became more pronounced over time. 90 minutes after addition of Deltarasin

first cells started to show signs of cell death. 150 minutes after treatment cell death was massive and started to impede the observation of Ras relocalization. DMSO only had mild effects on Ras localization. But cell death started to show first signs between 90 and 120 minutes after addition of DMSO to the medium with Ras relocalization as an additional consequence (figure 26). Nevertheless, the results of the experiment clearly show that Deltarasin is capable to relocalize mTFP-KrasG12D in small intestine organoids.

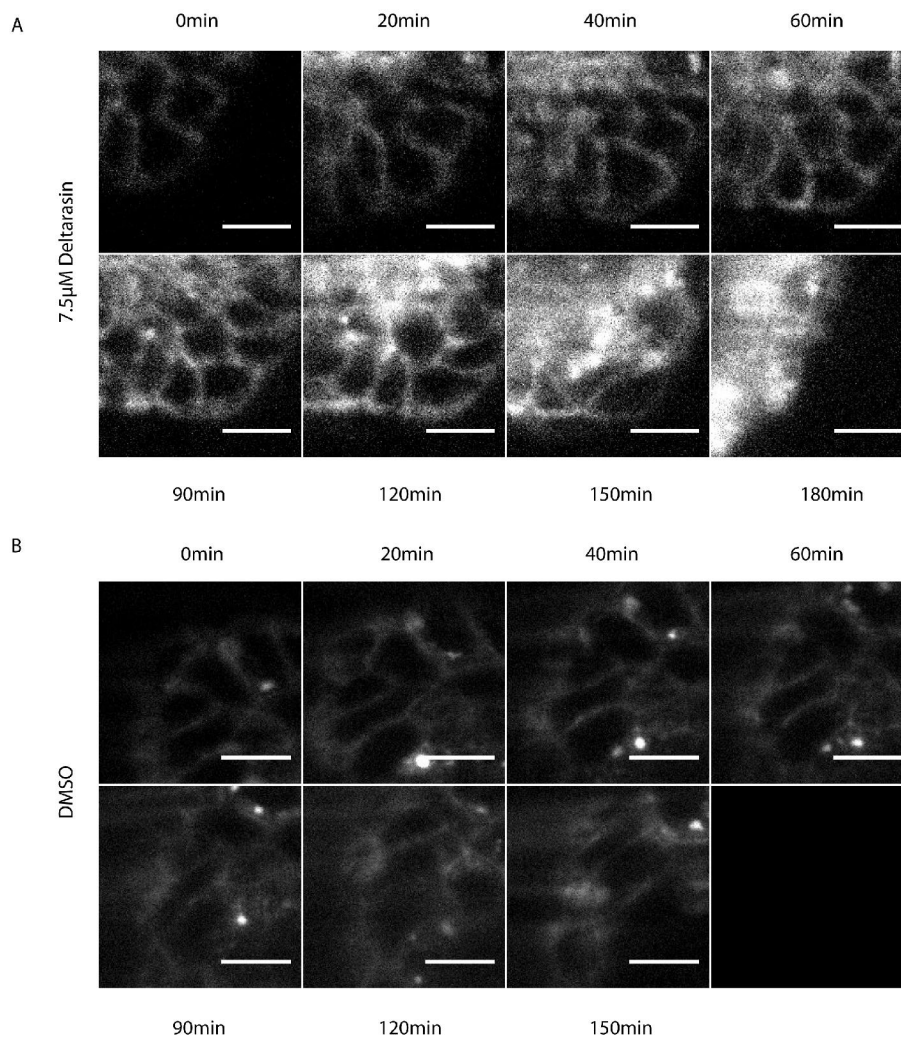


Figure 26: Relocalization of mTFP-Kras G12D in small intestine Organoids upon Deltarasin administration in high magnification and resolution

Organoids were treated with 7.5 μ M Deltarasin or DMSO and constantly observed with the Leica SP8 in DLS mode using a 25fold magnification Objective. One stack of pictures was taken in five minutes during the first hour of investigation. Afterwards one stack of pictures was taken in ten minutes. The organoids were observed for 2.5h or 3h.

200x200 pixel were taken from pictures used in figure 25 in highest resolution to get a part of the image that can be analyzed in high magnification; scale bars 10 μ m.

8 Discussion

This work investigated whether human cancer cells from different tumour origins and murine small intestine organoids are affected by the PDE inhibitor Deltarasin and a new PDE inhibitor called Deltazinone 1. Using state of the art microscopy, the localization of (K) Ras in space and time was acquired and analyzed. In addition it was determined whether there are any differences between Kras-dependent and -independent cell lines in Ras localization after chronic perturbation by PDE inhibition. The overall goal was to ascertain whether PDE constitutes a valid target for inhibiting oncogenic Kras-dependent signalling through interference with Kras localization, and to confirm that PDE inhibition results in Ras relocalization from the plasma membrane towards the endomembranes.

8.1 mCherry Kras^{WT} and mCitrine Hras^{G12V} relocalize in parallel in MDCK cells upon PDE δ inhibition by Deltarasin but not by Deltazinone 1

It was already known that in pancreatic ductal adenocarcinoma cells, fluorescently labelled Kras relocalizes from the plasma membrane towards the endomembranes upon treatment with the PDE inhibitor Deltarasin (Zimmermann et al., 2013) and that PDE inhibition also mislocalizes Hras (Chandra et al., 2012). Whether both Ras isoforms would relocalize from the plasma membrane towards the endomembranes in a similar manner if studied in parallel was unknown and investigated in this work. To test this, live cell imaging experiments were carried out in Kras-independent MDCK cells transfected with both fluorescently labelled Ras isoforms. Upon treatment with 5 μ M Deltarasin, both Ras isoforms indeed mislocalized in parallel (figure 10). Treatment with up to 20 μ M of the more specific PDE inhibitor Deltazinone 1 resulted in Hras relocalization, but Kras remained at the plasma membrane (figure 10).

Localization of Kras and Hras is dependent on PDE as part of the respective cycle (Schmick et al., 2015). Deltarasin and Deltazinone 1 affect the localization of (K)Ras at the plasma membrane by competitively binding to the prenyl-binding pocket of PDE. Deltarasin also binds to different G-protein coupled receptors, ion channels and transporters, but unspecific binding partners for Deltazinone 1 that could cause cytotoxic side effects are not known (Papke et al., 2016). Consequently, Deltazinone 1 caused specific cell death without displaying any general cytotoxicity for concentrations up to 24 μ M, while Deltarasin exhibits cytotoxic effects at concentrations above 9 μ M in all tested cell lines (Papke et al., 2016). All these unspecific interactions of Deltarasin may in some part affect Ras localization by

interfering with cell cycle events or other pathways which have a regulatory impact on Ras signalling and survival of the cell in general via crosstalk. PI3K/Akt and MAPK signalling pathways, for example, are connected via crosstalk in multiple ways. Deltarasin could simultaneously hit some regulatory proteins of both pathways in parallel to exhibit cytotoxic effects and further affect Ras localization by blocking the binding pocket of PDE . It is known that PI3K positively regulates the Ras/MAPK cascade to facilitate maximal ERK responses to physiological stimuli. The PI3K/Akt pathway is in turn negatively controlled by activated ERK. Cancer cells are able to evade apoptosis if just one of the pathways is therapeutically blocked as crosstalk leads to activation of compensatory signalling of the other pathway. Thus cancer cell growth can be more efficiently suppressed by blocking PI3K and MAPK in parallel rather than targeting components of each pathway alone (Aksamitiene et al., 2012). This finding strongly suggests that Deltarasin hits both pathways simultaneously. On the one hand it blocks PDE , leading to Ras relocalization and therefore down regulation of PI3K and MAPK pathways. On the other hand proteins of the cascades may itself be targets of Deltarasin e.g. G-protein coupled receptors in PI3K signalling and thus the pathways are down-regulated in more than one way in parallel. If Deltazinone 1 is not capable of hitting additional targets it may not have such strong effects on cells which would at the end be fatal for them. Nevertheless, the pathways are impaired upon Deltazinone 1 treatment, because Ras relocalization takes place although to a lesser extent compared to Deltarasin, and thus cells may display growth arrest or grow slower.

In all probability, Deltarasin also hits additional targets as it displays cytotoxic effects at concentrations above 9 μ M (Papke et al., 2016). Exposition of cells to Deltarasin results in cell death occurring sooner for higher doses than for lower ones. As cells shrink during apoptosis internalisation of plasma membrane to form cytoplasmic vesicles occurs and is followed by Ca^{2+} -dependent trafficking of some of these vesicles back to the cell surface, leading to phosphatidylserine externalisation. It is assumed that the vesicles formed upon internalisation as cells shrink may not traffic to specific compartments as ordinary endocytic vesicles would (Lee et al., 2013). Therefore, proteins that usually localize at the plasma membrane - including Ras isoforms δ may also relocalize towards the inner part of the cell. As Deltarasin also affects the localization of Ras at the plasma membrane by competitively binding to the prenyl-binding pocket of PDE , this will lead to relatively strong relocalization effects of Ras during death of the cells. Cytoplasmic vesicles also explain the relocalization effect that could be observed when cells shrink upon treatment with DMSO.

In the Kras-dependent cell line PancTuI, it has also been shown that Deltarasin is more efficient in down regulating Erk phosphorylation than Deltazinone 1. Therefore, it is likely either that Deltarasin has a tighter interaction with PDE in comparison to Deltazinone 1 or that Deltazinone 1 is more efficiently displaced from PDE by Arl2 activity in comparison to Deltarasin. If the latter point was true as a consequence more free PDE available at steady state can reinstate localization of Kras at the plasma membrane. This would explain why higher doses of Deltazinone 1 than Deltarasin are needed to affect oncogenic Kras localization in cells and subsequently signalling to counter the allosteric displacement activity of Arl2 (Papke et al., 2016).

For Hras, the dose of Deltazinone 1 that is required for relocalization appears to be lower than for Kras (figure 10). A dose of 20 μ M Deltazinone 1 is sufficient to relocalize Hras in Kras-independent cells in such a way that the effect can be seen with the naked eye. This may be due to the structural differences between Kras and Hras. While Kras displays a relatively strong electrostatic interaction with negatively charged membranes because of its polybasic stretch (Schmick et al., 2014), Hras contains two cysteines in place of the stretch and these cysteines can be reversibly palmitoylated (Hancock et al., 1989). When it is depalmitoylated, Hras is able to interact with PDE via its farnesyl tail, leading to its solubilisation (Schmick et al., 2015). This binding can be prevented by palmitoylation (Chandra et al., 2012), which is controlled by the activity of palmitoyl transferases (PATs) (Rocks et al., 2005; Rocks et al., 2010; Goodwin et al., 2005) and the depalmitoylating activity of acyl protein thioesterase (APT) 1/2 (Vartak et al., 2014; Dekker et al., 2010). APT activity is ubiquitous while PAT activity is localized to the Golgi apparatus. Consequently, depalmitoylated Hras can be kinetically trapped at the Golgi apparatus and directed to the plasma membrane via the secretory pathway (Schroeder et al., 1997; Schmick et al., 2015). Once palmitoylation is lost, solubilisation of Hras via binding to PDE keeps its cycle running. Although Hras has trapping compartments inside the cell (plasma membrane and Golgi apparatus), its entropic leakage may be higher in comparison to Kras. After loss of its palmitoylation, Hras may behave similarly to Rheb, which has no trapping compartment inside the cell and therefore displays quite high entropic leakage that must be compensated for by high countering activity of the PDE-Arl2 system (Schmick et al., 2015). In such cases, lower doses of PDE inhibitors are sufficient to relocalize the small GTPase.

8.2 Endogenous Ras relocates in Kras-independent cells upon PDE δ inhibition by Deltarasin in a dose dependent manner

Another question to be answered was whether endogenous Ras exhibits the same effects as observed for the over expressed fluorescently labelled constructs used in all previous experiments. Using immunofluorescence, different Kras-independent cancer cell lines were tested for relocalization of endogenous Ras upon treatment with different doses of Deltarasin for 24h (figures 12 and 13 in results). A dose dependent effect of Deltarasin on localization of endogenous Ras was observed and was shown to be statistically significant (figure 13 in results). As Ras cycles are general mechanisms and depend on PDE, these data were expected.

Deltazinone 1 was also examined for its ability to relocalize endogenous Ras in one of the cell lines (A431) that was used. The fact that cells reacted in DMSO controls with Ras relocalization to a similar extent to those in the actual samples with addition of Deltazinone 1 impedes interpretation of the results (figure 12). Any observed effect could be caused either by the compound or by the solvent. For Kras-independent cell lines it therefore remains ambiguous whether or not endogenous Ras could be relocalized by Deltazinone 1. With the doses typically used in the experiments in this work (10-20 μ M), no relocalization effect can be definitively viewed as certain in these cells. These data were unexpected, as Deltazinone 1 binds PDE in a similar manner to Deltarasin. The difference between the two compounds is the higher specificity and lower cytotoxicity of Deltazinone 1 (Papke et al., 2016). Both inhibitors are able to block the PDE binding-pocket to induce an interaction break between PDE and farnesylated cargo, which subsequently dilutes to endomembranes (Papke et al., 2016). The possibilities that Deltarasin has a tighter interaction with PDE in comparison to Deltazinone 1 or that Deltazinone 1 is more efficiently displaced from PDE by Arl2 activity in comparison to Deltarasin may be the key to this conundrum. If the latter point was true as a consequence more free PDE available at steady state can reinstate localization of Kras at the plasma membrane. Thus, higher doses of Deltazinone 1 than Deltarasin are needed to affect oncogenic Kras localization in cells and subsequently signalling to counter the allosteric displacement activity of Arl2 (Papke et al., 2016).

Another possibility is the induction of multi drug resistance (MDR) mechanisms in the cells, leading to displacement of the compound from the cells e.g. via pump mechanisms. MDR in combination with the possibility that Deltazinone 1 is more efficiently displaced from PDE by Arl2 activity than Deltarasin (Papke et al., 2016) could explain why A431 cells do not

react to treatment with Deltazinone 1, but exhibit Ras relocalization effects when treated with Deltarasin. Another interesting point to be addressed is the amount of compound that would be necessary to induce complete Kras relocalization. It was not possible to investigate this in detail with the A431 system as the solvent had already displayed an influence on Ras localization.

8.3 mCherry Kras^{WT} relocalizes in Kras-dependent cells upon PDE δ inhibition by Deltarasin and Deltazinone 1

Regulation of signal transduction and gene expression in cancer cells is very different in comparison to normal cells. This is a possible explanation for the fact that cancer cells may depend more on the activity of a specific oncogene than normal cells (Weinstein and Joe 2006). PancTuI cells are a Kras-dependent pancreatic ductal adenocarcinoma cell line. These cells are δ dependent on Kras for cell survival and maintenance of the malignant phenotype and therefore if Kras is affected in any way (e.g. through the use of a compound that changes its localization), it is likely to have dramatic consequences for the cells. To determine whether Kras dependency could be an important factor in conjunction with PDE δ availability, and potentially to discover whether a compound is capable of relocalizing Kras, the cell system was changed to PancTuI cells. This was necessary as the cell lines used in the previous experiments (MDCK, A431, DiFi) were all independent of Kras and came from varying backgrounds.

In RTCA experiments, PancTuI cells die when treated with 5 μ M Deltarasin and also react to addition of 10 μ M Deltazinone 1. However, Deltazinone 1 does not seem to induce death (cytotoxicity) here but rather a cytostatic effect, resulting in growth arrest (Papke et al., 2016). In live cell imaging experiments it was possible to demonstrate that transfected mCherry Kras^{WT} relocalizes in PancTuI cells from the plasma membrane towards the endomembranes upon treatment with 5 μ M Deltarasin and also upon treatment with doses \times 20 μ M of Deltazinone 1 (figure 17).

Kras relocalization using Deltazinone 1 can be observed in the first 30 minutes after addition of the drug with a dose four times as high as the equivalent dose of Deltarasin (figure 14). The effect that could be observed for treatment with Deltarasin is much stronger than for Deltazinone 1 (figure 15). It is likely that this is due to the additional targets hit by Deltarasin and the possibility that Deltazinone 1 is more efficiently displaced from PDE δ by Arl2 activity than Deltarasin (Papke et al., 2016; see above). As a result of the lower doses of

Deltarasin, the DMSO concentration in these samples was also lower, reducing the chance of possible side effects from the solvent.

As PancTuI cells are dependent on Kras, even the more specific inhibitor Deltazinone 1 induces growth arrest (Papke et al., 2016) and can lead to relocalization of Kras (figure 15) if the dose is sufficiently high.

Kras displays a relatively strong electrostatic interaction with negatively charged membranes which results in a very slow entropic leakage from the plasma membrane (slow off-rate) (Schmick et al., 2014). Already a low countering activity of the PDE β -Arl2 system is sufficient to reinstate its localization at the plasma membrane (Schmick et al., 2015). Therefore, PDE β saturating doses of inhibitors like Deltarasin or Deltazinone 1 are necessary to deplete the amount of available PDE β sufficient to delocalize Kras to endomembranes (figure 4 and figure 15). Relatively long incubation times with the inhibitors are required as relocalization to the endomembrane system after PDE β inhibition occurs somewhat slowly (Schmick et al., 2015). It takes approximately 30 minutes until the first effects of the compounds on Kras localization can be observed (figure 14 and 15). As Deltazinone 1 is possibly more efficiently displaced from PDE β by Arl2 activity than Deltarasin (Papke et al., 2016), the doses of Deltazinone 1 need to be higher than the dose of Deltarasin necessary to shut down the Kras cycle.

When the Kras cycle is disturbed in PancTuI cells, the MAPK and PI3K pathways will also be (partially) inhibited. It is very likely that the PI3K pathway is not able to compensate in this case, as in cancer cells the β -wiring diagram that regulates signal transduction and gene expression is not equivalent to that of normal cells (Weinstein and Joe, 2006). In terms of the oncogene addiction theory, the genetic streamlining theory could explain the results. This theory states that non-essential pathways are deactivated during tumour evolution to ensure that dominant pathways are not surrogated by compensatory signals. If dominant signals are abrogated, cells go into cell-cycle arrest or apoptosis (Torti and Trusolino, 2011). This is precisely what can be observed with the compounds in PancTuI cells. When treated with Deltarasin cells die, while Deltazinone 1 results in a cytostatic effect (Papke et al., 2016).

Concluding, a novel inhibitor class for PDE β , Deltazinone 1, with comparable potency to the previously developed Deltarasin but higher selectivity was characterised in 2D culture with regard to its effectiveness in Kras relocalization. Deltazinone 1 represents a more specific second chemotype of PDE β inhibitors and thus resembles a non-cytotoxic compound for future medicinal chemistry studies. As pharmacological characterization of Deltazinone 1

revealed that this compound is rapidly metabolized in mice, it is unsuitable for in vivo experiments (Papke et al., 2016). As Deltazinone 1 and Deltarasin both had a demonstrable effect on cell growth/survival, it appears that PDE constitutes a valid target for the pharmacological therapy of Kras-dependent tumours.

8.4 Why use small intestinal organoids?

Although they are generally used in preclinical cancer research, there is increasing evidence that 2D monolayers do not constitute the best system to test the efficacy of drugs. This is principally due to the fact that they do not accurately reflect the biological complexity of a tumour. 2D cultures lack the complex stroma-cancer interactions that can be cell-cell and cell-matrix interactions. Furthermore, they lack the architecture of the tissue and gradients in oxygenation, nutrition and pH that are present in tumours in vivo. This may explain why drugs that pass preclinical in vitro testing in 2D cultures later fail in patient studies (Zeeberg et al., 2016).

In the case of cancers like the pancreatic ductal adenocarcinoma (PDAC), the tumour's microenvironment is an important factor for metastatic spread, therapeutic resistance and carcinogenesis in general. Displaying a strong interplay between stromal components and tumour cells, the dense desmoplastic stroma of PDAC can represent as much as 90% of the total volume of the tumour (Zeeberg et al., 2016).

Three-dimensional (3D) cultures have a number of advantages over 2D monolayers as they more precisely reflect the bio-mechanical properties and structural design of the tumour and therefore they appear to represent a better model (Zeeberg et al., 2016). The differences between 3D models and 2D models can be seen in, for example, response of cells to growth factors and therapeutic treatment, as well as growth dynamics of the cells in general (Coleman et al., 2014).

Since the 1970s, it has been possible to keep normal cells and their malignant counterparts in 3D culture using a semi-solid matrix including components such as collagen, laminin and fibronectin. This allows epithelial cells to develop cell-matrix interactions simulating the basement membrane and polarized structures forming cell-cell contacts (Hwang et al., 2016). Comparison of the expression profiles of cells grown in 2D or 3D cultures revealed that cell-matrix interactions have a great impact on gene expression (Zschenker et al., 2012; Ghosh et al., 2005; Ridky et al., 2010; Hwang et al., 2016).

In this work, it was possible to verify in 2D cultures that two small molecule inhibitors which block the binding pocket of PDE mislocalize Kras. In a next step, they should be tested in a model system closer to the in vivo situation than standard cell culture systems.

In the last decade, an alternative in vitro 3D model for tissues has been developed: organoids. Adult stem cells self-organize in a 3D matrix into epithelial structures that resemble the respective organ of origin. The stem cells can be prepared from diverse adult tissues of human or mouse origin (Jung et al., 2011; Barker et al., 2010; Huch et al., 2013; Sato et al., 2009; Sato et al., 2011). The homeostatic environment of the normal tissue stem cells is mimicked and the organoid cultures are able to self-renew while remaining genetically stable and being long-term expanded (Sato et al., 2011; Huch et al., 2015).

Thus organoid culture represents a system where cellular signalling can be studied in an accessible 3D system outside the organism in the presence of a near in vivo environmental niche.

8.5 The mTFP-KrasG12D organoid system

Phenotypic effects of the expression of endogenous levels of oncogenic KrasG12D and the effects of Deltarasin application on Kras localization were investigated in murine small intestine organoids.

Organoids were isolated from two groups of mice: WT mice and Kras mice, in which one WT Kras allele is exchanged by mTFP-KrasG12D and this can be switched on using Cre recombinase. WT organoids were used as controls and organoids derived from Kras mice (ΔKras organoids) were infected with Cre recombinase to switch on mTFP-KrasG12D expression.

The isolation of organoids was successful and immunofluorescence data confirmed their small intestinal origin (figure 18). The combination and amount of paneth cells, enteroendocrine cells, goblet cells and stem cells (staining for stem cells and goblet cells was unsuccessful) are unique for the small intestine (Schuijers and Clevers, 2012; Clevers, 2013).

After DNA recombination took place in Kras organoids, three kinds of organoids were available for experiments: WT organoids that harbour two WT alleles, Kras organoids harbouring both one WT allele and one allele that has not recombined, and Kras organoids infected with Cre recombinase that harbour one WT allele and one allele that has recombined and expresses the mutant mTFP-KrasG12D protein. Successful recombination in Kras

organoids after infection with Cre recombinase was confirmed with a panel of four PCR reactions (figure 20). Infection with a control vector DNA did not result in recombination.

In mice when KrasG12D is expressed throughout the colonic epithelium from the endogenous genomic locus, it causes widespread hyperplasia typified by an extreme lengthening of the crypts in comparison to the wild-type colon and by the development of large, prominent goblet cells (Haigis et al., 2008). However, as the animals did not develop colon cancer (Haigis et al., 2008), it can be concluded that when activated from its endogenous locus, KrasG12D is sufficient to promote hyperplasia, but not neoplasia. It has also been shown that in this case KrasG12D is able to activate both Mek and Erk and to down regulate phospho-Akt (Haigis et al., 2008). The authors showed that all cells expressing KrasG12D also possessed high levels of phospho-Mek and despite the fact that Erk is its direct target, it is only found to be phosphorylated in the differentiated cells at the top of the crypt. Whether or not Mek can maintain a high steady state concentration of phosphorylated Erk appears to depend upon cell type (Haigis et al., 2008). The number of proliferative progenitor cells down in the crypts was also increased, which was suggested to be one of the causes of the colon's hyperplasia. The other cause was the activation of a Mek dependent pathway via KrasG12D (Haigis et al., 2008). In analysis of tumours expressing KrasG12D, it was shown that they express elevated levels of the Erk phosphatase *Mkp3* and this was viewed as a possible explanation for the inability of mutant Kras to up regulate phospho-Erk in the mouse colon. Subsequently it was shown in colon cancer cells that up regulation of *Mkp3* was indeed responsible for this inability (Haigis et al., 2008). This may explain why in Western Blot experiments performed with different organoid populations for test purposes there no differences in the phospho-Erk levels were found (data not shown). As for the phenotypic changes, such as a higher number of stem cells in the crypt or larger goblet cells that were seen in the mouse colon and lead to elevated proliferation rates, these results were not found in organoids expressing KrasG12D from one endogenous locus. They displayed a normal phenotype and grew with the same speed as the WT or controls that were not infected with Cre recombinase, indicating a normal number of stem cells (figure 23).

8.6 Ras status in small intestinal organoids after recombination

To demonstrate the existence of mTFP-KrasG12D protein Kras organoids after recombination, Western Blot experiments were performed (figure 21). In Kras organoids, an additional band around 50 kDa appeared with an antibody against all Ras isoforms. Even without infection with Cre recombinase, the additional band for mTFP-KrasG12D could be observed. After recombination, the mTFP-KrasG12D signal was slightly elevated. This increase proved to be statistically significant (figure 22). The fact that the band for mTFP-KrasG12D appeared even without the organoids being infected with Cre recombinase demonstrated that the stop codon flanked by loxP sites in Kras organoids leaked.

For further evaluation of the Ras status, a pan-Ras staining was performed with organoids from different conditions (WT, Kras, infected with Cre) and analyzed using the SPIM setup. It was found that the signals for pan-Ras and mTFP-Kras co-localized at the plasma membrane of the single cells of the organoids, meaning that the signal for KrasG12D localized correctly. The mutated protein with the mTFP-tag within the organoid was very likely to be Kras. In a second finding, not all organoids possessed equal mTFP-KrasG12D levels. Three populations could be distinguished: The first displayed a high amount of mTFP-KrasG12D; in a second population, medium level of mTFP-signal was detected; and a third population showed no mTFP-signal at all, although a *monoculture* derived from one organoid was investigated where each cell should have recombined (figure 23 and data not shown).

The differences in mTFP levels were not quantified as the intensity of the signal depends on many factors that were not equally performed in all experiments conducted. One important factor is the dependence on the width of the light sheet. If it is wider, the field of view is larger, leading to a decrease in signal intensity, thus weak signals will not be detected. To detect weaker signals, the light sheet can be adjusted narrower, in parallel decreasing the field of view and increasing background fluorescence. Other factors that play a role for the intensity of the signal detected are general characteristics, such as the sample's fluorescence intensity, its position in the matrigel and its position relatively to the mirrors. If other organoids block the light path between mirrors and sample or lens and sample, respectively or a position close enough to the light path is sufficient to do so - the signal intensity will decrease as well. As a result, the observation made with wide field microscopy that the organoids show different levels of mTFP-KrasG12D could be verified by SPIM but not quantified.

There are also strong indicators for the existence of a complex regulatory machinery that ensures correct maintenance of Kras levels in healthy cells. Therefore, the differences in mTFP-KrasD12D levels may be due to this cellular regulatory machinery which keeps Kras levels in check. While directed expression of KrasG12D stimulates abnormal proliferation in tissues that harbour Kras mutations in human cancer, widespread expression of KrasG12D causes embryonic lethality in mice (Tuveson et al., 2004). Inhibition of Kras function during embryogenesis of mice is lethal as Kras may have specific functions in signal transduction for which other family members such as Nras or Hras cannot compensate (Johnson et al., 1997).

The messenger RNA (mRNA) of the Kras gene contains an exceptionally long 3' untranslated region (UTR). Therefore, it is likely to be subject to a complex set of regulatory processes since post-transcriptional gene regulation by non-coding RNAs, such as microRNAs (miRNAs), requires recognition motifs in the 3' UTR of their target genes (Kim et al., 2016). It has been shown that the endogenous 3' UTR is of importance for expression, processing and translation of the Kras mRNA. If it is missing, Kras mRNA is not handled correctly in the cell, leading to changes in protein expression and signalling (Haigis et al., 2008).

As the Kras alleles in the organoids used in this work are mostly endogenous (with the exception of the changes near the 5' end due to the insertion of the mutation in the case of the Kras organoids), the 3' UTR is the endogenous one in all cases. Consequently Kras expression can be regulated in the normal way.

Endogenous Kras mRNA and protein expression have been shown to be repressed, e.g. by miR-185 over expression in vitro, and the results of this study further suggest that it functions in a tissue and cell-type-specific manner. As it has been reported to be deregulated in various cancers, miR-185 also has clinical relevance (Kim et al., 2016). This paper and others (reviewed in Kim and Slack, 2014) have shown that many miRNAs target and regulate Kras in cancer and that in every kind of cancer a different miRNA seems to be the key player. It could therefore very well be that Kras and mTFP-KrasG12D expression levels in small intestine organoids are regulated by an unknown miRNA. That could be an explanation for the different expression levels of mTFP-KrasG12D examined in the organoids.

8.7 Endogenous levels of mTFP-KrasG12D relocate small intestinal organoids upon PDE δ inhibition by Deltarasin

mTFP-KrasG12D was present in the organoids and located correctly at the plasma membrane of the single cells, but it was not clear whether it would be mislocalized upon organoid exposure to Deltarasin. To avoid possible interference caused by unequal mTFP-KrasG12D levels organoids with relatively high mTFP-KrasG12D levels were selected for the experiments further conducted. To address whether mTFP-KrasG12D would be mislocalized upon organoid exposure to Deltarasin, live cell imaging experiments were performed with the organoids using the SPIM setup. When treated with 7.5 μ M of the drug, first relocalization effects could be seen in organoids 20 minutes after Deltarasin administration (figure 25). 150 minutes after addition of Deltarasin cytotoxic effects were clearly visible and at this time point the first toxic effects of the solvent could also be observed in the DMSO control.

In tumours containing stroma and extracellular matrix are important contributors to aggressiveness and resistance towards chemotherapy (Le Calve et al., 2016). Organoids in contrast are purely epithelial populations of different cell types (Hwang et al., 2016). Nevertheless, they constitute a 3D model with an organized structure and the dose of Deltarasin used in 2D monocultures (5 μ M) was not expected to work as response of cells to growth factors and therapeutic treatment differ in 2D and 3D models (Coleman et al., 2014). Even higher cell densities prevented cytotoxic effects of Deltarasin in experiments with 2D cultures (Holger Vogel and Dina Truxius, personal communication). This may be due to an increased amount of extracellular messengers as a consequence of the larger number of cells and therefore to elevated signalling (paracrine and autocrine). One consequence of a higher density of cells is a higher number of contacts between the cells. This may also save some cells from the effect of the compound as it is unable to reach the entire surface of all cells. Therefore the amount of Deltarasin absorbed is not high enough to cause Ras relocalization or apoptosis. This may explain why higher doses of Deltarasin are needed to cause Kras relocalization in organoids than in 2D cell cultures.

However, it was possible to demonstrate that PDE δ inhibition also functions in 3D cultures, cultures that are significantly closer to the situation in a tumour. Compounds that pass this test are less likely to fail in patients in comparison to the usual preclinical in vitro testing in 2D cultures.

This work demonstrates that two specific PDE δ inhibitors with completely different lead structures are capable of mislocalizing Kras to endomembranes. In sum, it demonstrates that

the availability of PDE is essential to ensure (K)Ras localization at the plasma membrane in Kras-dependent cancer cells and thus that the survival of those cells are ultimately dependent on PDE .

9 Outlook

In this work it has been shown that small molecule PDE inhibitors affect (K)Ras localization in space and time. PDE inhibition causes Ras relocalization from the plasma membrane towards the endomembranes in different human cancer cell lines and in organoids.

The results of cell culture studies with fluorescently labelled Ras proteins to investigate its localization upon treatment with the small molecule PDE inhibitor Deltarasin (Chandra et al. 2012; Zimmermann et al, 2013) could be reproduced in this work. It was possible to demonstrate that Hras relocalizes in a manner similar to Kras and it could be shown that endogenous Ras also mislocalizes in different cancer cell lines. In addition, it was shown that fluorescently labelled KrasG12D relocalizes in organoids upon treatment with Deltarasin.

Another small molecule PDE inhibitor, Deltazinone 1, was also tested for its ability to relocalize Kras in different oncogenic cell lines. It was shown that in Kras-dependent PancTuI cells it is possible to mislocalize Kras with this inhibitor providing the dose is high enough to completely block the PDE system.

A number of open questions remain. Why does Deltazinone 1 work only in Kras-dependent cell lines? In this work and in Papke et al. 2016 it has been demonstrated that Deltazinone 1 mislocalizes Kras in PancTuI cells and induces growth inhibitory effects in both those and other Kras-dependent cell lines. In non-Kras-dependent cell lines, this compound has no obvious effect on cell growth and survival. So what exactly occurs in Kras-dependent cell lines causing them to be sensitive to Deltazinone 1 treatment? Could genetic streamlining be the reason? To test this cells that do not depend on Kras could be treated with inhibitors for different pathways or key factors of them e.g. PI3K and in parallel be exposed to Deltazinone 1. Thus, pathways that are silenced in Kras-dependent cells may be identified which could cause the sensitivity of the cells to Deltazinone 1.

With this in mind, it would be interesting to test other inhibitors with similar properties to Deltazinone 1 or Deltarasin in PancTuI cells and compare the results to Kras-independent cell lines. Will inhibitors that are more like Deltarasin also exhibit cytotoxic effects and will compounds which have more in common with Deltazinone 1 also work in Kras-dependent cells or any other cell line?

Although Deltarasin and Deltazinone 1 both relocalize Kras in PancTuI cells, the time profiles of the relocalization curves are somewhat dissimilar. This may be due to e.g. the cytotoxic

effects of Deltarasin or this compound binds better to PDE or it does not get so easily displaced from PDE by Arl2 activity compared to Deltazinone 1. This could be tested with a titration assay using synthetic biology by adding simultaneously fluorescently labelled Deltazinone 1 and labelled Deltarasin to labelled PDE. The amount of Deltazinone 1 can be kept constant; the amount of Deltarasin will be increased with time. The fluorophores have to be designed in a way that FRET can be measured once Deltazinone 1 binds PDE. If Deltarasin binds there, either the FRET signal could vanish or building another FRET pair would be possible as well. By measuring the signals the amount of each compound binding to PDE can be determined. Titration has to be performed the other way round as well and the experiment could also be conducted in presence of active Arl2.

Another question to be investigated is whether signal transduction by Ras is impaired and e.g. whether the MAPK pathway is blocked in organoids upon treatment with Deltarasin. To date, only mislocalization of Ras could be shown for treatment of organoids with Deltarasin. Other inhibitors such as Deltazinone 1 should also be tested to determine whether they are capable of relocalizing Ras in organoids. Here, it would be interesting to see whether all cells of the whole organoid exhibit relocalization or only a subpopulation of cells. It may also be the case that Deltazinone 1 fails to have any effect in the small intestine organoids that were used in this work as they are derived from mice. In previous studies conducted by Dina Truxius with mouse cell lines, the compound did not show any effect on the cells. Moreover, the organoids were presumably not dependent on Kras as they were not derived from any tumour but from organoids which are supposed to have a normal DNA profile, except the mutated Kras allele. Thus, it is not likely they became Kras-dependent, especially in such a short time, but it has not been tested. This should be done to find out for sure if organoids stay Kras-independent upon mTFP-KrasG12D activation.

As a final recommendation, the organoid system could be expanded (e.g. pancreas, liver) to investigate the effects of PDE inhibition on growth, Ras localization and survival of organoids derived from those organs.

List of Figures

Figure 1: Topological structure of ras proteins	5
Figure 2: GTPase cycle	7
Figure 3: Domain structure of the Ras proteins	12
Figure 4: One delivery system to rule them all	16
Figure 5: Ras signalling networks	19
Figure 6: The tumor suppressor effect of Ras	20
Figure 7: Multiple sequence alignment of the amino acids in the Kras4A and Kras4B proteins	22
Figure 8: modified Vogelgram	27
Figure 9: The three models of oncogene addiction	31
Figure 10: Localization of different Ras isoforms upon Deltarasin or Deltazinone 1 treatment	85
Figure 11: Quantification of the effects of Deltarasin or Deltazinone 1 treatment on different Ras isoforms in MDCK cells	86
Figure 12: Localization of endogenous Ras in A431 cells upon Deltarasin or Deltazinone 1 treatment	87
Figure 13: Localization of endogenous Ras in DiFi cells upon Deltarasin treatment	89
Figure 14: mCherry Kras^{WT} relocalization in PancTuI cells upon treatment with Deltarasin	91
Figure 15: mCherry Kras^{WT} relocalization in PancTuI cells upon treatment with Deltazinone 1	92
Figure 16: mCherry Kras^{WT} relocalization in PancTu1 cells upon treatment with DMSO	93

Figure 17: mCherry Kras^{WT} relocalization in PancTuI cells	94
Figure 18: Detection of different marker cell types in small intestinal organoids	95
Figure 19: Switching mTFP-Kras^{G12D} on via Cre-mediated recombination	96
Figure 20: Genotyping of organoids	100
Figure 21: mTFP-Kras^{G12D} in organoids	101
Figure 22: Quantification of mTFP-Kras^{G12D} levels in organoids	102
Figure 23: mTFP-Kras ^{G12D} and panRas in organoids	104
Figure 24: mTFP-Kras ^{G12D} and panRas in organoids in high magnification and resolution	105
Figure 25: Relocalization of mTFP-Kras ^{G12D} in small intestine Organoids upon Deltarasin administration	107
Figure 26: Relocalization of mTFP-Kras ^{G12D} in small intestine Organoids upon Deltarasin administration in high magnification and resolution	108

List of Tables

Table 1: Primary antibodies for Western Blots	35
Table 2: Secondary antibodies for Western Blots	35
Table 3: Antibodies for Immunofluorescence	36
Table 4: Secondary antibodies for Immunofluorescence	36

Abbreviations

°C	degree Celsius
µg	microgram
µl	micro litre
µM	micromole
a.b.	aqua bidest
ab	antibody
AF-6	acute lymphoblastic leukaemia-1 fused gene on chromosome 6
AKT/PKB	Ak tyoma/ protein kinase B
ALL	acute lymphoblastic leukaemia
AMP	Adenosine monophosphate
AMPK	AMP-activated protein kinase
APC	adenomatous polyposis coli
APS	Ammonium persulfate
APTs	acyl protein thioesterases
Arf	ADP ribosylation factor
Arl	ADP-ribosylation factor-like protein
ATP	Adenosine triphosphate
bp	base pair
BSA	bovine serum albumin
C57/B16	inbred mouse strain
CD1	cadherin domain-1
CDC42	cell division cycle-42
CDKN2A	cyclin-dependent kinase Inhibitor 2A, encodes p16 and p14Arf
CIAP	calf intestine alkaline phosphatase
cm	centimetre
CRC	colorectal adenocarcinoma / colorectal cancer
C-terminus	carboxy-terminus
DAG	diacylglycerol
DCC	Deleted in Colon Cancer
ddH ₂ O	aqua bidest
DMEM	Dulbecco's modified Eagle's medium

DMSO	Dimethyl sulfoxide
DNA	deoxyribonucleic acid
dNTP	deoxyribonucleoside triphosphate
ds	double strand
DTT	Dithiothreitol
E1A	Adenovirus early region 1A
E6/E7	viral oncogenes promoting cell growth by inactivating the tumour suppressor proteins p53 and Rb
EDTA	Ethylenediaminetetraacetic acid
EGF	epidermal growth factor
EGFR	epidermal growth factor receptor
ELK	ETS-like protein
ER	endoplasmatic reticulum
ERK	extracellular signal-regulated kinase
EtOH	ethanol
ETS	E26-transcription factor proteins
FCS	fetal calf serum
FDA	The US Food and Drug Administration
FLIM	fluorescence lifetime imaging microscopy
FRET	fluorescence resonance energy transfer
FTI	farnesyl transferase-inhibitors
g	gram
GAPs	GTPase-activating proteins
GDP	guanosine diphosphate
GEFs	Guanine-nucleotide exchange factors
GF	growth factor
GFR	growth factor reduced
Golgi	Golgi apparatus
Grb2	Growth factor receptor-bound protein 2
GSK3	glycogen synthase kinase 3
GTP	guanosine triphosphate
h	hour
Hras	Harvey-Ras

HVR	hyper variable region
Icmt	isoprenylcysteine carboxyl methyltransferase
IgG	Immunoglobulin G
Ins(1,4,5)P3	inositol-1,4,5- trisphosphate
ISCs	intestinal stem cells
JNK	Jun N-terminal kinase
kb	kilo base
kDa	kilo Dalton
KI allele	knock in allele
Kras	Kirsten-Ras
LAC	lung adenocarcinoma
LB	lysogeny broth
LPS	lipopolysaccharides
MAPK	mitogen-activated protein kinase
mCherry	monomeric variant of red fluorescent protein
mCitrine	monomeric variant of yellow fluorescent protein
MDCK	Madin-Darby canine kidney
MDM2	murine double minute-2
MDR	multi drug resistance
MEK	mitogen-activated protein kinase/ERK kinase
MeOH	methanol
min	minute
miRNA	microRNA
Mkp3	Erk phosphatase 16
ml	millilitre
mM	mill molar
mm	millimetre
mRNA	messenger RNA
MST	mammalian sterile-20-like protein kinase
mTFP	monomeric Teal fluorescent protein
mTORC1	mammalian target of rapamycin complex 1
NEAA	non-essential amino acid solution
NF1	neurofibromin
NF- B	nuclear factor- B

ng	nanogramm
Nras	neuroblastoma-Ras
nt	nucleotide
N-terminus	amino-terminus
p14/p19 Arf	alternate reading frame of the CDKN2A locus
p16INK4A	cyclin-dependent kinase inhibitor 2A
p21WAF	cyclin-dependent kinase inhibitor 1 or CDK-interacting protein 1
p53	tumour suppressor
PA	phosphatidic acid
PAGE	polyacrylamide gel electrophoresis
pan Ras	all Ras isoforms
PanIN	pancreatic intraepithelial neoplasia
PATs	palmitoyl transferases
PBS	phosphate buffered saline
PCR	Polymerase Chain Reaction
PDAC	pancreatic ductal adenocarcinoma
PDE6	phosphodiesterase 6
PDE	PDE6D, subunit of PDE6
PFA	paraformadlehyde
PI3K	phosphoinositide 3-kinases
PKB/C	protein kinase B/C
PLC	phospholipase C-
PM	plasma membrane
PRAK	p38-regulated/activated protein kinase
PtdIns(4,5)P2	Phosphatidylinositol 4,5-bisphosphate
PVDF	Polyvinylidene difluoride
Rab	subfamily of Ras GTPases
Rac	Ras-related C3 botulinum toxin substrate 1
Raf	serine/threonine-protein kinase, MAPKKK
Ral	Ras-like
RalGDS	Ral guanine nucleotide-dissociation stimulator
Ran	subfamily of Ras GTPases; Ras in nucleus
Raptor	Regulatory-associated protein of mTOR
Ras	Rat Sarcoma

RASSF	Ras association domain-containing family
Rb	Retinoblastoma
Rce1	Ras and a-factor converting enzyme
RE	recycling endosome
REM	Ras exchange motif
RGL	RalGDS-like protein
Rheb	Ras homolog enriched in brain
Rho	subfamily of Ras GTPases
RIN1	Ras interaction/interference protein-1
RIPA	radioimmunoprecipitation assay buffer
ROS	reactive oxygen species
rpm	rounds per minute
RSV	Rous sarcoma virus
RT	room temperature
RTCA	Real Time Cell Analysis
RTK	receptor tyrosine kinase
S6RP	S6 ribosomal protein
SAPK	stress-activated protein kinase
SDS	Sodium dodecyl sulfate
SH2 domain	Src-homology-domain 2
SH3 domain	Src-homology-domain 3
SHP2	Src-homology-2 domain-containing protein Tyr phosphatase-2
SMAD4	SMAD family member n°4, Mothers against decapentaplegic homolog 4
SOB	Super Optimal Broth
SOC	Super Optimal broth with Catabolite repression
Sos	Son of sevenless
SPIM	Single Plane Illumination Microscopy
ss	single strand
STK33	Serine/threonine-protein kinase 33
SV40	Simian vacuolating virus 40
SYK	spleen tyrosine kinase
TAE	Tris-acetate-EDTA
TBS	Tris-buffered saline
TE	Tris EDTA

TEMED	Tetra methyl ethylene diamin
TIAM1	T-cell lymphoma invasion and metastasis-1
Tm	Melting temperature
Tris	2-amino-2-hydroxymethyl-propane-1,3-diol
TSC2	Tuberous Sclerosis Complex 2
U	units
UTR	untranslated region
V	Volt
WT	wild type

Literature cited

- Aksamitiene, E., Kiyatkin, A., Kholodenko, B.N.* (2012), *Biochemical Society Transactions* Feb; 40(1):139-46.
- Allegra, C.J., Jessup, J.M., Somerfield, M.R., Hamilton, S.R., Hammond, E.H., Hayes, D.F., McAllister, P.K., Morton, R.F., Schilsky, R.L.* (2009), *Journal of Clinical Oncology*, Apr 20, 27(12):2091-6.
- Baker, S.J., Fearon, E.R., Nigro, J.M., Hamilton, S.R., Preisinger, A.C., Jessup, J.M., vanTuinen, P., Ledbetter, D.H., Barker, D.F., Nakamura, Y., White, R., Vogelstein, B.* (1989), *Science*, Apr 14, 244(4901):217-21.
- Bardeesy, N., Aguirre, A.J., Chu, G.C., Cheng, K.H., Lopez, L.V., Hezel, A.F., Feng, B., Brennan, C., Weissleder, R., Mahmood, U., Hanahan, D., Redston, M.S., Chin, L., Depinho, R.A.* (2006), *Proceedings of the National Academy of Sciences of the U S A.*, Apr 11, 103(15):5947-52.
- Barker, N., Huch, M., Kujala, P., van de Wetering, M., Snippert, H.J., van Es, J.H., Sato, T., Stange, D.E., Begthel, H., van den Born, M., Danenberg, E., van den Brink, S., Korving, J., Abo, A., Peters, P.J., Wright, N., Poulsom, R., Clevers, H.* (2010), *Cell Stem Cell*; Jan 8;6(1):25-36.
- Blum, R. and Kloog, Y.* (2005), *Drug Resistance Updates*, Dec, 8(6):369-80.
- Blum, R., Cox, A.D., Kloog, Y.* (2008), *Recent Patents on Anticancer Drug Discovery*, Jan, 3(1):31-47.
- Boriack-Sjodin, P.A., Margarit, S.M., Bar-Sagi, D., Kuriyan, J.* (1998), *Nature*, Jul 23, 394(6691):337-43.
- Bos, J.L., Fearon, E.R., Hamilton, S.R., Verlaan-de Vries, M., van Boom, J.H., van der Eb, A.J., Vogelstein, B.* (1987) *Nature*, May 28-Jun 3, 327(6120):293-7.
- Bos, J.L., Rehmann, H., Wittinghofer, A.* (2007), *Cell*, 129, 865-877.
- Buhrman, G., Holzapfel, G., Fetics, S., Mattos, C.* (2010), *Proceedings of the National Academy of Sciences of the U S A.*, Mar 16, 107(11):4931-6.
- Buhrman, G., O'Connor, C., Zerbe, B., Kearney, B.M., Napoleon, R., Kovrigina, E.A., Vajda, S., Kozakov, D., Kovrigin, E.L., Mattos, C.* (2011), *Journal of Molecular Biology*, Nov 4, 413(4):773-89.
- Butz, J.A., Roberts, K.G., Edwards, J.S.* (2004), *Biotechnology Progress*, Nov-Dec, 20(6):1836-9.
- Carta, C., Pantaleoni, F., Bocchinfuso, G., Stella, L., Vasta, I., Sarkozy, A., Digilio, C., Palleschi, A., Pizzuti, A., Grammatico, P., Zampino, G., Dallapiccola, B., Gelb, B.D., Tartaglia, M.* (2006), *American Journal of Human Genetics*, Jul, 79(1):129-35.

- Chakrabarti, M., Jang, H., Nussinov, R.* (2016), *The Journal of Physical Chemistry B.*, Feb 4, 120(4):667-79.
- Chandra, A., Grecco, H.E., Pisupati, V., Perera, D., Cassidy, L., Skoulidis, F., Ismail, S.A., Hedberg, C., Hanzal-Bayer, M., Venkitaraman, A.R., Wittinghofer, A., Bastiaens, P.I.* (2012), *Nature Cell Biology*, 14,2, 148-158.
- Chang, E.H., Gonda, M.A., Ellis, R.W., Scolnick, E.M., Lowy, D.R.* (1982), *Proceedings of the National Academy of Sciences of the U S A.*, 79(16):4848-52.
- Chen, B., Jiang, Y., Zeng, S., Yan, J., Li, X., Zhang, Y., Zou, W., Wang, X.* (2010), *PLoS genetics*, Dec 9, 6(12), e1001235.
- Chien, Y. and White, M.A.* (2003), *EMBO Reports*, Aug, 4(8):800-6.
- Clevers, H.* (2013), *Cell*, Jul 18, 154(2), 274-84.
- Clevers, H. and Battle, E.*, (2013) *Cell*, Feb 28, 152(5), 1198-1198.
- Coleman, S.J., Watt, J., Arumugam, P., Solaini, L., Carapuca, E., Ghallab, M., Grose, R.P., Kocher, H.M.* (2014,) *World Journal of Gastroenterology*, Jul 14;20, (26):8471-81.
- Courtney, K.D., Corcoran, R.B., Engelman, J.A.* (2010), *Journal of Clinical Oncology*, 28, 1075-1083.
- Cox, A.D. and Der, C.J.* (2002), *Cancer Biology & Therapy* 1 (6): 5996606.
- Cox, A.D., Fesik, S.W., Kimmelman, A.C., Luo, J., Der, C.J.* (2014), *Nature Reviews Drug Discovery*, Nov, 13(11):828-51.
- Deer, E.L., González-Hernández, J., Coursen, J.D., Shea, J.E., Ngatia, J., Scaife, C.L., Firpo, M.A., Mulvihill, S.J.* (2010), *Pancreas*, May, 39(4):425-35.
- DeFeo, D., Gonda, M.A., Young, H.A., Chang, E.H., Lowy, D.R., Scolnick, E.M., Ellis, R.W.* (1981), *Proceedings of the National Academy of Sciences of the U S A.*, Jun, 78(6):3328-32.
- Dekker, F.J., Rocks, O., Vartak, N., Menninger, S., Hedberg, C., Balamurugan, R., Wetzel, S., Renner, S., Gerauer, M., Schölermann, B., Rusch, M., Kramer, J.W., Rauh, D., Coates, G.W., Brunsveld, L., Bastiaens, P.I., Waldmann, H.* (2010), *Nature Chemical Biology*, Jun, 6(6), 449-56.
- Delattre, O., Olschwang, S., Law, D.J., Melot, T., Remvikos, Y., Salmon, R.J., Sastre, X., Validire, P., Feinberg, A.P., Thomas, G.* (1989), *Lancet*, Aug 12, 2(8659):353-6.
- Der, C.J., Krontiris, T.G., Cooper, G.M.*, (1982), *Proceedings of the National Academy of Sciences of the U S A.*, 79, 3637-3640.
- Donovan, S., Shannon, K.M., Bollag, G.* (2002), *Biochim Biophys Acta*, 1602, 23-45.
- Eisenberg, S., Laude, A. J., Beckett, A. J., Mageean, C. J., Aran, V., Hernandez-Valladares, M., Henis, Y. I., Prior, I. A.* (2013), *Biochemical Society Transactions*, 41,1: 79-83.

- Ellis, R.W., DeFeo, D., Furth, M.E., Scolnick, E.M.* (1982), *Molecular and Cellular Biology*, Nov, 2(11):1339-45.
- Farr, C.J., Marshall, C.J., Easty, D.J., Wright, N.A., Powell, S.C., Paraskeva, C.* (1988), *Oncogene*, Dec, 3(6):673-8.
- Fearon, E.R., Hamilton, S.R., Vogelstein, B.* (1987), *Science*, Oct 9, 238(4824):193-7.
- Fearon, E.R. and Vogelstein, B.* (1990), *Cell*, Jun 1, 61(5):759-67.
- Forrester, K., Almoguera, C., Han, K., Grizzle, W.E., Perucho, M.* (1987), *Nature*, May 28-Jun 3, 327(6120):298-303.
- Goodwin, J.S., Drake, K.R., Rogers, C., Wright, L., Lippincott-Schwartz, J., Philips, M.R., Kenworthy, A.K.* (2005), *The Journal of Cell Biology*, Jul 18, 170(2), 261-72.
- Ghosh, S., Spagnoli, G.C., Martin, I., Ploegert, S., Demougin, P., Heberer, M., Reschner, A.* (2005), *Journal of Cellular Physiology*; 204:522-531.
- Grady, W.M.* (2004), *Cancer Metastasis Reviews*, Jan-Jun, 23(1-2):11-27.
- Gysin, S., Salt, M., Young, A., McCormick, F.* (2011), *Genes & Cancer*, 2011 Mar, 2(3):359-72.
- Haigis, K.M., Kendall, K.R., Wang, Y., Cheung, A., Haigis, M.C., Glickman, J.N., Niwa-Kawakita, M., Sweet-Cordero, A., Sebolt-Leopold, J., Shannon, K.M., Settleman, J., Giovannini, M., Jacks, T.* (2008), *Nature Genetics*, May; 40(5):600-8.
- Hamad, N.M., Elconin, J.H., Karnoub, A.E., Bai, W., Rich, J.N., Abraham, R.T., Der, C.J., Counter, C.M.* (2002), *Genes & Development*, Aug 15, 16(16):2045-57.
- Han, L and Colicelli, J.* (1995), *Molecular and Cellular Biology*, Mar, 15(3):1318-23.
- Hancock, J.F., Magee, A.I., Childs, J.E., Marshall, C.J.* (1989), *Cell*, 57, 7, 30,6, 1167-1177.
- Hancock, J.F., Paterson, H., Marshall, C.J.* (1990), *Cell* 63 (1): 133-639.
- Hancock, J.F.* (2003), *Nature Reviews Molecular Cell Biology*, May, 4(5):373-84.
- Hanzal-Bayer, M., Renault, L., Roversi, P., Wittinghofer, A., Hillig, R.C.* (2002), *EMBO Journal*, May 1, 21(9):2095-106.
- Hein, C., Wittinghofer, A., Dötsch, V.* (2013), *Elife*, Jul 30;2:e01159.
- Hingorani, S.R., Wang, L., Multani, A.S., Combs, C., Deramandt, T.B., Hruban, R.H., Rustgi, A.K., Chang, S., Tuveson, D.A.* (2005), *Cancer Cell*, May, 7(5):469-83.
- Hobbs, G.A., Der, C.J., Rossman, K.L.* (2016), *Journal of Cell Science*, Apr 1, 129(7):1287-92.
- Hofer, F., Fields, S., Schneider, C., Martin, G.S.* (1994), *Proceedings of the National Academy of Sciences of the U S A.*, Nov 8, 91(23):11089-93.

- Hruban, R.H., Adsay, N.V., Albores-Saavedra, J., Compton, C., Garrett, E.S., Goodman, S.N., Kern, S.E., Klimstra, D.S., Klöppel, G., Longnecker, D.S., Lüttges, J., Offerhaus, G.J.* (2001), *The American Journal of Surgical Pathology*, May, 25(5):579-86.
- Huch, M., Dorrell, C., Boj, S.F., van Es, J.H., Li, V.S., van de Wetering, M., Sato, T., Hamer, K., Sasaki, N., Finegold, M.J., Haft, A., Vries, R.G., Grompe, M., Clevers, H.* (2013), *Nature*; Feb 14;494(7436):247-50.
- Huch, M., Gehart, H., van Boxtel, R., Hamer, K., Blokzijl, F., Verstegen, M.M., Ellis, E., van Wenum, M., Fuchs, S.A., de Ligt, J., van de Wetering, M., Sasaki, N., Boers, S.J., Kemperman, H., de Jonge, J., Ijzermans, J.N., Nieuwenhuis, E.E., Hoekstra, R., Strom, S., Vries, R.R., van der Laan, L.J., Cuppen, E., Clevers, H.* (2015) *Cell*; Jan 15;160 (1-2): 299-312.
- Hwang, C.I., Boj, S.F., Clevers, H., Tuveson, D.A.* (2016), *The Journal of Pathology*. Jan; 238(2):197-204.
- Ismail, S.A., Chen, Y.X., Rusinova, A., Chandra, A., Bierbaum, M., Gremer, L., Triola, G., Waldmann, H., Bastiaens, P.I., Wittinghofer, A.* (2011), *Nature Chemical Biology*, Oct 16, 7(12):942-9.
- Iwig, J.S. and Kuriyan, J.* (2013), *Cell*, 153,6, 1191-1193.
- Jackson, J.H., Li, J.W., Buss, J.E., Der, C.J., Cochrane, C.G.* (1994), *Proceedings of the National Academy of Sciences of the U S A.*, Dec 20, 91(26):12730-4.
- Johnson, L., Greenbaum, D., Cichowski, K., Mercer, K., Murphy, E., Schmitt, E., Bronson, R.T., Umanoff, H., Edelmann, W., Kucherlapati, R., Jacks, T.* (1997), *Genes & Development* Oct 1;11(19):2468-81.
- Johnson, L., Mercer, K., Greenbaum, D., Bronson, R.T., Crowley, D., Tuveson, D.A., Jacks, T.* (2001), *Nature*, Apr 26, 410(6832):1111-6.
- Jung, P., Sato, T., Merlos-Suarez, A., Barriga, F.M., Iglesias, M., Rossell, D., Auer, H., Gallardo, M., Blasco, M.A., Sancho, E., Clevers, H., Batlle, E.* (2011), *Nature Medicine*; Sep 4, 17(10):1225-7.
- Kaelin, W.G. Jr.* (2005), *Nature Reviews Cancer*, Sep, 5(9):689-98.
- Kanda, M., Matthaei, H., Wu, J., Hong, S.M., Yu, J., Borges, M., Hruban, R.H., Maitra, A., Kinzler, K., Vogelstein, B., Goggins, M.* (2012), *Gastroenterology*, Apr, 142(4):730-733.e9.
- Karnoub, A.E. and Weinberg, R.A.* (2008), *Nature Reviews Molecular Cell Biology* Jul, 9(7):517-31.
- Kelley, G.G., Reks, S.E., Ondrako, J.M., Smrcka, A.V.* (2001), *EMBO Journal*, Feb 15, 20(4):743-54.
- Khokhlatchev, A., Rabizadeh, S., Xavier, R., Nedwidek, M., Chen, T., Zhang, X.F., Seed, B., Avruch, J.* (2002), *Current Biology*, Feb 19, 12(4):253-65.

- Khawaja, A., Rodriguez-Viciana, P., Wennström, S., Warne, P.H., Downward, J. (1997), EMBO Journal, May 15, 16(10):2783-93.*
- Kim, M. and Slack, F.J. (2014), Journal of Hematology and Oncology, Nov 30; 7:84.*
- Kim, M., Kogan, N., Slack, F.J. (2016), Oncotarget, Mar 15; 7(11):11770-84.*
- King, P.D., Lubeck, B.A., Lapinski, P.E (2013), Cell Signaling, 6, 264, 1-11.*
- Kinzler, K.W. and Vogelstein, B. (1996), Cell, Oct 18, 87(2):159-70.*
- Khosravi-Far, R., Solski, P.A., Clark, G.J., Kinch, M.S., Der, C.J. (1995), Molecular and Cellular Biology, Nov, 15(11):6443-53.*
- Konstantinopoulos, P.A., Karamouzis, M.V., Papavassiliou, A.G. (2007), Nature Reviews Drug Discovery, Jul, 6(7):541-55.*
- Koo, B.K., Sasselli, V., Clevers, H. (2013), Current Protocols in Stem Cell Biology, Nov 13, 27: Unit 5A.6.*
- Lampson, B.L., Pershing, N.L., Prinz, J.A., Lacsina, J.R., Marzluff, W.F., Nicchitta, C.V., MacAlpine, D.M., Counter, C.M. (2013), Current Biology, Jan 7, 23(1):70-5.*
- Land, H., Parada, L.F., Weinberg, R.A. (1983), Nature, Aug 18-24, 304(5927):596-602.*
- Le Calvé, B., Griveau, A., Vindrieux, D., Maréchal, R., Wiel, C., Svrcek, M., Gout, J., Azzi, L., Payen, L., Cros, J., de la Fouchardière, C., Dubus, P., Guitton, J., Bartholin, L., Bachet, J.B., Bernard, D. (2016), Oncotarget, May 31;7(22):32100-12.*
- Lee, S.H., Meng, X.W., Flatten, K.S., Loegering, D.A., Kaufmann, S.H. (2013), Cell Death and Differentiation, Jan, 20(1):64-76.*
- Leever, S.J. and Marshall, C.J. (1992), EMBO Journal, Feb, 11(2):569-74.*
- Leever, S.J., Paterson, H.F., Marshall, C.J. (1994), Nature, Jun 2, 369(6479):411-4.*
- Lopez, I., Mak, E.C., Ding, J., Hamm, H.E., Lomasney, J.W. (2001), The Journal of Biological Chemistry, Jan 26, 276(4):2758-65.*
- Lorentzen, A., Kinkhabwala, A., Rocks, O., Vartak, N., Bastiaens, P.I. (2010), Science Signaling 3 (140): ra68óra68.*
- Luo, F., Ye, H., Hamoudi, R., Dong, G., Zhang, W., Patek, C.E., Poulogiannis, G., Arends, M.J. (2010), The Journal of Pathology, Apr, 220(5):542-50.*
- Malliri, A., van der Kammen, R.A., Clark, K., van der Valk, M., Michiels, F., Collard, J.G. (2002), Nature, Jun 20, 417(6891):867-71.*
- Mandai, K., Nakanishi, H., Satoh, A., Obaishi, H., Wada, M., Nishioka, H., Itoh, M., Mizoguchi, A., Aoki, T., Fujimoto, T., Matsuda, Y., Tsukita, S., Takai, Y. (1997), The Journal of Cell Biology, Oct 20, 139(2):517-28.*
- Marte, B.M. and Downward, J. (1997), Trends in Biochemical Sciences, Sep, 22(9):355-8.*

- Mayo, M.W., Wang, C.Y., Cogswell, P.C., Rogers-Graham, K.S., Lowe, S.W., Der, C.J., Baldwin, A.S. Jr. (1997), *Science*, Dec 5, 278(5344):1812-5.
- McCubrey, J.A., Steelman, L.S., Abrams, S.L., Lee, J.T., Chang, F., Bertrand, F.E., Navolanic, P.M., Terrian, D.M., Franklin, R.A., D'Assoro, A.B., Salisbury, J.L., Mazzarino, M.C., Stivala, F., Libra, M. (2006), *Advances in Enzyme Regulation*, 46,1, 249-279.
- McGrath, J.P., Capon, D.J., Smith, D.H., Chen, E.Y., Seeburg, P.H., Goeddel, D.V., Levinson, A.D. (1983), *Nature*, Aug 11-17, 304(5926):501-6.
- Mendoza, M.C., Er, E.E., Blenis, J. (2011), *Trends in Biochemical Sciences*, Jun, 36(6):320-8.
- Milburn, M.V., Tong, L., deVos, A.M., Brünger, A., Yamaizumi, Z., Nishimura, S., Kim, S.H. (1990) *Science*, Feb 23;247(4945):939-45.
- Mitin, N., Rossman, K.L., Der, C.J. (2005), *Current Biology*, 15, R563-R574.
- Moodie, S.A., Willumsen, B.M., Weber, M.J., Wolfman, A. (1993), *Science*, Jun 11, 260(5114):1658-61.
- Morris, J.P. 4th, Wang, S.C., Hebrok, M. (2010), *Nature Reviews Cancer*, Oct, 10(10):683-95.
- Muleris, M., Salmon, R.J., Zafrani, B., Girodet, J., Dutrillaux, B. (1985), *Annales de Genetique*, 28(4):206-13.
- Mullis, K., Faloona, F., Scharf, S., Saiki, R., Horn, G., Erlich, H. (1986), *Cold Spring Harbour Symposia on Quantitative Biology*, 51 Pt 1:263-73.
- Nakano, H., Yamamoto, F., Neville, C., Evans, D., Mizuno, T., Perucho, M. (1984), *Proceedings of the National Academy of Sciences of the U S A.*, Jan, 81(1):71-5.
- Nandan, M.O. and Yang, V.W. (2011), *Current Colorectal Cancer Report* Jun 1, 7(2):113-120.
- Nigro, J.M., Baker, S.J., Preisinger, A.C., Jessup, J.M., Hostetter, R., Cleary, K., Bigner, S.H., Davidson, N., Baylin, S., Devilee, P., Glover, T., Collins, F.S., Weston, A., Modali, R., Harris, C.C., Vogelstein, B. (1989), *Nature*, Dec 7, 342(6250):705-8.
- Normanno, N., Tejpar, S., Morgillo, F., De Luca, A., Van Cutsem, E., Ciardiello, F. (2009), *Nature Reviews Clinical Oncology*, Sep, 6(9):519-27.
- Nussinov, R., Tsai, C.J., Mattos, C. (2013), *Trends in Molecular Medicine*, Nov, 19(11):695-704.
- O'Brien, S.J., Nash, W.G., Goodwin, J.L., Lowy, D.R., Chang, E.H. (1983), *Nature*, Apr 28, 302(5911):839-42.
- Ogura, T., Yamao, K., Hara, K., Mizuno, N., Hijioka, S., Imaoka, H., Sawaki, A., Niwa, Y., Tajika, M., Kondo, S., Tanaka, T., Shimizu, Y., Bhatia, V., Higuchi, K., Hosoda, W., Yatabe, Y. (2013), *Journal of Gastroenterology*, May, 48(5):640-6.

- Olive, M., Untawale, S., Coffey, R.J., Siciliano, M.J., Wildrick, D.M., Fritsche, H., Pathak, S., Cherry, L.M., Blick, M., Lointier, P., Roubein, L.D., Levin, B., Boman, B.M.* (1993), *In Vitro Cellular and Developmental Biology*, 29A (3 Pt 1), 239-48.
- Papke, B., Murarka, S., Vogel, H.A., Martín-Gago, P., Kovacevic, M., Truxius, D.C., Fansa, E.K., Ismail, S., Zimmermann, G., Heinelt, K., Schultz-Fademrecht, C., Al Saabi, A., Baumann, M., Nussbaumer, P., Wittinghofer, A., Waldmann, H., Bastiaens, P.I.* (2016), *Nature Communications*, Apr 20, 7:11360.
- Pells, S., Divjak, M., Romanowski, P., Impey, H., Hawkins, N.J., Clarke, A.R., Hooper, M.L., Williamson, D.J.* (1997), *Oncogene*, Oct 9, 15(15):1781-6.
- Plowman, S.J., Berry, R.L., Bader, S.A., Luo, F., Arends, M.J., Harrison, D.J., Hooper, M.L., Patek, C.E.* (2006), *Journal of Experimental and Clinical Cancer Research*, Jun, 25(2):259-67.
- Ponder, B.A. and Wilkinson, M.M.* (1986), *Journal of the National Cancer Institute*, Oct, 77(4):967-76.
- Ponting, C.P. and Benjamin, D.R.* (1996), *Trends in Biochemical Sciences*, Nov, 21(11):422-5.
- Rajagopalan, H., Bardelli, A., Lengauer, C., Kinzler, K.W., Vogelstein, B., Velculescu, V.E.* (2002), *Nature*, Aug 29, 418(6901):934.
- Rao, C.V. and Yamada, H.Y.* (2013), *Frontiers in Oncology*, May 21, 3:130.
- Reichmann, A., Martin, P., Levin, B.* (1981), *International Journal of Cancer*, Oct 15, 28(4):431-40.
- Ridky, T.W., Chow, J.M., Wong, D.J., Khavari, P.A.* (2010), *Nature Medicine*; 16 (12): 1450-1455.
- Roberts, P.J. and Der, C.J.* (2007), *Oncogene*, May 14, 26(22):3291-310.
- Rocks, O., Peyker, A., Kahms, M., Verveer, P.J., Koerner, C., Lumbierres, M., Kuhlmann, J., Waldmann, H., Wittinghofer, A., Bastiaens, P.I.* (2005) *Science*, Mar 18, 307(5716), 1746-52.
- Rocks, O., Gerauer, M., Vartak, N., Koch, S., Huang, Z.P., Pechlivanis, M., Kuhlmann, J., Brunsveld, L., Chandra, A., Ellinger, B., Waldmann, H., Bastiaens, P.I.* (2010), *Cell*, Apr 30, 141(3), 458-71.
- Rodriguez-Viciano, P., Warne, P.H., Dhand, R., Vanhaesebroeck, B., Gout, I., Fry, M.J., Waterfield, M.D., Downward, J.* (1994), *Nature*, Aug 18, 370(6490):527-32.
- Rodriguez-Viciano, P., Warne, P.H., Khwaja, A., Marte, B.M., Pappin, D., Das, P., Waterfield, M.D., Ridley, A., Downward, J.* (1997), *Cell*, May 2, 89(3):457-67.
- Ruley, H.E.* (1983), *Nature*, Aug 18-24, 304(5927):602-6.
- Rossmann, K.L., Der, C.J., Sondek, J.* (2005), *Nature Reviews Molecular Cell Biology*, Feb, 6(2):167-80.

- Sakaguchi, A.Y., Naylor, S.L., Shows, T.B., Toole, J.J., McCoy, M., Weinberg, R.A.* (1983), *Science*, Mar 4, 219(4588):1081-3.
- Santos, E., Martin-Zanca, D., Reddy, E.P., Pierotti, M.A., Della Porta, G., Barbacid, M.* (1984), *Science*, Feb 17, 223(4637):661-4.
- Sasaki, M., Okamoto, M., Sato, C., Sugio, K., Soejima, J., Iwama, T., Ikeuchi, T., Tonomura, A., Miyaki, M., Sasazuki, T.* (1989), *Cancer Research*, Aug 15, 49(16):4402-6.
- Sato, T., Vries, R.G., Snippert, H.J., van de Wetering, M., Barker, N., Stange, D.E., van Es, J.H., Abo, A., Kujala, P., Peters, P.J., Clevers, H.* (2009), *Nature*; May 14;459(7244), 262-5.
- Sato, T., Stange, D.E., Ferrante, M., Vries, R.G., Van Es, J.H., Van den Brink, S., Van Houdt, W.J., Pronk, A., Van Gorp, J., Siersema, P.D., Clevers, H.* (2011), *Gastroenterology*; Nov;141(5):1762-72.
- Sato, T. and Clevers, H.* (2013), *Methods in Molecular Biology*, 945:319-28.
- Scheffzek, K., Ahmadian, M.R., Kabsch, W., Wiesmüller, L., Lautwein, A., Schmitz, F., Wittinghofer, A.* (1997), *Science*, Jul 18;277(5324):333-8.
- Schmick, M., Vartak, N., Papke, B., Kovacevic, M., Truxius, D.C., Rossmannek, L., Bastiaens, P.I.* (2014), *Cell*, 157, 2, 459-471.
- Schmick, M., Kraemer, A., Bastiaens, P.I.* (2015), *Trends in cell biology*, 25, 190-197.
- Scholl, C., Fröhling, S., Dunn, I.F., Schinzel, A.C., Barbie, D.A., Kim, S.Y., Silver, S.J., Tamayo, P., Wadlow, R.C., Ramaswamy, S., Döhner, K., Bullinger, L., Sandy, P., Boehm, J.S., Root, D.E., Jacks, T., Hahn, W.C., Gilliland, D.G.* (2009), *Cell*, May 29, 137(5):821-34.
- Schroeder, H., Leventis, R., Rex, S., Schelhaas, M., Nägele, E., Waldmann, H., Silviu, J.R.* (1997), *Biochemistry*, Oct 21, 36(42), 13102-9.
- Schuijers, J. and Clevers H.* (2012), *EMBO Journal*, Jun 13, 31(12), 2685-96.
- Serrano, M., Lin, A.W., McCurrach, M.E., Beach, D., Lowe, S.W.* (1997), *Cell*, Mar 7, 88(5):593-602.
- Shimizu, K., Goldfarb, M., Suard, Y., Perucho, M., Li, Y., Kamata, T., Feramisco, J., Stavnezer, E., Fogh, J., Wigler, M.H.* (1983), *Proceedings of the National Academy of Sciences of the U S A.*, 80, 2112-2116.
- Singh, A., Greninger, P., Rhodes, D., Koopman, L., Violette, S., Bardeesy, N., Settleman, J.* (2009), *Cancer Cell*, 15, 6, 489-500.
- Smith, M.J., Neel, B.G., Ikura, M.* (2013), *Proceedings of the National Academy of Sciences of the U S A.*, Mar 19, 110(12):4574-9.
- Solomon, E., Voss, R., Hall, V., Bodmer, W.F., Jass, J.R., Jeffreys, A.J., Lucibello, F.C., Patel, I., Rider, S.H.* (1987), *Nature*, Aug 13-19, 328(6131):616-9.

- Song, C., Hu, C.D., Masago, M., Kariyai, K., Yamawaki-Kataoka, Y., Shibatohe, M., Wu, D., Satoh, T., Kataoka, T. (2001), *The Journal of Biological Chemistry*, Jan 26, 276(4):2752-7.
- Spaargaren, M. and Bischoff, J.R. (1994), *Proceedings of the National Academy of Sciences of the U S A.*, Dec 20, 91(26):12609-13.
- Stehelin, D., Varmus, H.E., Bishop, J.M., Vogt, P.K. (1976), *Nature*, Mar 11, 260(5547):170-3.
- Stokoe, D., Macdonald, S.G., Cadwallader, K., Symons, M., Hancock, J.F. (1994), *Science*, Jun 3, 264(5164):1463-7.
- Stone, J.C. (2011), *Genes & Cancer*, Mar, 2(3):320-34.
- Tejpar, S., Celik, I., Schlichting, M., Sartorius, U., Bokemeyer, C., Van Cutsem, E. (2012), *Journal of Clinical Oncology*, Oct 10, 30(29):3570-7.
- Thumar, J., Shahbazian, D., Aziz, S.A., Jilaveanu, L.B., Kluger, H.M. (2014), *Molecular Cancer*, Mar 4, 13:45.
- Torti, D. and Trusolino, L. (2011), *EMBO Molecular Medicine*, Nov, 3(11):623-36.
- Tran, N.H., Cavalcante, L.L., Lubner, S.J., Mulkerin, D.L., LoConte, N.K., Clipson, L., Matkowskyj, K.A., Deming, D.A. (2015), *Therapeutic Advances in Medical Oncology*, Sep, 7(5):252-62.
- Tsai, F.D., Lopes, M.S., Zhou, M., Court, H., Ponce, O., Fiordalisi, J.J., Gierut, J.J., Cox, A.D., Haigis, K.M., Philips, M.R. (2015), *Proceedings of the National Academy of Sciences of the U S A.*, Jan 20, 112(3):779-84.
- Tuveson, D.A., Shaw, A.T., Willis, N.A., Silver, D.P., Jackson, E.L., Chang, S., Mercer, K.L., Grochow, R., Hock, H., Crowley, D., Hingorani, S.R., Zaks, T., King, C., Jacobetz, M.A., Wang, L., Bronson, R.T., Orkin, S.H., DePinho, R.A., Jacks, T. (2004), *Cancer Cell*. Apr; 5(4):375-87.
- van Hattum, H. and Waldmann, H. (2014), *Chemistry & Biology*, Sep 18, 21(9):1185-95.
- Vartak, N. and Bastiaens, P. (2010), *EMBO Journal*, 29, 2689-99.
- Vartak, N., Papke, B., Grecco, H.E., Rossmannek, L., Waldmann, H., Hedberg, C., Bastiaens, P.I. (2014), *Biophysical Journal*, Jan 7, 106(1), 93-105.
- Vetter, I. R., and Wittinghofer, A. (2001), *Science (New York, N.Y.)* 294 (5545): 129961304.
- Vogelstein, B., Fearon, E.R., Hamilton, S.R., Kern, S.E., Preisinger, A.C., Leppert, M., Smits, A.M.M., Bos, J.L. (1988), *New England Journal of Medicine*, 319, 525-532.
- Vogelstein, B., Fearon, E.R., Kern, S.E., Hamilton, S.R., Preisinger, A.C., Nakamura, Y., White, R. (1989), *Science*, Apr 14, 244(4901):207-11.
- Vojtek, A.B., Hollenberg, S.M., Cooper, J.A. (1993), *Cell*, Jul 16, 74(1):205-14.

- Voorhoeve, P.M. and Agami, R. (2003), *Cancer Cell*, Oct, 4(4):311-9.
- Vos, M.D., Ellis, C.A., Elam, C., Ulku, A.S., Taylor, B.J., Clark, G.J. (2003), *The Journal of Biological Chemistry*, Jul 25, 278(30):28045-51.
- Vos, M.D., Martinez, A., Ellis, C.A., Vallecorsa, T., Clark, G.J. (2003a), *The Journal of Biological Chemistry* Jun 13, 278(24):21938-43.
- Warne, P.H., Viciano, P.R., Downward, J. (1993), *Nature*, Jul 22, 364(6435):352-5.
- Wei, W., Jobling, W.A., Chen, W., Hahn, W.C., Sedivy, J.M. (2003), *Molecular and Cellular Biology*, Apr, 23(8):2859-70.
- Weinstein, I. B. (2000), *Carcinogenesis*, 21, 5, 857-64.
- Weinstein, I.B., and Joe, A.K. (2006), *Nature Clinical Practice Oncology* 3 (8): 448657.
- Wennerberg, K., Rossman, K.L., Der, C.J. (2005), *Journal of Cell Science* 118 (5): 843646.
- White, M.A., Nicolette, C., Minden, A., Polverino, A., Van Aelst, L., Karin, M., Wigler, M.H. (1995), *Cell*, Feb 24, 80(4):533-41.
- Witkiewicz, A.K., McMillan, E.A., Balaji, U., Baek, G., Lin, W.C., Mansour, J., Mollaei, M., Wagner, K.U., Koduru, P., Yopp, A., Choti, M.A., Yeo, C.J., McCue, P., White, M.A., Knudsen, E.S. (2015), *Nature Communications*, Apr 9, 6:6744.
- Wood, K.W., Sarnecki, C., Roberts, T.M., Blenis, J. (1992), *Cell*, Mar 20, 68(6):1041-50.
- Yeung, T., Terebiznik, M., Yu, L., Silvius, J., Abidi, W.M., Philips, M., Levine, T., Kapus, A., Grinstein, S. (2006), *Science*, Jul 21, 313(5785):347-51.
- Zeeberg, K., Cardone, R.A., Greco, M.R., Saccomano, M., Nøhr-Nielsen, A., Alves, F., Pedersen, S.F., Reshkin, S.J. (2016), *International Journal of Oncology* Jul;49(1):243-52.
- Zhang, X.F., Settleman, J., Kyriakis, J.M., Takeuchi-Suzuki, E., Elledge, S.J., Marshall, M.S., Bruder, J.T., Rapp, U.R., Avruch, J. (1993), *Nature*, Jul 22, 364(6435):308-13.
- Zimmermann, G., Papke, B., Ismail, S., Vartak, N., Chandra, A., Hoffmann, M., Hahn, S.A., Triola, G., Wittinghofer, A., Bastiaens, P.I., Waldmann, H., (2013) *Nature*, 497, 7451, 638-642.
- Zschenker, O., Streichert, T., Hehlhans, S., Cordes, N. (2012), *PloS One*; 7(4): e34279.

Acknowledgements

I would like to thank Prof. Dr. Philippe Bastiaens for providing a great scientific environment and for his supervision and guidance in a difficult but also exciting project.

For taking over the second supervisor position I would like to thank PD Dr. Leif Dehmelt.

I want to thank Dr. Astrid Krämer for her great support. Not only by proof-reading my thesis, but also she constantly was helping me in the course of the project when I got lost and of course for her efforts in running the department.

I would like to express special thanks to Dr. Sven A. H. Müller, who spend hours with me at the Leica SP8 to get the SPIM system running.

For making it possible for me to go to work every day by taking care of my beloved dog Hannes I would like to thank Stefan Dietz and Suzanne Bisterfeld. Even when I had to work quite long or went to further education for more than one week he was always well taken care of.

Special thanks go to Manuela Grygier, Lisaweta Roßmannek, Dr. Sina Koch and Michael Reichl for taking care of the mice and helping to get the organoid culture started.

I would also like to thank our technicians Michael Reichl, Hendrike Schütz, Kirsten Michel, Manuela Grygier, Jutta Luig, Lisaweta Roßmannek, Sabine Dongard, Jana Seidel, Petra Glitz, Gaby Beetz, Anette Langerak, Michelle Protzek, and our ölab soulö Nimetka Seloska for their support.

I am also thankful to the past and present staff of the department II I met within the time I spent at the MPI, with special regards (but without order) to Dr. Klaus Schuermann, Dr. Dina Truxius, Dr. Sina Koch, Katia van Eickels, Christian Klein, Holger Vogel, Dr. Björn Koos, Dr. Marton Gelleri, Dr. Jens Christmann, Dr. Martin Masip, Dr. Jan Hübinger and Lisa Baak.

I would also like to thank Walburga Hecker, Birgitø Bistro, especially Birgit and Sandra, and the permanent employees at the MPI in the central units.

Last but not least I want to thank my family and friends, especially Daniel, Stephanie, Dina, Uwe and Hannes, for their support or just being there for me when I needed them during the past 3.5 years and also the times before that were not so easy.